Molecular Analysis of Translational Readthrough in *Tobacco necrosis virus-D*

Laura Rachelle Newburn

A DISSERTATION SUBMITTED TO THE FACULTY OF GRADUATE STUDIES IN PARTIAL FULFILLMENT OF THE REQUIREMENTS FOR THE DEGREE OF

DOCTOR OF PHILOSOPHY

GRADUATE PROGRAM IN BIOLOGY

YORK UNIVERSITY

TORONTO, ONTARIO

CANADA

MARCH 2021

ABSTRACT

Plus-sense single-stranded RNA plant viruses are a large group of agriculturally and economically important plant pathogens. These viruses encode their own RNA-dependent RNA polymerase (RdRp), whose translation from the viral genome is critical for a successful viral infection. Due to the limited size of their genomes, RNA plant viruses have developed several alternative methods of gene expression, including stop codon recoding. Recoding events, such as readthrough, allow for the translating ribosome to bypass a termination signal by incorporating an amino acid from a near-cognate tRNA. Several plant viruses, including those within the *Tombusviridae* family, utilize readthrough to produce their RdRp. Using a combination of *in vitro* and *in vivo* techniques, the importance of several RNA sequences and structures on readthrough efficiency were studied in the *Betanecrovirus Tobacco necrosis virus strain D* (TNV-D). The overall goal of this dissertation was to identify the RNA sequences and structures that are involved in promoting efficient translational readthrough of the TNV-D RdRp.

In this study, I show that readthrough production of the TNV-D RdRp requires multiple local RNA structures, as well as two long-range intra-genomic base-pairing interactions. A large RNA stem-loop structure (termed RTSL), located immediately downstream from the readthrough site, was found to be critical for readthrough, and was functional only when base-paired via a long-range RNA-RNA interaction with a sequence in the genomic 3'-untranslated region (3'UTR). RNA elements positioned just upstream and downstream from the RTSL were also investigated, and both Pre- and Post-RTSL RNA structures were found to be important for

efficient readthrough. Within the 3'UTR, SLII, and an RNA pseudoknot structure involving the 3'-terminus of the viral genome were both determined to be required for readthrough, as well as a second long-range RNA-RNA interaction involving the 3'UTR. Finally, SLX, also located in the 3'UTR, was not required for readthrough, but was important for viral RNA accumulation.

Collectively, these findings have helped to expand our understanding of the RNA elements involved in the mechanism of TNV-D translational readthrough. These results have also provided possible insight into other viruses that utilize type-III translational readthrough as a gene expression strategy.

AKNOWLEDGEMENTS

First and foremost, I would like to thank my supervisor Dr. K. Andrew White for allowing me to complete this research under his guidance. Throughout my time as a graduate student I have been able to experience many wonderful opportunities that would not have been possible without his support and encouragement.

My committee members, Dr. Katalin Hudak and Dr. Mark Bayfield have also been instrumental in my success as a graduate student. I sincerely appreciate your reviews of my research progress through the years.

I would like to thank the current and previous members of the lab. A special thank you to my initial mentor Dr. Beth Nicholson, and Tamari Chkuaseli who has made these past years so enjoyable.

My family and friends have been a great source of comfort and strength during my graduate studies. Thank you to my parents Bill Newburn and Lorna Morochove, as well as my brother Kyle Newburn for their unwavering support.

Last, but certainly not least, I would like to thank my husband Evert Timberg for his encouragement, support, and love throughout my graduate studies.

TABLE OF CONTENTS

LIST OF FIGURES

CHAPTER 1

CHAPTER 2

CHAPTER 3

CHAPTER 4

CHAPTER 5

APPENDICES

LIST OF ABBREVIATIONS

A-site:	aminoacyl-site
aa-tRNA	aminoacyl tRNA
ABCE1:	ATP-binding cassette subfamily member 1
AQP4:	aquaporin 4
AQP4ex:	aquaporin 4 extended
ATP:	adenosine triphosphate
BBSV:	*Beet black scorch virus*
BMV:	*Brome mosaic virus*
BTE:	BYDV-like translation element
BYDV:	*Barley yellow dwarf virus*
BYV:	*Beet yellows virus*
C-:	carboxyl
cDNA:	copy DNA
CIRV:	*Carnation Italian ringspot virus*
CITE:	cap-independent translational enhancer
CNV:	*Cucumber necrosis virus*
CP:	capsid protein
DI:	defective interfering
DL:	downstream linker

DNA:	deoxyribonucleic acid
DRTE:	distal readthrough element
ds:	double stranded
E-site:	exit-site
eEF:	eukaryotic elongation factor
eIF:	eukaryotic initiation factor
eRF:	eukaryotic release factor
FS:	frameshift
g:	genome
GDP:	guanosine diphosphase
GTP:	guanosine triphosphase
HCRSV:	*Hibiscus chlorotic ringspot virus*
hdc:	headcase
Hsc70-2:	Hsp70 cognate 2
Hsp70:	heat shock protein 70
IRE:	internal replication element
IRES:	internal ribosome entry site
IS:	intervening sequence
kb:	kilobase
LWSV:	*Leek white stripe virus*
M-domain:	middle-domain
Mo-MuLV:	*Moloney murine leukemia virus*
MP:	movement protein

mRNA:	messenger RNA
N-:	amino
nt:	nucleotide
OAS:	origin of assembly
ORF:	open reading frame
P-site:	peptidyl-site
PABP:	polyadenylated binding protein
PCR:	polymerase chain reaction
PEMV:	*Pea enation mosaic virus*
PFBV:	*Pelargonium flower break virus*
PIC:	preinitiation complex
PK:	pseudoknot
poly(A):	polyadenylated
PRTE:	proximal readthrough element
PVX:	*Potato virus X*
Rap-1:	replicase-associated protein 1
RCNMV:	*Red clover necrotic mosaic virus*
Rel:	relative
RdRp:	RNA-dependent RNA-polymerase
RII:	region II
RIV:	region IV
RNA:	ribonucleic acid
rRNA:	ribosomal RNA

RT:	readthrough
RTSL:	readthrough stemloop
SDS-PAGE:	sodium dodecyl sulfate-polyacrylamide gel electrophoresis
sg:	subgenomic
SH:	shifty heptanucleotide
SHAPE:	selective 2'hydroyl acylation analyzed by primer extension
SL:	stem-loop
ss:	single-stranded
TBSV:	*Tomato bushy stunt virus*
TCV:	*Turnip crinkle virus*
TMV:	*Tobacco mosaic virus*
TNV-D:	*Tobacco necrosis virus strain D*
tRNA:	transfer RNA
UL:	upstream linker
UTR:	untranslated region
wge:	wheat germ extract
wt:	wild-type

CHAPTER 1

Introduction

1.1 Plus-strand RNA Plant Viruses

Viruses are infectious biological agents that can infect a wide variety of hosts, from prokaryotes to eukaryotes. They are composed of two major constituents, a nucleic acid genome and a protein capsid that encases the genome. Virus capsids are typically spherical or rod-shaped and consist of multiple copies of one or more capsid protein subunit. Additionally, virus particles may also contain extra layers, such as a secondary protein matrix layer and a host-derived lipid bilayer that forms an outer envelope (Acheson, 2011).

Plant viruses are obligate intracellular parasites whose survival depends on hijacking host components. Plant virus genomes can be composed of single-stranded (ss) or double-stranded DNA or RNA and be segmented (*i.e* a genome composed of two or more molecules) or non-segmented. Segmented genomes can be packaged into particles either separately (multipartite viruses) or collectively (segmented viruses). Most plant viruses are spherical or rod-shaped and do not contain a lipid envelope. The vast majority of plant viruses also contain plus-sense (*i.e.* messenger-sense) ssRNA genomes, and encode an RNA-dependent RNA-polymerase (RdRp) responsible for RNA genome replication (Bustamante and Hull, 1998). Upon entry into host cells, plus-strand RNA viral genomes are unpackaged and directly translated by the host's translational machinery to produce some or all of their encoded proteins. At minimum, these

viruses must translate an RdRp and a capsid protein, to allow for synthesis of progeny genomes and subsequent packaging, respectively. However, in reality, additional viral proteins with different important functions are also produced.

Many plus-strand RNA plant viruses are agriculturally important worldwide (*i.e.* potyviruses, luteoviruses) and have been the subject of intense research. Viral infection in crops such as wheat, corn, rice, and olive trees can result in a reduction in yield or crop death, both of which have a significant negative socio-economic impact (Patil, 2020).

1.2 Viral Life Cycle

The life cycle of plus-sense RNA plant viruses can be broken down into six distinct stages: entry/disassembly, translation, genome replication, virus assembly, intra-host movement, and finally, inter-host transmission (**Figure 1**). Each stage is briefly described below.

1.2.1 Virus Entry/Disassembly

Plant cells are encased by both a plasma membrane and an outer cell wall. The rigid nature of the cell wall makes it difficult for a plant virus to enter a plant cell. Instead, viruses must gain entry through a breach in the plant cell's protective layer (**Figure 1(i)**). This is usually accomplished with the help of biological vectors such as insects, fungi, and nematodes. When feeding on or infecting plants, these pathogens cause damage that provides a mode of entry into plant cells for associated viruses (Hull, 2002). Once inside the cell, a virion disassembles or uncoats to release the viral RNA genome and allow for expression of the viral genes, mediated by the host translation machinery (**Figure 1(ii)**). Unpackaging is a critical process, although for most plant viruses the exact mechanism is not well understood. *Cucumber necrosis virus* (CNV)

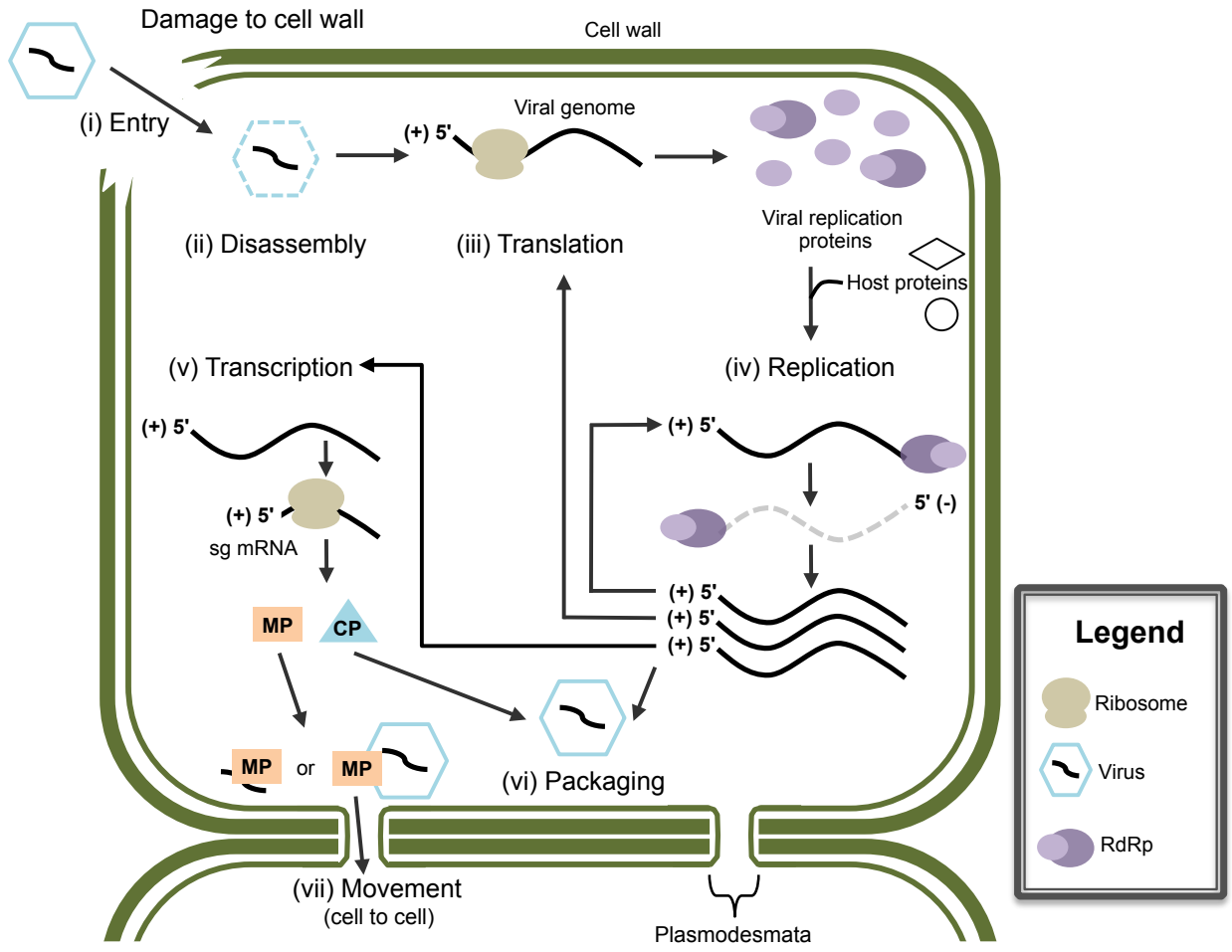

Figure 1. **Simplified infectious cycle of a plus-sense RNA plant virus**. **(i)** Entry of the viral particle via damage to the plant cell wall. **(ii)** Disassembly of the viral particle, releasing the viral genome into the cytoplasm. **(iii)** Translation of early proteins from genomic RNA, including viral replication proteins. **(iv)** Replication of the viral genome via a minus-strand RNA intermediate. **(v)** Transcription of subgenomic mRNA and expression of late stage viral proteins, including the capsid protein (CP) and movement protein (MP). **(vi)** Packaging of the viral RNA genomes into progeny viral particles. **(vii)** Movement of the progeny virus/genome via the plasmodesmata into adjacent cells, as mediated by the movement protein. See text for details.

(Family: *Tombusviridae*, Genus: *Tombusvirus*), a spherical virus, utilizes the chaperone heat shock protein 70 (Hsp70) and/or Hsp70 cognate 2 (Hsc70-2) to promote the disassembly process. The surface of CNV particles associates with Hsc70-2. This interaction leads to a conformation change and partial disassembly of the capsid, which likely makes the capsid more sensitive to protease digestion to further mediate genome release (Alam and Rochon, 2016).

1.2.2 Translation of Viral Proteins

After disassembly, the plus-sense RNA viral genomes must co-opt the host cell's translation machinery to initiate translation of their encoded proteins (**Figure 1(iii)**). Some viruses, such as *Potato virus X* (PVX) (Family: *Alphaflexiviridae*, Genus: *Potexvirus*), utilize traditional 5'-cap and a 3'-polyadenylated tail structures, and thus recruit cellular translation initiation factors in a manner similar to cellular mRNAs (Sonenberg et al., 1978; Dreher and Miller, 2006); see section **1.3** for more detail on canonical translation. However, many viruses lack one or both of these conventional terminal structures and, instead, have developed alternative strategies to overcome such deficiencies. *Tobacco mosaic virus* (TMV) (Family: *Virgaviridae*, Genus: *Tobamovirus*) possesses a 5'-cap, but not a 3'-polyadenylated tail; instead it encodes a transfer RNA (tRNA)-like structure at its 3'-terminus that, together with upstream pseudoknots, is able support translation initiation by assisting in the recruitment of translational machinery (Leathers et al., 1993). Members of the virus family *Tombusviridae*, termed tombusvirids, lack both 5'-cap and 3'-polyadenylated tail structures. Instead, they possess a 3'-cap independent translation enhancer (3'CITE) in their 3'-untranslated regions (3'UTRs) that recruits eukaryotic translation initiation factors (eIFs), such as eIF4E or 4G, and thus functionally replaces the 5'-cap (Fabian and White, 2004; 2006; Nicholson et al., 2010). Most, but not all,

3'CITEs interact with the 5'UTR of the viral RNA genome through an RNA-RNA base-pairing interaction, which repositions the 3'CITE-bound eIFs to the 5'-end of the genome, where translation initiation occurs (Fabian and White, 2004; 2006). Beyond the unique translation initiation strategies utilized by RNA virus genomes, those that are polycistronic have developed additional approaches to mediate translation of open reading frames (ORFs) positioned internally, and these strategies are discussed in section **1.4**.

1.2.3 Viral Genome Replication

Once the virally-encoded RdRp and other viral replication associated proteins have been translated, they, in conjunction with host factors, direct replication of the viral genome (**Figure 1(iv)**). The replication of plus-sense ssRNA plant virus genomes occurs in two distinct stages: (1) synthesis of a full-length complementary minus-sense RNA copy, using the infecting plus-strand as a template, followed by (2) synthesis of multiple plus-sense progeny RNA genomes using the minus-strand as a template. Initially, the RdRp engages the 3'-terminus of the infecting plus-strand RNA genome and initiates synthesis of the intermediate minus-sense genome (Miller and White, 2006). Viral RNA elements, *i.e.* promoters, are required to position the replication machinery at the 3'-end of the viral genome, and these RNA elements can involve primary sequence as well as higher order RNA structures (Miller and White, 2006). For subsequent plus-sense progeny genome synthesis, there are also promoter elements in the 3'-region of the minus-strand genome that are responsible for directing RdRp initiation. In infections, plus-sense progeny copies of the viral genome are commonly ~100-fold more abundant than corresponding minus-sense templates, indicating that the minus-strand RNA intermediates are reused as templates multiple times (Buck, 1999). In addition to synthesis of viral genomes, some viruses

produce smaller partial copies of the genome, termed subgenomic (sg) mRNAs, which are used to express downstream-encoded ORFs (**Figure 1(v)**). The synthesis of sg mRNAs is referred to as transcription, to distinguish it from genome replication, and is described in section **1.4.5**.

1.2.4 Packaging

Packaging, or encapsidation, is the last stage of viral reproduction where capsid or coat protein subunits assemble around the progeny viral genome (**Figure 1(vi)**). Encapsidation occurs at later stages of infections when large amounts of viral coat protein accumulate. The coat protein recognizes a specific RNA element(s) in viral genomes, termed the packaging signal or origin of assembly (OAS), which allows for discrimination between progeny viral RNA and cellular RNAs. The OAS acts as a nucleation site for assembly of the capsid that forms a protein shell around the viral genome. The OAS can be located at different locations within different viral genomes. For example, the OAS of *Turnip crinkle virus* (TCV) (Family: *Tombusviridae*, Genus: *Carmovirus*) is within a 28nt region of a stem-loop (SL) near the 3'-end of the capsid protein gene, ~300nt from the 3'-end of the RNA genome (Qu and Morris, 1997). In contrast, the PVX OAS is a 107nt stem-loop structure located at the very 5'-terminus of the genome (Kwon et al., 2005). Following the initial nucleation of assembly at the OAS, additional coat protein subunits associate and polymerise around the viral RNA until a complete particle has formed. This process is facilitated by dimerized coat protein subunits whereby the basic domains of the coat protein interact with the negatively charged RNA genome (Rao, 2006). Encapsidation of the viral genome protects it from degradation and can be important for mediating viral transmission between plants; as described in section **1.2.6**.

1.2.5 Intercellular and Systemic Movement

An additional important event during plant infection is the spread of the infection beyond the initially infected cell to adjacent cells. A virally encoded protein, referred to as the movement protein, facilitates this cell-to-cell movement between adjacent plant cells via the plasmodesmata (**Figure 1(vii)**). Plasmodesmata are narrow intercellular channels between adjacent plant cells that allow for intercellular communication and material exchange (Lee and Lu, 2011). Both viral genomes and virus particles are too large to pass through plasmodesmata openings unaided. Accordingly, the virally encoded movement protein functions to increase the size exclusion limit of the plasmodesmata, thus allowing passage of the virus or its RNA genome into adjacent cells (Lee and Lu, 2011).

To continue the spread of the virus from a local infection to a whole plant/systemic infection, the viral particle has to enter the phloem network of the plant (Roberts et al., 1997). The vascular system of the plant allows for fast transport of virus to more distant regions of the plant, permitting systemic infection. However, the exact mechanism of systemic spread remains largely unknown (Hipper et al., 2013).

1.2.6 Transmission

To further the scale of infection, plant viruses must move between host plants. Transmission can occur through many different mechanisms, such as seeds (Carroll, 1972) or soil movement/cultivation (Roberts, 2014). However, as plants are essentially immobile, plant viruses tend to rely on biological vectors for transmission. These vectors are often arthropods, with aphids and whiteflies accounting for ~50% of all vector-using plant virus transmission (Ziegler-Graff, 2020). Along with their comparably larger range of movement, biological vectors cause

damage to the plant cell wall, thus overcoming this barrier, and allowing associated virions entry to the cell. Virus association with their vectors is mediated by the interaction of their capsid proteins with the mouthparts of arthropods (Ziegler-Graff, 2020).

Other vectors include soil-dwelling organisms, such as nematodes and fungi (Roberts, 2014). Vector transmission through soil results in infecting the host plant through the root tissue. Fungi, such as *Olpidium sp.*, are able to transmit several members of the *Tombusviridae* family, including CNV (McLean et al., 1994). The capsid protein plays an important role in transmission by associating with the surface of the fungal zoospores. When the zoospores protrude into the root cells, the zoospore-associated virus also gains entry and is able to initiate an infection (McLean et al., 1994).

1.3 Canonical Translation

Translation is the decoding of mRNAs by ribosomes, accessory protein factors, and transfer RNAs (tRNAs), to synthesize their corresponding proteins. The eukaryotic 80S ribosome is composed of two major subunits; the large 60S subunit and the small 40S subunit (Hinnebusch, 2014). The large subunit contains the catalytic site that directs the formation of peptide bonds, while the small subunit includes the decoding site, where base pairing between the mRNA codon and tRNA anticodon occurs (Hinnebusch, 2014). Below, the three stages of protein synthesis, initiation, elongation, and termination, are briefly described.

1.3.1 Initiation

The initiation step in translation is considered to be the rate-limiting step in canonical translation initiation, and it can be divided into three distinct steps: assembly of the preinitiation complex (PIC), scanning, and recognition (**Figure 2**).

1.3.1.1 Preinitiation Complex Assembly

Prior to entering the cytoplasm for translation, eukaryotic mRNA undergoes post-transcriptional modification in the nucleus to include a 5'-m^7GpppN cap structure and a 3'-polyadenylated tail. These modifications are required for canonical translation initiation and subsequence expression of the encoded protein (Thiébeauld et al., 2007). A key goal of translation initiation is to position the ribosome at the start codon of an ORF in a state ready to begin protein synthesis; this is a complex process involving many steps, including protein-protein and protein-mRNA interactions (**Figure 2(i)**). Initially, the 5'-cap structure interacts with eIF4E (Marcotrigiano et al., 1997; Matsou et al., 1997). eIF4E interacts with the large scaffolding protein eIF4G, which in turn recruits the RNA helicase eIF4A; collectively, this complex is known as eIF4F (Gingras et al., 1997). eIF4G also interacts with polyadenylated-binding protein (PABP), which is bound to the 3'- polyadenylated tail, effectively circularizing the mRNA and simultaneously enhancing both 5'-cap/eIF4E and 3'-polyadenylated tail/PABP binding activity (Gallie, 1998; Hinnebusche, 2014). eIF4A unwinds secondary structure in the 5'UTR of mRNA to facilitate ribosome binding (Rogers et al., 2001; Rozovsky et al., 2008). eIF4G is a key interactor in the recruitment of the 43S pre-initiation complex, which is composed of the 40S ribosomal subunit, eIF1, eIF1A, the eIF2 ternary complex (eIF2, $tRNA_i^{met}$, and GTP), eIF3, and

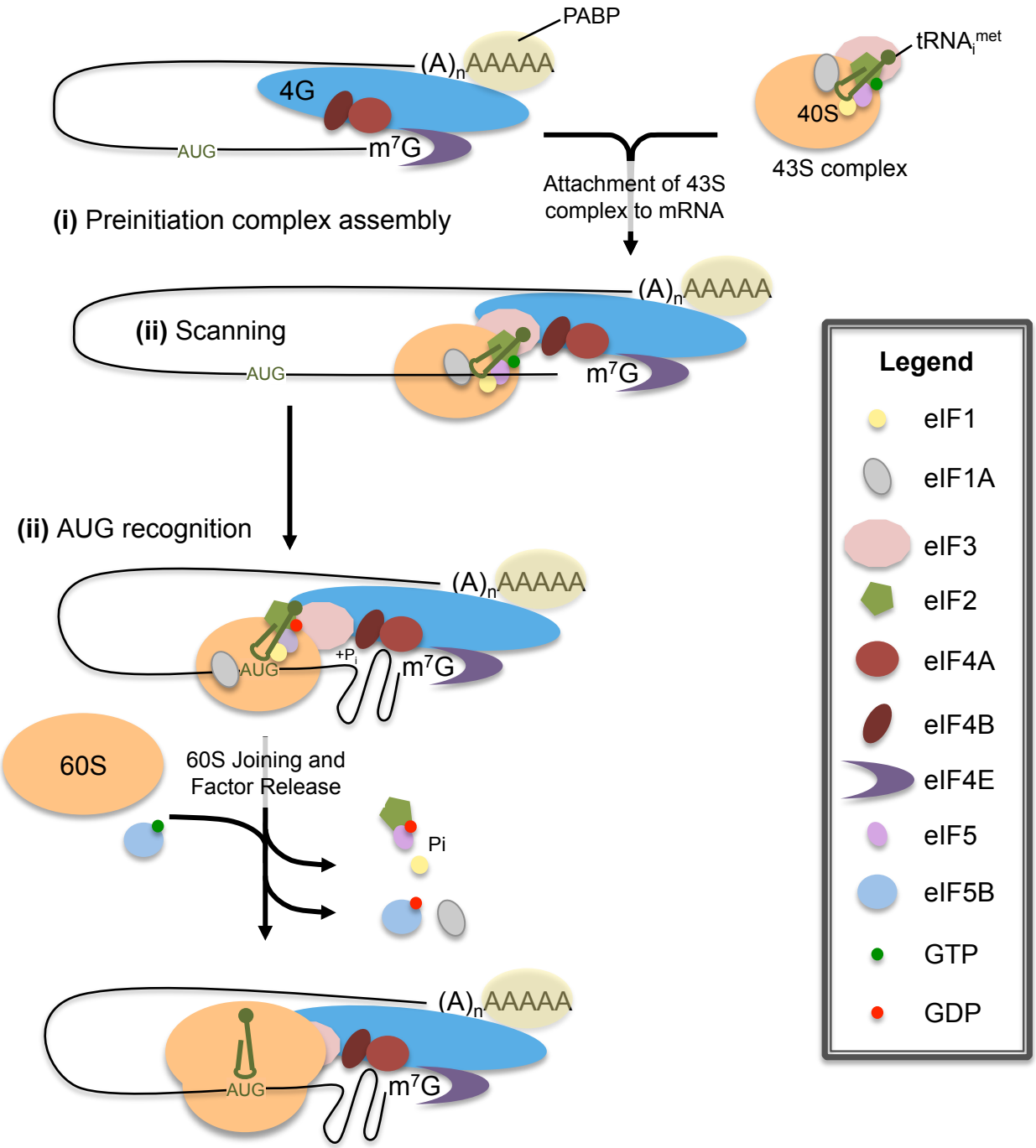

Figure 2. **Canonical eukaryotic translation initiation**. (i) The 43S complex binds to the 5'-end of the mRNA via an interaction between eukaryotic initiation factor (eIF) 4G and eIF3. (ii) The complex scans the mRNA in the 5'-to-3' direction until it encounters a start codon in the ribosomal A-site. (iii) eIF5B mediates 60S subunit joining, and the resulting 80S initiation complex is competent for elongation. See text for more details. Figure is adapted from Hinnebusch, 2014.

eIF5 (Hinnebusch, 2014), and this interaction is mediated through a direct connection between eIF3 with eIF4G (Korneeva et al., 2000; LeFebvre et al., 2006).

1.3.1.2 Scanning

Ribosome scanning occurs in the 5'-to-3' direction until the 43S complex reaches the start codon (Vassilenki et al., 2011). Many of the initiation factors, such as eIF4A, eIF4B, eIF4G, eIF1 and eIF1A, enhance scanning (**Figure 2(ii)**). The ATP-dependent helicase activity of eIF4A stimulates PIC scanning through structured 5'UTRs, with its activity supported by eIF4B and eIF4G (Pestova and Kolupaeva, 2002). Interestingly, eIF4G may still remain bound to eIF4E during scanning, though its exact role remains unclear. eIF1 and eIF1A are also necessary to maintain the PIC in an open scanning conformation (Pestova and Koulpaeva, 2002; Passmore et al., 2007).

1.3.1.3 Recognition

A critical aspect of the PIC scanning mechanism is the ability to recognize the appropriate start codon (**Figure 2(iii)**). eIF1 functions to block the recognition of non-AUG triplets or AUGs in poor contexts (Pestova and Koulpaeva, 2002; Passmore et al., 2007). The optimal start codon nucleotide context for vertebrates is (A/G)CCAUGG (Kozak, 1987), with monocot and dicot plants preferring (A/G)(A/C)CAUGGC and A(A/C)AAUGGC respectively (Joshi et al., 1997). Upon recognition of the start codon by the $tRNA_i^{met}$, the PIC undergoes a conformational change that triggers eIF1 dissociation and release of phosphate from eIF2-GTP, catalyzed by GTPase-activator protein eIF5, forming the 48S complex (Paulin et al., 2001; Unbehaun et al., 2004; Algire et al., 2005). Following the release of the above eIFs, eIF5B-GTP accelerates the joining

of the 60S ribosomal subunit to the 40S subunit with the assistance of eIF1A (Pestova et al., 2000; Acker et al., 2006). GTP hydrolysis by eIF5B reduces its affinity for the 60S subunit and eIF5B dissociates; this GTP hydrolysis is also instrumental in the release of eIF1A from the ribosome complex (Acker et al., 2006; Acker et al., 2009). The resulting 80S initiation complex is competent for elongation. Some eIFs may remain associated with the 80S complex during early elongation, although their function is unclear (Valášek et al., 2017).

1.3.2 Elongation

Translation elongation is composed of three basic steps, decoding, peptide-bond formation, and translocation (**Figure 3**). These steps are repeated until the ribosome reaches a stop codon. Decoding, or tRNA selection, is a process where the GTPase eukaryotic elongation factor (eEF) 1A delivers an aminoacyl-tRNA into the ribosomal aminoacyl-site (A-site) in a tertiary complex with GTP. If the tRNA anticodon is able to base pair with the mRNA codon in the ribosomal A-site, GTP hydrolysis by eEF1A enables the acceptance of the aminoacyl-tRNA in the ribosomal A-site, and eEF1A-GDP is released (**Figure 3(i)**). Peptide-bond formation occurs rapidly, catalyzed by the peptidyl-transferase activity of the ribosome, and the nascent peptide chain is transferred from the peptidyl-tRNA in the peptidyl-site (P-site) to the newly seated aminoacyl-tRNA in the A-site, resulting in the extension of the nascent peptide chain (**Figure 3(ii)**). This transfer causes the ribosome to rotate so that the peptidyl- and deacylated-tRNAs are spanning the A/P- and P/Exit -sites (E-site) of the large subunit while remaining in the A- and P-sites of the small subunit respectively. eEF2-GTP binds the ribosomal A-site and, in conjunction with the reverse rotation of the small ribosomal subunit, promotes translocation of the tRNAs fully into the P- and E-sites of the ribosome (**Figure 3(iii)**). With the peptidyl-tRNA

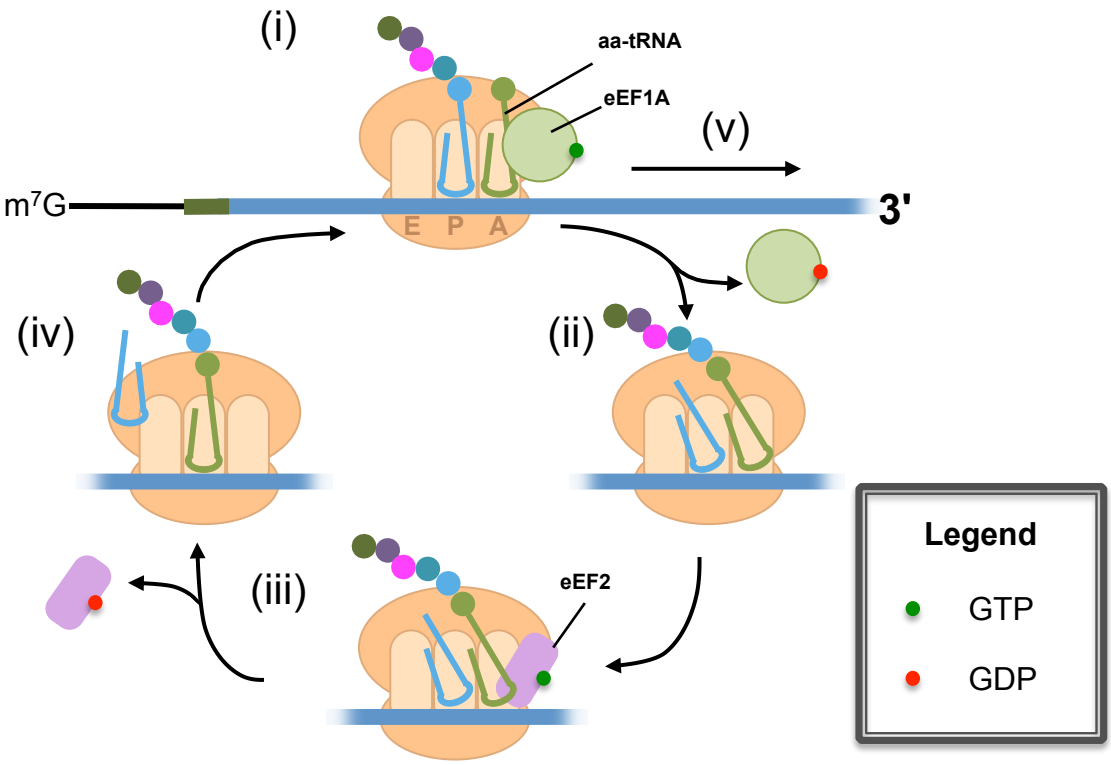

Figure 3. **Canonical eukaryotic translation elongation**. **(i)** Eukaryotic elongation factor (eEF) 1A delivers an aminoacyl-tRNA (aa-tRNA) to the 80S ribosomal A-site. **(ii)** Peptide bond formation occurs and the ribosome rotates so that the peptidyl- and deacylated-tRNAs are spanning the A/P- and P/E-sites of the large subunit while remaining in the A- and P-sites of the small subunit. **(iii)** eEF2 binds the ribosomal A-site and helps promote the translocation of tRNAs. **(iv)** The deacylated-tRNA leaves the E-site and **(v)** elongation continues in the same manner until protein synthesis is complete. See text for additional details.

in the P-site (**Figure 3(iv)**), a new codon can be positioned in the A-site and the elongation cycle continues until protein synthesis is complete (**Figure 3(v)**) (Dever et al., 2018; Schuller and Green, 2018).

1.3.3 Termination

Translation termination is initiated when the translating ribosome encounters a stop codon in the ribosomal A-site (**Figure 4(i)**). In eukaryotes, all three stop codons – UGA, UAA, and UGA – are recognized by eukaryotic release factor (eRF) 1, a protein that is similar in size and shape to a tRNA (**Figure 4(ii)**) (Song et al., 2000). eRF1 is composed of three functional domains, the N-terminal domain responsible for stop codon recognition in the ribosomal A-site, the middle (M) domain that is responsible for stimulating peptide release, and the C-terminal domain that interacts with other termination factors such as eRF3 (**Figure 4(ii)**) (Hellen, 2018).

Largely the eRF1 N-terminal domain is responsible for stop codon recognition through the combined effort of three conserved motifs; TAS-NIKS$_{(58\text{-}64)}$, YxCxxxF$_{(125\text{-}131)}$, and GTS$_{(31\text{-}33)}$ (Chavatta et al., 2002; Frolova et al., 2002; Bulygin et al., 2010; Wong et al., 2012; Brown et al., 2015). The TAS-NIKS$_{(58\text{-}64)}$, motif is responsible for recognizing uridine in the +1 stop codon position (Chavatta et al., 2002; Brown et al., 2015). The YxCxxxF$_{(125\text{-}131)}$ motif along with E$_{(55)}$ and GTS$_{(31\text{-}33)}$ are responsible for decoding the +2 and +3 stop codon positions through hydrogen bonding interactions involving Y$_{(125)}$, E$_{(55)}$, and T$_{(32)}$ (Kolosov et al., 2005; Wong et al., 2012; Brown et al., 2015). Additionally the C$_{(127)}$ side chain can form two hydrogen bonds with the 18S rRNA A1825 residue, stabilizing its 'flipped out' conformation upon which the +2 and +3 stop codon nucleotides stack allowing the +4 nucleotide to be drawn into the ribosomal A-site (**Figure**

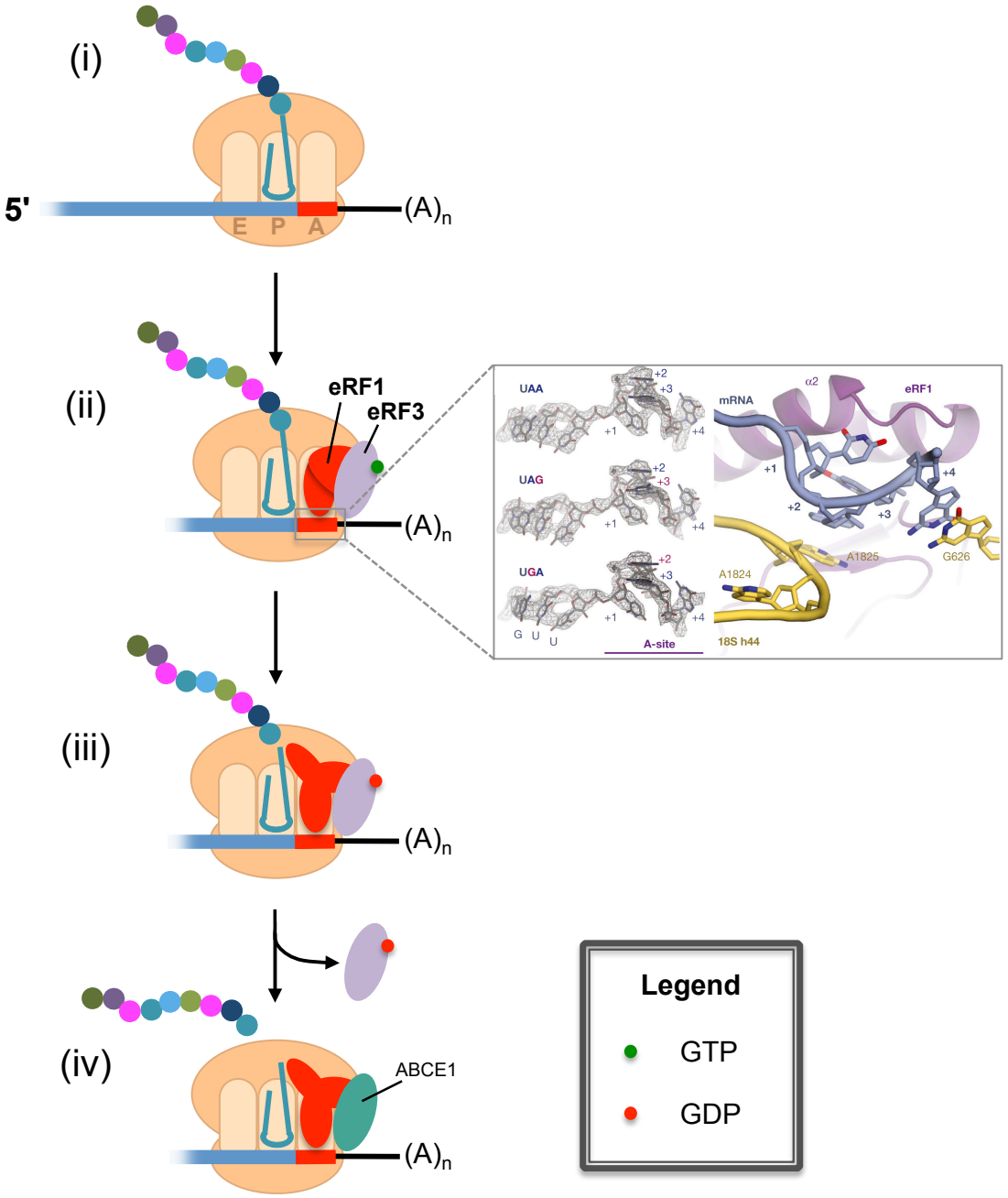

Figure 4. **Canonical eukaryotic translation termination**. **(i)** Translation termination is signalled when the translating ribosome encounters a stop codon in the ribosomal A-site. **(ii)** The stop codon is recognized by a complex consisting of eukaryotic release factor (eRF) 1 and eRF3. Grey boxed area left: electron microscope map densities of all three stop codons in the ribosomal A-site, right: interactions between eRF1 (purple), stop codon mRNA (blue), and 18S rRNA (yellow). Grey boxed area adapted from Brown et al., 2015. **(iii)** eRF1 undergoes a conformational change that stimulates nascent polypeptide release. (**iv**) ATP-binding cassette subfamily E member 1 (ABCE1) may stabilize this conformation of eRF1 and promotes ribosome recycling. See text for more details.

4(ii)) (Brown et al., 2015). All together, these three motifs are required for optimal stop codon recognition.

The activity of eRF1 is supported by eRF3, a GTPase that is engaged with the C-terminal domain of eRF1 when entering the ribosomal A-site, and after GTP hydrolysis eRF3 disassociates (**Figure 4(iii)**) (Alkalaeva et al., 2006; Preis et al., 2014). The conformation of eRF1 changes so that the M-domain GGQ motif is extended towards the large ribosomal subunits' peptidyl transferase center triggering peptidyl-tRNA hydrolysis and thereby nascent peptide release (Frolova et al., 1999). Binding of ATP-binding cassette subfamily E member 1 (ABCE1) to eRF1 may stabilize this conformation of eRF1 (**Figure 4(iv)**) (Preis et al., 2014).

After nascent polypeptide release the post-termination complex is recycled in a process initiated by ABCE1. ABCE1 facilitates the release of the 60S subunit and eRF1 through ATP-hydrolysis (Pisarev et al., 2010; Hellen, 2018). The deacylated tRNA and mRNA are released from the 40S subunit through interactions with other cellular factors such as eIF3 (Pisarev et al., 2007; Hellen, 2018).

1.4. Gene Coding and Expression Strategies of Plus-sense RNA Plant Viruses

The genomes of plus-sense RNA plant viruses are coding, thus viral proteins can be translated directly from the infecting genome. However, the limited size of these viruses has led them to develop a variety of coding and expression strategies to regulate the synthesis of viral proteins and maximize the use of their coding space. These alternative strategies include segmented genomes, polyprotein synthesis, leaky scanning of ribosomes, internal ribosome entry

sites (IRESes), transcription of sg mRNAs, and programmed ribosome recoding events, such as translational frameshifting or readthrough mechanisms (**Figure 5**).

1.4.1 Viruses with Segmented Genomes

Some positive-strand RNA viruses split their genomes across two or more RNA fragments (**Figure 5A**). Both segmented and multipartite viruses consist of multiple genome strands, with the former containing all RNA segments in the same particle, and the latter packaging genome segments separately. For example, *Red clover necrotic mosaic virus* (RCNMV) (Family: *Tombusviridae*, Genus: *Dianthovirus*) is a segmented virus composed of two RNA segments, the tri-cistronic RNA1 and mono-cistronic RNA2, that are copackaged into a single capsid (Basnayake et al., 2006). In contrast, multipartite *Brome mosaic virus* (BMV) (Family: *Bromoviridae*, Genus: *Bromovirus*) is composed of three RNA segments, with RNA1 and RNA2 being mono-cistronic and RNA3 di-cistronic, and each of these genome segments is packaged into a separate virion (Choi et al., 2002; Choi and Rao, 2003). In these cases, the strategy of encoding viral genes in multiple genome segments helps to reduce the need for translation strategies to allow for expression of genes encoded downstream of the first ORF in a viral genome. Additionally, independent control of the accumulation levels of the different segments allows for modulation of the expression of encoded genes during infections.

1.4.2 Polyproteins and Proteolytic Processing

RNA plant viruses such as *Potato virus A* (Family: *Potyviridae*, Genus: *Potyvirus*) and *Turnip yellow mosaic virus* (Family: *Tymoviridae*, Genus: *Tymovirus*) translate polyproteins, as oppose to individual proteins (Puurand et al., 1994; Jakubiec et al., 2007). This method of gene

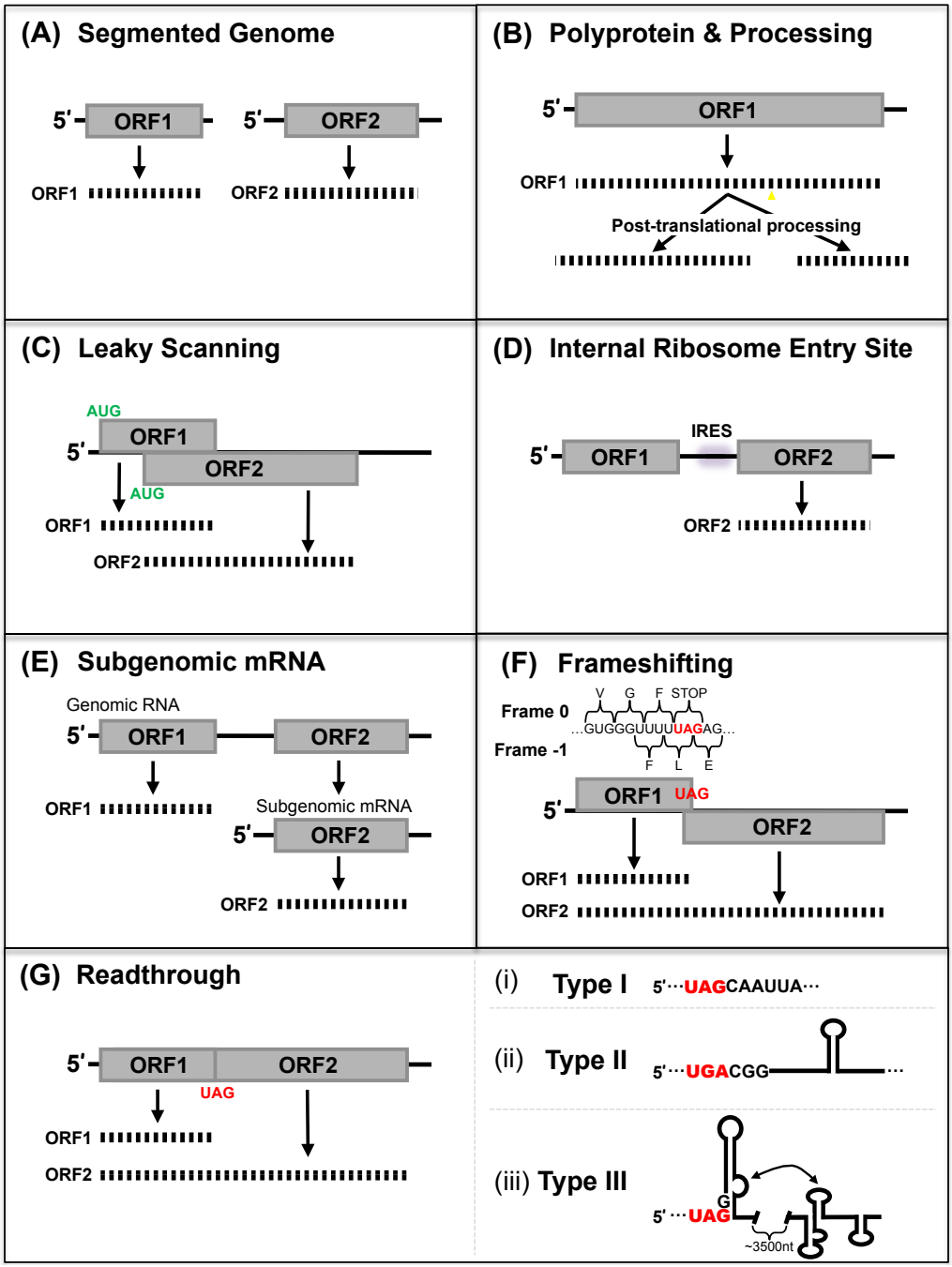

Figure 5. **A schematic representation of alternative gene expression strategies utilized by RNA plant viruses**. **(A)** Segmented genome, where a viral genome is composed of multiple segments. **(B)** Polyprotein synthesis, where one long polypeptide is translated and then proteolytically cleaved into individual proteins. **(C)** Leaky scanning, where the ribosome bypasses a viral protein-coding start codon in favour of another one further downstream. **(D)** Internal ribosome entry site (IRES), where an internal RNA element acts to recruit the ribosome. **(E)** Subgenomic mRNA, where a small RNA genome is produced that positions downstream open reading frame (ORF) in the genome to be in a more 5'-position. **(F)** Frameshifting, where a translating ribosome bypasses a stop codon by moving into an alternative reading frame. The slippery sequence shown belongs to Barley yellow dwarf virus. **(G)** Readthrough, a translating ribosome decodes a stop codon as a sense codon and continues translation producing a C-terminally extended protein. (i), (ii) and (iii) correspond to the three types of readthrough elements. See text for additional details

expression involves the translation of a long polyprotein from a large single ORF, which is subsequently proteolytically cleaved to generate multiple individual viral proteins (**Figure 5B**). Generally, virally-encoded proteases are responsible for cleaving the polyprotein into individual proteins, and the rate of this occurrence provides a post-translational mechanism to control expression of the individual genes (Puurand et al., 1994; Jakubiec et al., 2007).

1.4.3 Leaky Scanning

As described previously, the ribosomal PIC scans an mRNA linearly until it encounters a start codon in a favourable Kozak consensus sequence (Kozak, 1987; Joshi et al., 1997). However, the scanning ribosome can bypass the initiation site of a viral protein and continue scanning further downstream until it reaches the next favourable initiation site (**Figure 5C**). The 'leakiness' of the initial start codon (*i.e.* its divergence from the Kozak optimum) allows for the translation of an overlapping 3'ORF encoded in a different reading frame, thereby increasing the coding capacity for that section of RNA. Several plus-sense RNA plant viruses use leaky scanning to express their genes, including tombusvirids such as *Tomato bushy stunt virus* (TBSV) and CNV, which use leaky scanning to express their movement and suppressor of gene silencing proteins (Scholthof et al., 1999; Johnston and Rochon, 1996).

1.4.4 Internal Ribosome Entry Sites

Internal ribosomes entry sites provide a cap-independent method of recruiting ribosomes to mRNA (**Figure 5D**). Plant virus IRESes are generally short RNA sequences lacking notable secondary structure (Zhang et al., 2015). These IRESes can be within non-coding or coding regions. The *Carmoviruses Pelargonium flower break virus* (PFBV), *Hibiscus chlorotic ringspot*

virus (HCRSV), and TCV direct translation of the capsid protein ORF in the full-length viral RNA via an IRES located just upstream of the capsid protein start codon (Fernández-Miragall and Hernández, 2011; Koh et al., 2003; May et al., 2017). This occurs despite the fact that the capsid protein is also expressed from a sg mRNA during infection. Notably, when the PFBV IRES was disrupted, viral infectivity declined, indicating that early expression of capsid protein is important for viral infectivity, and consistent with the fact that the capsid protein is also a suppressor of host antiviral gene silencing (Fernández-Miragall and Hernández, 2011). Interestingly, IRESes do not necessarily need to be located upstream of the protein ORF that they control. The replicase-associated protein 1 (Rap1) of *Potato leafroll polerovirus* (Family: *Luteoviridae*) is translated utilizing an IRES with a functional motif of GGAGAGAGAGG that is located within the Rap1 ORF (Jaag et al., 2003).

1.4.5 Subgenomic mRNA

The expression of downstream ORF(s) encoded in a polycistronic viral genome can be achieved through the transcription of sg mRNAs. Sg mRNAs are short viral messages that are transcribed from the full-length genome (**Figure 5E**). They place the more 3'-proximal ORF(s) at the 5'-end of the mRNA, thereby allowing 5'-entering ribosomes to efficiently access the ORF. Members of the family *Tombusviridae* produce their sg mRNA(s) through a premature termination mechanism. During minus-strand synthesis of the genome, the RdRp encounters a stop signal formed by an RNA secondary structure, which causes the RdRp to terminate prematurely (Choi and White, 2002). This early termination produces a smaller-sized minus-strand RNA that is used as a template by the RdRp to produce many plus-strand copies, which are 3'-coterminal to the genome (White, 2002).

1.4.6 Translation Recoding

Translation termination is prompted by one of three stop codons, UAG, UGA, or UAA. However, signals within mRNA can redefine the reading of codons. Recoding mechanisms such as frameshifting and readthrough, are able to produce a C-terminally unique protein. During frameshifting, the ribosome encounters a slippery nucleotide sequence and shifts its reading frame either in the 5' or 3' direction (Barry and Miller, 2002; Tajima et al., 2011; Gao and Simon, 2016). In contrast, during readthrough the stop codon is deciphered by a near-cognate tRNA, thus the resulting protein remains in the same reading frame as it initiated (Skuzeski et al., 1991; Firth et al., 2011; Cimino et al., 2011). Several advantages are gained through translational recoding such as regulation of gene expression, and maximization of the limited coding capacity of viruses.

1.4.6.1 Translational Frameshifting

Ribosomal frameshifting is a translation strategy used by many RNA viruses to regulate gene expression. Frameshifting has been implicated as a translation strategy in several plus-sense RNA plant viruses, such as RCNMV, *Barley yellow dwarf virus* (BYDV) (Family: *Luteoviridae*, Genus: *Luteovirus*), *Pea enation mosaic virus 2* (PEMV-2) (Family: *Tombusviridae*, Genus: *Umbravirus*), and *Beet yellows virus* (BYV) (Family: *Closteroviridae*, Genus: *Closterovirus*) to name a few (Xiong et al., 1993; Brault and Miller, 1992; Gao and Simon, 2016; Agranovsky et al., 1994). The resulting C-terminally extended protein is often the viral RdRp protein (Firth and Brierley, 2012). RCNMV, BYDV, and PEMV-2 utilize -1 programmed frameshifting where the ribosome shifts in the reverse direction by one nucleotide into a new reading frame (**Figure 5F**),

whereas BYV is predicted to utilize +1 programmed frameshifting where the ribosome is advanced by one nucleotide into a new reading frame (Agranovsky et al., 1994).

Minus-one frameshifting, the most common frameshifting mechanism in plant viruses, generally requires specific primary RNA sequence, as well as secondary and/or tertiary structures. The primary sequence requirement is a slippery heptanucleotide sequence in the original reading frame of X_XXY_YYZ where X is any nucleotide, Y is adenine or uracil, and Z is adenine, uracil or cytosine (Firth and Brierley, 2012) When the ribosome reaches this sequence, the tRNAs present in the ribosome shift by one nucleotide backwards resulting in a near-cognate re-pairing between the anti-codon and new codon. Higher order RNA structures such as a pseudoknot, or a stem-loop downstream of the slippery sequence are also involved in promoting efficient -1 frameshifting (Garcia et al., 1993; Nixon et al., 2002; Lucchesi et al., 2000). In addition, a long-range RNA-RNA interaction between a higher order structure proximal to the frameshift site and distant downstream regions can be important. BYDV uses -1 frameshifting to control the production of the viral RdRp. In addition to the slippery heptanucleotide sequence of G_GGU_UUU, a large stem-loop structure five nucleotides downstream of the heptanucleotide sequence undergoes a long-range RNA-RNA interaction with the 3'UTR located ~4kb away (Barry and Miller, 2002). A similar long-range interaction is also required for frameshifting production of the RdRp in RCNMV (Tajima et al., 2011), and PEMV-2 (Gao and Simon, 2016).

In contrast to the abundance of -1 frameshifting examples in plant viruses, +1 frameshifting has only been suggested in plus-sense RNA plant viruses belonging to the *Closteroviridae* family (Agranovsky et al., 1994; Karasev et al., 1995). Similar to -1 frameshifting, +1 frameshifting also requires a run of slippery bases and RNA secondary

structure bordering this region. In the case of BYV, a slippery sequence of GGG_UUU followed by a UAG stop codon in combination with two stem-loops flanking the UAG stop codon are necessary to promote efficient +1 frameshifting (Agranovsky et al., 1994).

1.4.6.2 Translational Readthrough

In some plant viruses, the stop codon of a gene is "leaky" and ribosomes, at a low frequency, are able to decode the stop codon with a near cognate tRNA (**Figure 5G**). Translation elongation then continues in the original reading frame to produce a C-terminally extended protein. This process is mediated by competition between near cognate tRNAs and eukaryotic release factors during recognition of the stop codon. Readthrough is often used to produce viral RdRp replicase proteins (Firth and Brierley, 2012), however in *Luteoviruses*, *Benyviruses*, and *Pomoviruses* it is used to produce an extended coat protein product that is important for insect transmission (Brault et al., 1995; Chay et al., 1996).

The failure of release factors to recognize a stop codon often depends on the context of the stop codon. There are three distinct classes of RNA readthrough signals that use a unique mix of primary sequence, secondary structure, and tertiary structure. The consensus sequence for type I readthrough elements is a stop codon followed by CAR_YYA where R is a purine, and Y is a pyrimidine (**Figure 5G(i)**). TMV uses a type I readthrough context that consists of a UAG stop codon followed by a short local sequence of CAA_UUA (Skuzeski et al., 1991). Type II readthrough elements typically consist of a UGA stop codon followed by either CGG or CUA, with a large RNA stem-loop structure downstream of the stop codon that is important for promoting readthrough (**Figure 5G(ii)**) (Firth et al., 2011; Firth and Brierley, 2012). Some members of *Virgaviridae* use a type II readthrough element to produce their RdRp and, in some

cases, a C-terminally extended coat protein (Urban et al., 1996; Cowen et al., 1997; Firth et al., 2011).

Type III readthrough elements use a UAG stop codon followed by a guanine residue. They also involve an RNA secondary structure immediately following the stop codon known as the readthrough stem-loop (RTSL) (**Figure 5G(iii)**). In addition to the UAG_G stop codon context and RTSL, readthrough in the tombusvirid *Carnation Italian ringspot virus* (CIRV) requires a long-range interaction between the proximal readthrough element (PRTE), located in a bulge of the RTSL, and an area in the 3'UTR known as the distal readthrough element (DRTE). This interaction has been proposed to act as a regulatory switch to coordinate the opposing viral genome processes of 5'-to-3' translation and 3'-to-5' minus-stand synthesis (Cimino et al., 2011).

1.5 TNV-D Overview

Tobacco necrosis virus stain D (TNV-D) is a plus-sense ssRNA plant virus in the family *Tombusviridae*. *Tombusviridae* currently consists of 16 genera, whose grouping is primarily based on the relatedness of their viral RdRps (White, 2020). TNV-D is the type-member of the genus *Betanecrovirus*, which also includes *Beet black scorch virus* (BBSV) and *Leek white stripe virus* (LWSV) (Rochon et al., 2012). TNV-D is packaged into a T=3 iscosahedral capsid that is ~28nm in diameter (Cardoso et al., 2004). Transmission of TNV-D is mediated by the soil dwelling fungus *Olpidium brassicae*, which can infect the roots of several plant species, including tobacco, lettuce, mung beans, tulips, olive trees, citrus fruits, pears, apples, and grapevines (Kassanis and MacFarlane, 1964; Coutts et al., 1991; Cardoso et al., 2004).

1.5.1 Genome Organization

The genome of TNV-D is 3,763 nucleotides in length and encodes five ORFs (Coutts et al., 1991). The five open reading frames correspond to, from 5'-to-3', the viral replication proteins p22 and p82, movement proteins p7a and p7b, and coat protein, p29 (**Figure 6**). The 5' and 3'UTRs of TNV-D are 38 and 305 nucleotides long, respectively (Molnár et al., 1997) and contain RNA elements critical for viral processes, such as replication and translation.

1.5.2 Gene Expression Strategies

As with other members of *Tombusviridae*, TNV-D lacks both a 5'-cap and a 3'-polyadenylated tail. Instead translation initiation relies on a 3'CITE within the 3'UTR, specifically, a *Barley yellow dwarf virus*-like translational enhancer (BTE) (Shen and Miller, 2004). The BTE is required for efficient initiation of translation and recruits eIF4F through binding eIF4G via a conserved 17 nucleotide sequence, GGAUCCUGGGAAACAGG (Shen and Miller, 2004; Treder et al., 2008). In TNV-D the 3'CITE/eIFs complex is repositioned to the 5-end of the virus through an unknown mechanism (Chkuaseli et al., 2015), however in BYDV this occurs via a long-range RNA-RNA base pairing interaction between the 3'CITE and the 5'UTR (Guo et al., 2001).

Proteins that are produced directly from the full-length viral genome include a viral RNA replication accessory protein (p22), and the RdRp (p82) that is synthesized via readthrough of the p22 stop codon (**Figure 6**) (Molnár et al., 1997; Fang and Coutts, 2013). Similar to the tombusvirid CIRV, it is proposed that TNV-D also utilizes a type III readthrough element (Cimino et al., 2011). All members of *Tombusviridae*, with the exception of *Dianthoviruses*, are predicted to use readthrough to produce their RdRps (White, 2020).

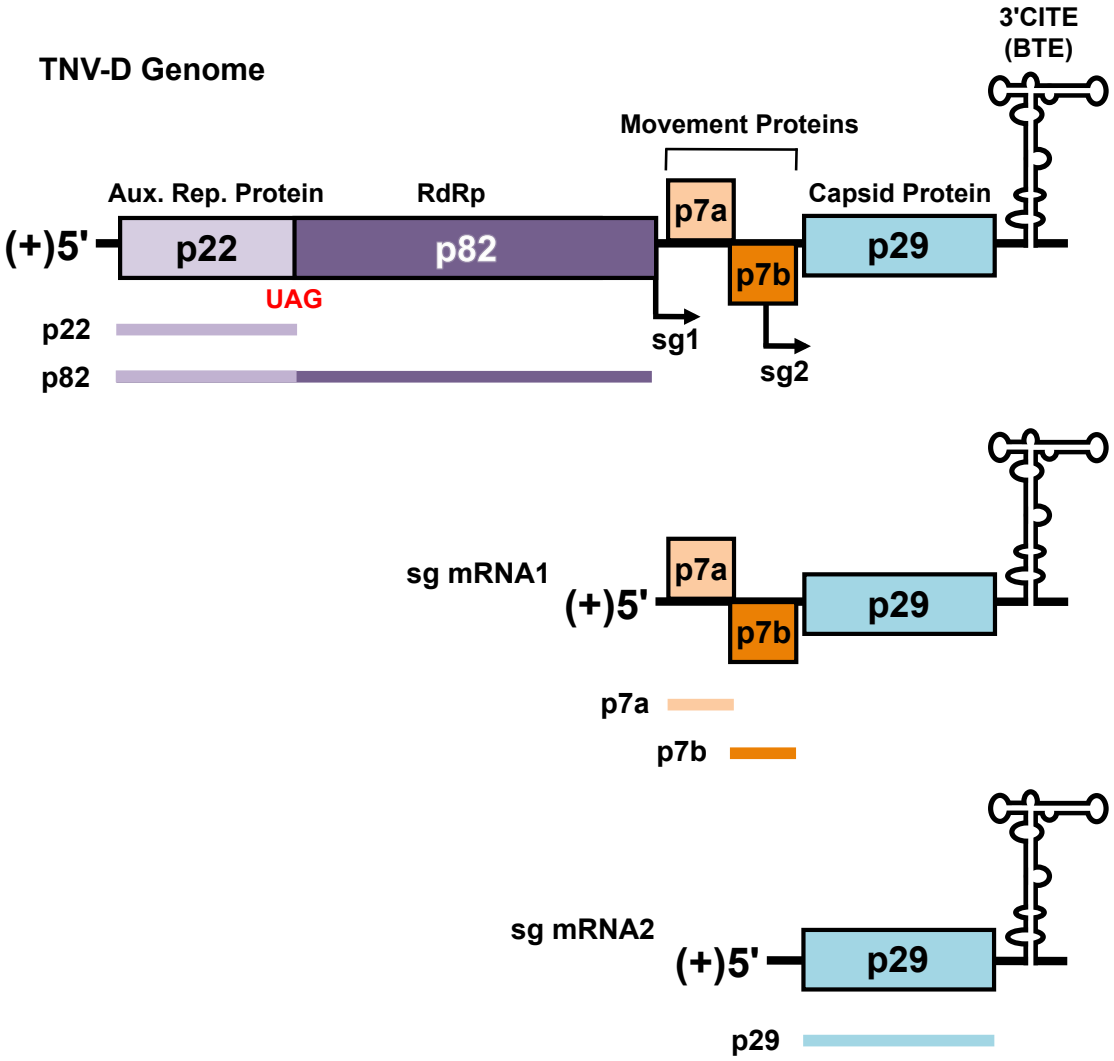

Figure 6. **Linear representation of the *Tobacco necrosis virus strain D* (TNV-D) RNA genome**. The black horizontal lines represent the plus-sense TNV-D RNA genome and subgenomic (sg) mRNAs. Transcription start sites of sg mRNAs are shown by arrows below the genome. The ORFs of the different viral proteins are colour-coded to correspond to their functions shown in **Figure 1**. Proteins translated from full length genomic TNV-D are the RNA-dependent RNA-polymerase (RdRp) associated protein p22, and the RdRp p82 (via readthrough). Movement proteins p7a and p7b are translated from sg mRNA1 (p7b via leaky scanning). The capsid protein p29 is translated from sg mRNA2.

The three proteins encoded downstream of the RdRp are translated from two sg mRNAs that are transcribed during infections (**Figure 6**). Several members of *Tombusviridae*, including TNV-D, utilize a premature termination mechanism to produce their sg mRNAs (Jiwan et al., 2011; Jiwan and White, 2011). In this process, an RNA structure, known as an attenuation structure, serves as a stop signal to the RdRp during minus-strand synthesis. This produces a truncated minus-strand RNA that contains a promoter at its 3'-end, which the RdRp uses to synthesize the plus-sense sg mRNA (White, 2002; Jiwan et al., 2011). Although recent evidence indicates that attenuation structures can be very complex and involve multiple long-range interactions, as in CIRV (Chkuaseli and White, 2020), the attenuation structures in TNV-D are believed to be localized and comparatively simple (Jiwan et al., 2011). The ~1.6 kb long sg mRNA1 of TNV-D encodes p7a and p7b, required for cell-to-cell movement, with the latter protein translated via leaky scanning (Offei et al., 1995; Molnár et al., 1997; Chkuaseli et al., 2015). Sg mRNA2 is ~1.3 kb and encodes p29, which in addition to being the viral capsid protein, is also required for systemic infection of host plants (Offei and Coutts, 1996; Molnár et al., 1997). The two sg mRNAs are 3'-co-terminal with the genome, and thus also contain the BTE that mediates their translation (**Figure 6**) (Coutts et al., 1991; Chkuaseli et al., 2015).

1.5.3 Viral Genome Replication

The study of replication elements within TNV-D is limited, however as members of *Tombusviridae* utilize a closely-related RdRp, their replication mechanisms likely share some similarities. TBSV is the type species of the *Tombusvirus* genus, and serves as a model for virus genome replication. Within the 3'UTR, tombusvirids requires two cis-acting RNA elements for replication and control of minus-strand synthesis (Panavas et al., 2002; Panaviene et al., 2005;

Fabian et al., 2003). SL1 is the core promoter for minus-strand synthesis, while an interaction between SL3 and the most 3'-end of the virus acts to modulate minus-strand synthesis and protect the 3'-end of the genome from 3'-to-5' exonuclease digestion (Panavas et al., 2002; Pogany et al., 2003; Panaviene et al., 2005; Fabian et al., 2003). Similar interactions between the 3'-end of the viral genome and internal regions also occur in other members of the *Tombusviridae* family, such as TCV (Zhang et al., 2004, Zhang et al., 2006), and TNV-D (Na and White, 2006).

TBSV also possesses an internal RNA element that is critical for efficient replication. The internal replication element (IRE), an extended stem-loop RNA structure containing a critical CC mismatch, is essential for RdRp template recognition and assembly of the viral replicase complex (Monkewich et al., 2005). The TBSV RdRp and accessory replication proteins bind to the IRE and recruit the genomic RNA to peroxisomal membranes, where genome replication occurs (Pogany et al., 2005). A sequence just 3' to the IRE (termed the upstream linker, UL) is complementary to a sequence within the 3'UTR of the TBSV genome (downstream linker, DL) and base pairing of these sequences is essential for genome replication (Wu et al., 2009). This interaction unites the IRE with the other RNA replication elements in the 3'UTR and positions the IRE-bound RdRp proximal to the 3'-end of the genome (Wu et al., 2009). Interestingly other tombusvirids, including TNV-D, have been proposed to contain IRE counterparts (Nicholson et al., 2012; Newburn and White, 2020), however these elements remain to be investigated further.

1.6 Project Purpose

Plus-sense RNA plant viruses, like TNV-D, must translate a virally encoded RdRp from the infecting viral genomic RNA. The RdRp is critical for the establishment and spread of a viral infection by (i) synthesizing progeny viral genomes, and (ii) transcribing sg mRNAs. Often,

recoding events such as readthrough are used to express the RdRp, therefore, the analysis of readthrough regulation is important for understanding viral infection and may aid in the characterization of readthrough elements involved in other viruses.

The goal of my research was to investigate the mechanism of RdRp production in TNV-D via readthrough using *in vitro* and *in vivo* approaches. This objective was accomplished in a series of three studies, which are presented as publications that corresponding to three chapters of this dissertation. The **specific objectives** related to each chapter/publication are listed below:

(1) Functional characterization of the core RNA elements involved in readthrough production of the RdRp (**Chapter 2**).

(2) Analysis of the RNA elements proximal to the core RNA elements that influence readthrough efficiency (**Chapter 3**).

(3) Investigation of the structures and sequences in the 3'UTR of the TNV-D genome that affect readthrough and virus accumulation (**Chapter 4**).

The overall results of this study revealed that readthrough in TNV-D is a complex process involving diverse RNA structures and interactions. The findings suggest a multifaceted regulatory mechanism in which distant regions of the genome function cooperatively to regulate the essential process of translational readthrough. The mechanism and its implications are discussed further in concluding **Chapter 5**, along with possible future directions for this research.

1.7 References

Acheson NH. 2011. *Fundamentals of Molecular Virology*. 2nd Edition. John Wiley & Sons, Inc. New Jersey.

Acker MG, Shin BS, Dever TE, Lorsch JR. 2006. Interaction between Eukaryotic Initiation Factors 1A and 5B is Required for Efficient Ribosomal Subunit Joining. *J Biol Chem*. **281**(13): 8469-75. doi: 10.1074/jbc.M600210200.

Acker MG, Shin BS, Nanda JS, Saini AK, Dever TE, Lorsch JR. 2009. Kinetic analysis of late steps of eukaryotic translation initiation. *J Mol Biol*. **385**(2): 491-506. doi:10.1016/j.jmb.2008.10.029

Agranovsky AA, Koonin EV, Boyko VP, Maiss E, Frötschl R, Lunina NA, Atabekov JG. 1994. Beet Yellows Closterovirus: Complete Genome Structure and Identification of a Leader Papain-like Thiol Protease. *Virology*. **198**(1): 311-24. doi: 10.1006/viro.1994.1034.

Alam SB, Rochon D. 2017. Evidence that Hsc70 Is Associated with Cucumber Necrosis Virus Particles and Plays a Role in Particle Disassembly. *J Virol*. **91**(2): e01555-16. doi:10.1128/JVI.01555-16.

Algire MA, Maag D, Lorsch JR. 2005. P_i Release from eIF2, Not GTP Hydrolysis, Is the Step Controlled by Start-Site Selection during Eukaryotic Translation Initiation. *Mol Cell*. **20**(2): 251-62. doi: 10.1016/j.molcel.2005.09.008.

Alkalaeva EZ, Pisarev AV, Frolova LY, Kisselev LL, Pestova TV. 2006. In Vitro Reconstitution of Eukaryotic Translation Reveals Cooperativity between Release Factors eRF1 and eRF3. *Cell*. **125**(6): 1125-36. doi: 10.1016/j.cell.2006.04.035.

Barry JK, Miller WA. 2002. A -1 ribosomal frameshift element that requires base pairing across four kilobases suggests a mechanism of regulating ribosome and replicase traffic on a viral RNA. *Proc Natl Acad Sci USA*. **99**(17): 11133-8. doi: 10.1073/pnas.162223099.

Basnayake VR, Sit TL, Lommel SA. 2006. The genomic RNA packaging scheme of *Red clover necrotic mosaic virus*. *Virology*. **345**(2): 532-9. doi: 10.1016/j.virol.2005.10.017.

Brault V, Miller WA. 1992. Translational frameshifting mediated by a viral sequence in plant cells. *Proc Natl Acad Sci USA*. **89**(6):2262-6. doi: 10.1073/pnas.89.6.2262.

Brault V, van den Heuvel JF, Verbeek M, Ziegler-Graff V, Reutenauer A, Herrbach E, Garaud JC, Guilley H, Richards K, Jonard G. 1995. Aphid transmission of beet western yellows luteovirus requires the minor capsid read-through protein P74. *EMBO J*. **14**(4): 650-9.

Brown A, Shao S, Murray J, Hegde RS, Ramakrishnan V. 2015. Structural basis for stop codon recognition in eukaryotes. *Nature*. **524**(7566): 493-496. doi: 10.1038/nature14896.

Buck KW. 1999. Replication of tobacco mosaic virus RNA. *Philos Trans R Soc Lond B Biol Sci*. **354**(1383): 613-627. doi:10.1098/rstb.1999.0413.

Bulygin KN, Khairulina YS, Kolosov PM, Ven'yaminova AG, Graifer DM, Vorobjev YN, Frolova LY, Kisselev LL, Karpova GG. 2010. Three distinct peptides from the N domain of translation termination factor eRF1 surround stop codon in the ribosome. *RNA*. **16**(10): 1902-14. doi: 10.1261/rna.2066910.

Bustamante PI, Hull R. 1998. Plant virus gene expression strategies. *Electron J Biotechnol.* **1**(2): 65-82.

Cardoso JM, Félix MR, Oliveira S, Clara MI. 2004. A *Tobacco necrosis virus D* isolate from *Olea europaea* L.: viral characterization and coat protein sequence analysis. *Arch Virol*. **149**(6): 1129-38. doi: 10.1007/s00705-003-0258-7.

Carroll TW. 1972. Seed Transmissibility of Two Strains of Barley Stripe Mosaic Virus. *Virology*. **48**(2):323-36. doi: 10.1016/0042-6822(72)90043-8.

Chavatte L, Seit-Nebi A, Dubovaya V, Favre A. 2002. The invariant uridine of stop codons contacts the conserved NIKSR loop of human eRF1 in the ribosome. *EMBO J*. **21**(19): 5302-11. doi: 10.1093/emboj/cdf484.

Chay CA, Gunasinge UB, Dinesh-Kumar SP, Miller WA, Gray SM. 1996. Aphid Transmission and Systemic Plant Infection Determinants of Barley Yellow Dwarf Luteovirus-PAV are Contained in the Coat Protein Readthrough Domain and 17-kDa Protein, Respectively. *Virology*. **219**(1): 57-65. doi: 10.1006/viro.1996.0222.

Chkuaseli T, Newburn LR, Bakhshinyan D, White KA. 2015. Protein expression strategies in Tobacco necrosis virus-D. *Virology*. **486**: 54-62. doi: 10.1016/j.virol.2015.08.032.

Chkuaseli T, White KA. 2020. Activation of viral transcription by stepwise largescale folding of an RNA virus genome. *Nucleic Acids Res.* **48**(16): 9285-9300. doi: 10.1093/nar/gkaa675.

Cimino PA, Nicholson BL, Wu B, Xu W, White KA. 2011. Multifaceted Regulation of Translational Readthrough by RNA Replication Elements in a Tombusvirus. *PLoS Pathog*. **7**(12): e1002423. doi: 10.1371/journal.ppat.1002423.

Choi YG, Dreher TW, Rao AL. 2002. tRNA elements mediate the assembly of an icosahedral RNA virus. *Proc Natl Acad Sci USA*. **99**(2): 655-60. doi: 10.1073/pnas.022618199.

Choi YG, Rao AL. 2003. Packaging of Brome Mosaic Virus RNA3 Is Mediated through a Bipartite Signal. *J Virol*. **77**(18): 9750-7. doi: 10.1128/jvi.77.18.9750-9757.2003.

Choi IR, White KA. 2002. An RNA Activator of Subgenomic mRNA1 Transcription in Tomato Bushy Stunt Virus. *J Biol Chem*. **277**(5): 3760-6. doi: 10.1074/jbc.M109067200.

Coutts RHA, Rigden JE, Slabas AR, Lomonossoff GP, Wise PJ. 1991. The complete nucleotide sequence of tobacco necrosis virus strain D. *J Gen Virol*. **72**(Pt 7): 1521-9. doi: 10.1099/0022-1317-72-7-1521.

Cowan GH, Torrance L, Reavy B. 1997. Detection of potato mop-top virus capsid readthrough protein in virus particles. *J Gen Virol*. **78** (Pt 7): 1779-83. doi: 10.1099/0022-1317-78-7-1779.

Dever TE, Dinman JD, Green R. 2018. Translation Elongation and Recoding in Eukaryotes. *Cold Spring Harb Perspect Biol.* **10**(8): a032649. doi: 10.1101/cshperspect.a032649.

Dreher TW, Miller WA. 2006. Translational control in positive strand RNA plant viruses. *Virology*. **344**(1): 185-97. doi: 10.1016/j.virol.2005.09.031.

Fabian MR, Na H, Ray D, White KA. 2003. 3'-Terminal RNA secondary structures are important for accumulation of tomato bushy stunt virus DI RNAs. *Virology*. **313**(2): 567-80. doi: 10.1016/s0042-6822(03)00349-0

Fabian MR, White KA. 2004. 5'-3' RNA-RNA Interaction Facilitates Cap- and Poly(A) Tail-Independent Translation of Tomato Bushy Stunt Virus mRNA: A Potential Common Mechanism for Tombusviridae. *J Biol Chem.* **279**(28): 28862-28872. doi: 10.1074/jbc.M401272200.

Fabian MR, White KA. 2006. Analysis of a 3'-translation enhancer in a tombusvirus: a dynamic model for RNA-RNA interactions of mRNA termini. *RNA*. **12**(7): 1304-1314. doi: 10.1261/rna.69506.

Fang L, Coutts RHA. 2013. Investigations on the *Tobacco Necrosis Virus D* p60 Replicase Protein. *PLoS One*. **8**(11): e80912. doi: 10.1371/journal.pone.0080912.

Fernández-Miragall O, Hernández C. 2011. An Internal Ribosome Entry Site Directs Translation of the 3'-Gene from *Pelargonium Flower Break Virus* Genomic RNA: Implications for Infectivity. *PLoS One*. **6**(7): e22617. doi: 10.1371/journal.pone.0022617.

Firth AE, Brierley I. 2012. Non-canonical translation in RNA viruses. *J Gen Virol*. 93(Pt 7): 1385-1409. doi: 10.1099/vir.0.042499-0.

Firth AE, Wills NM, Gesteland RF, Atkins JF. 2011. Stimulation of stop codon readthrough: frequent presence of an extended 3' RNA structural element. *Nucleic Acids Res*. **39**(15): 6679-91. doi: 10.1093/nar/gkr224.

Frolova L, Seit-Nebi A, Kisselev L. 2002. Highly conserved NIKS tetrapeptide is functionally essential in eukaryotic translation termination factor eRF1. *RNA*. **8**(2): 129-36. doi: 10.1017/s1355838202013262.

Frolova LY, Tsivkovskii RY, Sivolobova GF, Oparina NY, Serpinsky OI, Blinov VM, Tatkov SI, Kisselev LL. 1999. Mutations in the highly conserved GGQ motif of class 1 polypeptide release factors abolish ability of human eRF1 to trigger peptidyl-tRNA hydrolysis. *RNA*. **5**(8): 1014-20. doi: 10.1017/s135583829999043x.

Gallie DR. 1998. A tale of two termini: a functional interaction between the termini of an mRNA is a prerequisite for efficient translation initiation. *Gene*. **216**(1): 1-11. doi: 10.1016/s0378-1119(98)00318-7.

Gao F, Simon AE. 2016. Multiple Cis-acting elements modulate programmed -1 ribosomal frameshifting in Pea enation mosaic virus. *Nucleic Acids Res*. **44**(2): 878-95. doi: 10.1093/nar/gkv1241.

Garcia A, van Duin J, Pleij CW. 1993. Differential response to frameshift signals in eukaryotic and prokaryotic translational systems. *Nucleic Acids Res*. **21**(3): 401-6. doi: 10.1093/nar/21.3.401.

Gingras AC, Raught B, Sonenberg N. 1999. eIF4 Initiation Factors: Effectors of mRNA Recruitment to Ribosomes and Regulators of Translation. *Annu Rev Biochem*. **68**: 913-63. doi: 10.1146/annurev.biochem.68.1.913.

Guo L, Allen EM, Miller WA. 2001. Base-Pairing between Untranslated Regions Facilitates Translation of Uncapped, Nonpolyadenylated Viral RNA. *Mol Cell*. **7**(5): 1103-9. doi: 10.1016/s1097-2765(01)00252-0.

Hellen CUT. 2018. Translation Termination and Ribosome Recycling in Eukaryotes. *Cold Spring Harb Perspect Biol*. **10**(10):a032656. doi: 10.1101/cshperspect.a032656.

Hinnebusch AG. 2014 The Scanning Mechanism of Eukaryotic Translation Initiation. *Annu Rev Biochem*. **83**: 779-812. doi: 10.1146/annurev-biochem-060713-035802.

Hipper C, Brault V, Ziegler-Graff V, Revers F. 2013. Viral and cellular factors involved in phloem transport of plant viruses. *Front Plant Sci*. **4**: 154. doi: 10.3389/fpls.2013.00154.

Hull R. 2002. Introduction. In: *Matthews' Plant Virology*. 4th Edition. Academic Press. New York, pp. 1-12. doi:10.1016/b978-012361160-4/50052-9.

Jaag HM, Kawchuk L, Rohde W, Fischer R, Emans N, Prüfer D. 2003. An unusual internal ribosomal entry site of inverted symmetry directs expression of a potato leafroll polerovirus replication-associated protein. *Proc Natl Acad Sci USA*. **100**(15): 8939-44. doi: 10.1073/pnas.1332697100.

Jakubiec A, Drugeon G, Camborde L, Jupin I. 2007. Proteolytic Processing of *Turnip Yellow Mosaic Virus* Replication Proteins and Functional Impact on Infectivity. *J Virol*. **81**(20): 11402-12. doi: 10.1128/JVI.01428-07.

Jiwan SD, White KA. 2011. Subgenomic mRNA transcription in Tombusviridae. *RNA Biol*. **8**(2): 287-94. doi: 10.4161/rna.8.2.15195.

Jiwan SD, Wu B, White KA. 2011. Subgenomic mRNA transcription in tobacco necrosis virus. *Virology*. **418**(1): 1-11. doi: 10.1016/j.virol.2011.07.005.

Johnston JC, Rochon DM. 1996. Both Codon Context and Leader Length Contribute to Efficient Expression of Two Overlapping Open Reading Frames of a Cucumber Necrosis Virus Bifunctional Subgenomic mRNA. *Virology*. **221**(1): 232-9. doi: 10.1006/viro.1996.0370.

Joshi CP, Zhou H, Huang X, Chiang VL. 1997. Context sequences of translation initiation codon in plants. *Plant Mol Biol*. **35**(6): 993-1001. doi: 10.1023/a:1005816823636.

Karasev AV, Boyko VP, Gowda S, Nikolaeva OV, Hilf ME, Koonin EV, Niblett CL, Cline K, Gumpf DJ, Lee RF, Garnsey SM, Fwandowski DJI, Dawson WO. 1995. Complete Sequence of the Citrus Tristeza Virus RNA Genome. *Virology*. **208**(2): 511-20. doi: 10.1006/viro.1995.1182.

Koh DC, Wong SM, Liu DX. 2003. Synergism of the 3'-Untranslated Region and an Internal Ribosome Entry Site Differentially Enhances the Translation of a Plant Virus Coat Protein. *J Biol Chem*. **278**(23): 20565-73. doi: 10.1074/jbc.M210212200.

Kolosov P, Frolova L, Seit-Nebi A, Dubovaya V, Kononenko A, Oparina N, Justesen J, Efimov A, Kisselev L. 2005. Invariant amino acids essential for decoding function of polypeptide release factor eRF1. *Nucleic Acids Res*. **33**(19): 6418-25. doi: 10.1093/nar/gki927.

Korneeva NL, Lamphear BJ, Hennigan FL, Rhoads RE. 2000 Mutually Cooperative Binding of Eukaryotic Translation Initiation Factor (eIF) 3 and eIF4A to Human eIF4G-1. *J Biol Chem*. **275**(52): 41369-76. doi: 10.1074/jbc.M007525200.

Kozak M. 1987. An analysis of 5'-noncoding sequences from 699 vertebrate messenger RNAs. *Nucleic Acids Res*. **15**(20): 8125-48. doi: 10.1093/nar/15.20.8125.

Kwon SJ, Park MR, Kim KW, Plante CA, Hemenway CL, Kim KH. 2005. *cis*-Acting sequences required for coat protein binding and in vitro assembly of *Potato virus X*. *Virology*. **334**(1): 83-97. doi: 10.1016/j.virol.2005.01.018.

Leathers V, Tanguay R, Kobayashi M, Gallie DR. 1993. A Phylogenetically Conserved Sequence within Viral 3' Untranslated RNA Pseudoknots Regulates Translation. *Mol Cell Biol*. **13**(9): 5331-47. doi: 10.1128/mcb.13.9.5331.

Lee JY, Lu H. 2011. Plasmodesmata: the battleground against intruders. *Trends Plant Sci*. **16**(4): 201-10. doi: 10.1016/j.tplants.2011.01.004.

LeFebvre AK, Korneeva NL, Trutschl M, Cvek U, Duzan RD, Bradley CA, Hershey JW, Rhoads RE. 2006. Translation Initiation Factor eIF4G-1 Binds to eIF3 through the eIF3e Subunit. *J Biol Chem*. **281**(32): 22917-32. doi: 10.1074/jbc.M605418200.

Lucchesi J, Mäkeläinen K, Merits A, Tamm T, Mäkinen K. 2000. Regulation of -1 ribosomal frameshifting directed by Cocksfoot mottle sobemovirus genome. *Eur J Biochem*. **267**(12): 3523-9. doi: 10.1046/j.1432-1327.2000.01379.x.

Kassanis B, MacFarlane I. 1964. Transmission of Tobacco Necrosis Virus by Zoospores of *Olpidium brassicae*. *J Gen Microbiol*. **36**: 79-93. doi: 10.1099/00221287-36-1-79.

Marcotrigiano J, Gingras AC, Sonenberg N, Burley SK. 1997. Cocrystal Structure of the Messenger RNA 5' Cap-Binding Protein (eIF4E) Bound to 7-methyl-GDP. *Cell*. **89**(6): 951-61. doi: 10.1016/s0092-8674(00)80280-9.

Matsuo H, Li H, McGuire AM, Fletcher CM, Gingras AC, Sonenberg N, Wagner G. 1997. Structure of translation factor eIF4E bound to m^7GDP and interaction with 4E-binding protein. *Nat Struct Biol*. **4**(9): 717-24. doi: 10.1038/nsb0997-717.

May J, Johnson P, Saleem H, Simon AE. 2017. A Sequence-Independent, Unstructured Internal Ribosome Entry Site Is Responsible for Internal Expression of the Coat Protein of *Turnip Crinkle Virus*. *J Virol*. **91**(8): e02421-16. doi: 10.1128/JVI.02421-16.

McLean MA, Campbell RN, Hamilton RI, Rochon DM. 1994. Involvement of the Cucumber Necrosis Virus Coat Protein in the Specificity of Fungus Transmission by *Olpidium bornovanus*. *Virology*. **204**(2): 840-2. doi: 10.1006/viro.1994.1604.

Miller WA, White KA. 2006. Long-Distance RNA-RNA Interactions in Plant Virus Gene Expression and Replication. *Annu Rev Phytopathol*. **44**: 447-67. doi: 10.1146/annurev.phyto.44.070505.143353.

Molnár A, Havelda Z, Dalmay T, Szutorisz H, Burgyán J. 1997. Complete nucleotide sequence of tobacco necrosis virus strain D^H and genes required for RNA replication and virus movement. *J Gen Virol*. 78(Pt 6): 1235-9. doi: 10.1099/0022-1317-78-6-1235.

Monkewich S, Lin HX, Fabian MR, Xu W, Na H, Ray D, Chernysheva OA, Nagy PD, White KA. 2005. The p92 Polymerase Coding Region Contains an Internal RNA Element Required at an Early Step in Tombusvirus Genome Replication. *J Virol*. **79**(8): 4848-58. doi: 10.1128/JVI.79.8.4848-4858.2005.

Na H, White KA. 2006. Structure and prevalence of replication silencer-3' terminus RNA interactions in Tombusviridae. Virology. 2006 Feb 20;345(2):305-16. doi: 10.1016/j.virol.2005.09.008. Epub 2005 Nov 18. PMID: 16298411.

Newburn LR, White KA. 2020. A *trans*-activator-like structure in RCNMV RNA1 evokes the origin of the *trans*-activator in RNA2. *PLoS Pathog*. **16**(1): e1008271. doi: 10.1371/journal.ppat.1008271.

Nicholson BL, Lee PK, White KA. 2012. Internal RNA replication elements are prevalent in *Tombusviridae*. *Front Microbiol*. **3**: 279. doi: 10.3389/fmicb.2012.00279.

Nicholson BL, Wu B, Chevtchenko I, White KA. 2010. Tombusvirus recruitment of host translational machinery via the 3' UTR. *RNA*. **16**(7): 1402-1419. doi: 10.1261/rna.2135210.

Nixon PL, Rangan A, Kim YG, Rich A, Hoffman DW, Hennig M, Giedroc DP. 2002. Solution Structure of a Luteoviral P1-P2 Frameshifting mRNA Pseudoknot. *J Mol Biol*. **322**(3): 621-33. doi: 10.1016/s0022-2836(02)00779-9.

Offei SK, Coffin RS, Coutts RHA. 1995. The tobacco necrosis virus p7a protein is a nucleic acid-binding protein. *J Gen Virol*. **76**(Pt 6): 1493-6. doi: 10.1099/0022-1317-76-6-1493.

Offei SK, Coutts RHA. 1996. Location of the 5′ Termini of Tobacco Necrosis Virus Strain D Subgenomic mRNAs. *J Phytopathol*. **144**: 13-17. doi: 10.1111/j.1439-0434.1996.tb01481.x.

Panavas T, Pogany J, Nagy PD. 2002. Analysis of Minimal Promoter Sequences for Plus-Strand Synthesis by the *Cucumber necrosis virus* RNA-Dependent RNA Polymerase. *Virology*. **296**(2): 263-74. doi: 10.1006/viro.2002.1423.

Panaviene Z, Panavas T, Nagy PD. 2005. Role of an Internal and Two 3'-Terminal RNA Elements in Assembly of Tombusvirus Replicase. *J Virol*. **79**(16): 10608-18. doi: 10.1128/JVI.79.16.10608-10618.2005.

Passmore LA, Schmeing TM, Maag D, Applefield DJ, Acker MG, Algire MA, Lorsch JR, Ramakrishnan V. 2007. The Eukaryotic Translation Initiation Factors eIF1 and eIF1A Induce an Open Conformation of the 40S Ribosome. *Mol Cell*. **26**(1):41-50. doi: 10.1016/j.molcel.2007.03.018.

Patil BL. 2020. Plant Viral Diseases: Economic Implications. In: *Reference Module in Life Sciences*. doi: 10.1016/b978-0-12-809633-8.21307-1.

Paulin FE, Campbell LE, O'Brien K, Loughlin J, Proud CG. 2001. Eukaryotic translation initiation factor 5 (eIF5) acts as a classical GTPase-activator protein. *Curr Biol*. **11**(1): 55-9. doi: 10.1016/s0960-9822(00)00025-7.

Pestova TV, Kolupaeva VG. 2002 The roles of individual eukaryotic translation initiation factors in ribosomal scanning and initiation codon selection. *Genes Dev*. **16**(22): 2906-22. doi: 10.1101/gad.1020902.

Pestova TV, Lomakin IB, Lee JH, Choi SK, Dever TE, Hellen CU. 2000. The joining of ribosomal subunits in eukaryotes requires eIF5B. *Nature*. **403**(6767): 332-5. doi: 10.1038/35002118.

Pisarev AV, Hellen CU, Pestova TV. 2007. Recycling of eukaryotic post-termination ribosomal complexes. *Cell*. **131**(2): 286-99. doi: 10.1016/j.cell.2007.08.041.

Pisarev AV, Skabkin MA, Pisareva VP, Skabkina OV, Rakotondrafara AM, Hentze MW, Hellen CU, Pestova TV. 2010. The role of ABCE1 in eukaryotic post-termination ribosomal recycling. *Mol Cell*. **37**(2): 196-210. doi: 10.1016/j.molcel.2009.12.034.

Pogany J, Fabian MR, White KA, Nagy PD. 2003. A replication silencer element in a plus-strand RNA virus. *EMBO J*. **22**(20): 5602-11. doi: 10.1093/emboj/cdg523.

Pogany J, White KA, Nagy PD. 2005. Specific Binding of Tombusvirus Replication Protein p33 to an Internal Replication Element in the Viral RNA is Essential for Replication. *J Virol*. **79**(8): 4859-69. doi: 10.1128/JVI.79.8.4859-4869.2005.

Preis A, Heuer A, Barrio-Garcia C, Hauser A, Eyler DE, Berninghausen O, Green R, Becker T, Beckmann R. 2014. Cryoelectron Microscopic Structures of Eukaryotic Translation Termination Complexes Containing eRF1-eRF3 or eRF1-ABCE1. *Cell Rep*. **8**(1): 59-65. doi: 10.1016/j.celrep.2014.04.058.

Puurand Ü, Mäkinen K, Paulin L, Saarma M. 1994. The nucleotide sequence of potato virus A genomic RNA and its sequence similarities with other potyviruses. *J Gen Virol*. **75**(2): 457-61. doi: 10.1099/0022-1317-75-2-457.

Qu F, Morris TJ. 1997. Encapsidation of Turnip Crinkle Virus Is Defined by a Specific Packaging Signal and RNA Size. *J Virol*. **71**(2): 1428-1435. doi:10.1128/JVI.71.2.1428-1435.1997.

Rao ALN. 2006. Genome Packaging by Spherical Plant RNA Viruses. *Annu Rev Phytopathol*. **44**(1): 61-87. doi: 10.1146/annurev.phyto.44.070505.143334.

Roberts AG. 2014. Plant Viruses: Soil-borne. In: *eLS*. John Wiley & Sons, Ltd: Chichester. doi: 10.1002/9780470015902.a0000761.pub3.

Roberts AG, Cruz SS, Roberts IM, Prior D, Turgeon R, Oparka KJ. 1997. Phloem Unloading in Sink Leaves of *Nicotiana benthamiana*: Comparison of a Fluorescent Solute with a Fluorescent Virus. *Plant Cell*. **9**(8): 1381-1396. doi: 10.1105/tpc.9.8.1381.

Rochon D, Lommel SA, Martelli GP, Rubino L, Russo M. 2012. Tombusviridae. In: King, A.M.Q.; Adams M.J., Carstens E.B., Lefkowitz E.J., (Eds.).*Virus Taxonomy, Ninth Report of the International Committee on Taxonomy of Viruses*, *Elsevier*. Academic Press, London, pp. 1111–1138.

Rogers GW Jr, Richter NJ, Lima WF, Merrick WC. 2001. Modulation of the Helicase Activity of eIF4A by eIF4B, eIF4H, and eIF4F. *J Biol Chem*. **276**(33): 30914-22. doi: 10.1074/jbc.M100157200.

Rozovsky N, Butterworth AC, Moore MJ. 2008. Interactions between eIF4AI and its accessory factors eIF4B and eIF4H. *RNA*. **14**(10): 2136-48. doi: 10.1261/rna.1049608.

Scholthof HB, Desvoyes B, Kuecker J, Whitehead E. 1999. Biological Activity of Two Tombusvirus Proteins Translated from Nested Genes Is Influenced by Dosage Control via Context-Dependent Leaky Scanning. *Mol Plant-Microbe Interact*. **12**(8): 670–679. doi: 10.1094/MPMI.1999.12.8.670.

Schuller AP, Green R. 2018. Roadblocks and resolutions in eukaryotic translation. *Nat Rev Mol Cell Biol*. **19**(8): 526-541. doi: 10.1038/s41580-018-0011-4.

Shen R, Miller WA. 2004. The 3' Untranslated Region of Tobacco Necrosis Virus RNA Contains a Barley Yellow Dwarf Virus-Like Cap-Independent Translation Element. *J Virol*. **78**(9): 4655-64. doi: 10.1128/jvi.78.9.4655-4664.2004.

Skuzeski JM, Nichols LM, Gesteland RF, Atkins JF. 1991. The Signal for a Leaky UAG Stop Codon in Several Plant Viruses includes the Two Downstream Codons. *J Mol Biol*. **218**(2): 365-73. doi: 10.1016/0022-2836(91)90718-l.

Sonenberg N, Shatkin AJ, Ricciardi RP, Rubin M, Goodman RM. 1978. Analysis of terminal structures of RNA from potato virus X. *Nucleic Acids Res*. **5**(7): 2501-12. doi: 10.1093/nar/5.7.2501.

Song H, Mugnier P, Das AK, Webb HM, Evans DR, Tuite MF, Hemmings BA, Barford D. 2000. The Crystal Structure of Human Eukaryotic Release Factor eRF1–Mechanism of Stop Codon Recognition and Peptidyl-tRNA Hydrolysis. *Cell*. **100**(3): 311-21. doi: 10.1016/s0092-8674(00)80667-4.

Tajima Y, Iwakawa HO, Kaido M, Mise K, Okuno T. 2011. A long-distance RNA-RNA interaction plays an important role in programmed -1 ribosomal frameshifting in the translation of p88 replicase protein of *Red clover necrotic mosaic virus*. *Virology*. **417**(1): 169-78. doi: 10.1016/j.virol.2011.05.012.

Thiébeauld O, Pooggin MM, Ryabova LA. 2007. Alternative translation strategies in plant viruses. *Plant Viruses*. **1(1):** 1-20.

Treder K, Kneller EL, Allen EM, Wang Z, Browning KS, Miller WA. 2008. The 3' cap-independent translation element of Barley yellow dwarf virus binds eIF4F via the eIF4G subunit to initiate translation. *RNA*. **14**(1): 134-47. doi: 10.1261/rna.777308.

Unbehaun A, Borukhov SI, Hellen CU, Pestova TV. 2004. Release of initiation factors from 48S complexes during ribosomal subunit joining and the link between establishment of codon-anticodon base-pairing and hydrolysis of eIF2-bound GTP. *Genes Dev*. **18**(24): 3078-93. doi: 10.1101/gad.1255704.

Urban C, Zerfass K, Fingerhut C, Beier H. 1996. UGA suppression by $tRNA^{Trp}_{CmCA}$ occurs in diverse virus RNAs due to a limited influence of the codon context. *Nucleic Acids Res*. **24**(17): 3424-30. doi: 10.1093/nar/24.17.3424.

Valášek LS, Zeman J, Wagner S, Beznosková P, Pavlíková Z, Mohammad MP, Hronová V, Herrmannová A, Hashem Y, Gunišová S. 2017. Embraced by eIF3: structural and functional insights into the roles of eIF3 across the translation cycle. *Nucleic Acids Res*. **45**(19): 10948-10968. doi: 10.1093/nar/gkx805.

Vassilenko KS, Alekhina OM, Dmitriev SE, Shatsky IN, Spirin AS. 2011. Unidirectional constant rate motion of the ribosomal scanning particle during eukaryotic translation initiation. *Nucleic Acids Res*. **39**(13): 5555-67. doi: 10.1093/nar/gkr147.

White KA. 2002. The Premature Termination Model: A Possible Third Mechanism for Subgenomic mRNA Transcription in (+)-Strand RNA Viruses. *Virology*. **304**(2): 147-54. doi: 10.1006/viro.2002.1732.

White KA. 2020. Tombusvius-Like Viruses (Tombusviridae). In: *Reference Module in Life Sciences, Elsevier.* doi: 10.1016/B978-0-12-809633-8.21260-0.

Wong LE, Li Y, Pillay S, Frolova L, Pervushin K. 2012. Selectivity of stop codon recognition in translation termination is modulated by multiple conformations of GTS loop in eRF1. *Nucleic Acids Res*. **40**(12): 5751-65. doi: 10.1093/nar/gks192.

Wu B, Pogany J, Na H, Nicholson BL, Nagy PD, White KA. 2009. A Discontinuous RNA Platform Mediates RNA Virus Replication: Building an Integrated Model for RNA-based Regulation of Viral Processes. *PLoS Pathog*. **5**(3): e1000323. doi: 10.1371/journal.ppat.1000323.

Xiong Z, Kim KH, Kendall TL, Lommel SA. 1993. Synthesis of the Putative Red Clover Necrotic Mosaic Virus RNA Polymerase by Ribosomal Frameshifting *in Vitro*. *Virology*. **193**(1): 213-21. doi: 10.1006/viro.1993.1117.

Zhang J, Roberts R, Rakotondrafara AM. 2015. The role of the 5' untranslated regions of *Potyviridae* in translation. *Virus Res*. **206**: 74-81. doi: 10.1016/j.virusres.2015.02.005.

Zhang J, Zhang G, Guo R, Shapiro BA, Simon AE. 2006. A Pseudoknot in a Preactive Form of a Viral RNA is Part of a Structural Switch Activating Minus-Strand Synthesis. *J Virol*. **80**(18):9181-91. doi: 10.1128/JVI.00295-06..

Zhang G, Zhang J, Simon AE. 2004. Repression and Derepression of Minus-Strand Synthesis in a Plus-Strand RNA Virus Replicon. *J Virol*. **78**(14): 7619-33. doi: 10.1128/JVI.78.14.7619-7633.2004.

Ziegler-Graff V. 2020. Molecular Insights into Host and Vector Manipulation by Plant Viruses. *Viruses*. **12**(3): 263. doi: 10.3390/v12030263.

CHAPTER 2

Translational readthrough in Tobacco necrosis virus-D

TNV-D produces its RdRp via readthrough of the p22 stop codon. A previous readthrough investigation in a related virus indicated that a long-range RNA-RNA interaction between the PRTE and DRTE was critical for readthrough. A similar interaction was predicted to occur in TNV-D. This study has confirmed the necessity of the PRTE-DRTE interaction in TNV-D, confirming the use of type III readthrough. Additionally this study has characterized the importance of the lower stem of the RTSL, stop codon identity, and lack of interchangeability with other readthrough or frameshifting elements.

This chapter is presented as a research article published in *Virology* (Newburn et al., 2014). For this article, Dr. Beth Nicholson and Dr. K. Andrew White designed the investigation, and I performed approximately 50% of the experiments (Figure 3C, Figure 4, Figure 5, and Figure 6A-C), analyzed the data of these experiments, wrote the first draft of the materials and methods section as well as the figure captions, designed the first version of Figure 7, and proof-read and edited the manuscript written by Dr. K. Andrew White. The experiments shown in Figure 1 and Figure 2 were performed by Dr. Beth Nicholson. Michael Yosefi carried out cloning and preliminary experiments for Figure 3B. The experiments shown in Figure 6D-F were performed by Peter Cimino.

Virology 450-451 (2014) 258–265

Contents lists available at ScienceDirect

Virology

journal homepage: www.elsevier.com/locate/yviro

Translational readthrough in Tobacco necrosis virus-D

Laura R. Newburn, Beth L. Nicholson, Michael Yosefi, Peter A. Cimino, K. Andrew White*

Department of Biology, York University, Toronto, ON, Canada M3J 1P3

ARTICLE INFO

Article history:
Received 30 October 2013
Returned to author for revisions
23 November 2013
Accepted 8 December 2013
Available online 9 January 2014

Keywords:
Plant virus
RNA virus
Recoding
Readthrough
Frameshifting
Cap-independent translation
RNA structure
Tombusviridae
Necrovirus
Carmovirus

ABSTRACT

The plus-strand RNA genome of Tobacco necrosis virus-D (TNV-D) expresses its polymerase via translational readthrough. The RNA signals involved in this readthrough process were characterized *in vitro* using a wheat germ extract translation system and *in vivo* via protoplast infections. The results indicate that (i) TNV-D requires a long-range RNA-RNA interaction between an extended stem-loop (SL) structure proximal to the readthrough site and a sequence in the 3′-untranslated region of its genome; (ii) stability of the extended SL structure is important for its function; (iii) TNV-D readthrough elements are compatible with UAG and UGA, but not UAA; (iv) a readthrough defect can be rescued by a heterologous readthrough element *in vitro*, but not *in vivo*; and (v) readthrough elements can also mediate translational frameshifting. These results provide new information on determinants of readthrough in TNV-D and further support the concept of a common general mechanism for readthrough in Tombusviridae.

Introduction

Plus-strand RNA viruses use a variety of translational strategies for the expression of their encoded proteins. Some employ recoding mechanisms such as translational readthrough or frameshifting to further expand their coding capacity (Firth and Brierley, 2012). Translational readthrough occurs when a stop codon is read as a sense codon by a suppressor tRNA, resulting in a C-terminal extension of the initial protein. Translational frameshifting also results in a C-terminally extended protein, but this occurs when a translating ribosome shifts its reading frame. Frameshifting into the −1 reading frame is most common, and this event, as well as readthrough, are used to express the RNA-dependent RNA polymerases (RdRps) in many different viruses (Firth and Brierley, 2012; Firth et al., 2011; Cimino et al., 2011). For both of these recoding events, RNA sequences and/or structures that facilitate the processes are generally found 3′-proximal to the recoding sites (Firth and Brierley, 2012).

Interestingly, some viruses also require distal RNA elements in addition to those found proximal to recoding sites. Barley yellow dwarf virus (BYDV; genus *Luteovirus,* family Luteoviridae) uses −1 frameshifting to express its RdRp and this process requires an extended stem-loop (SL) structure located just downstream of the frameshift site as well as a sequence in the 3′UTR of the genome (Paul et al., 2001; Barry and Miller, 2002). The key sequence in the 3′UTR is located in the terminal loop of an RNA hairpin structure and it must base pair with a bulge in the extended stem-loop (SL) structure proximal to the frameshift site for efficient −1 frameshifting to occur (Barry and Miller, 2002). Frameshifting in Red clover necrotic mosaic virus (RCNMV; genus *Dianthovirus*, family Tombusviridae) has been shown to involve RNA structures and a long-range base pairing interaction similar to those present in BYDV (Tajima et al., 2011). Interestingly, comparable structures and interactions are also needed for readthrough in Carnation Italian ringspot virus (CIRV; genus *Tombusvirus*, Family Tombusviridae) and Turnip crinkle virus (TCV; genus *Carmovirus*, Family Tombusviridae) (Cimino et al., 2011). Accordingly, comparable sets of long-range RNA–RNA interactions are involved in different recoding events in these viruses and it has been proposed that other genera in Tombusviridae may have similar requirements (Cimino et al., 2011).

Tobacco necrosis virus-D (TNV-D) is a plus-strand RNA virus and the type member of the genus *Betanecrovirus* in the family Tombusviridae (Sit and Lommel, 2010). Its ~3.8 kb genome encodes five viral proteins (Coutts et al., 1991) (Fig. 1A). The RdRp, p82, is expressed from the genomic RNA via readthrough of the 5′-proximal open reading frame (ORF) coding for p22 (Molnár et al., 1997; Fang and Coutts, 2013). The movement (p7a and p7b) and capsid (p29) proteins are translated from two subgenomic (sg) mRNAs that are transcribed during infections (Offei et al.,1995;

* Correspondence to: Department of Biology, York University, 4700 Keele St. Toronto, Ontario, Canada M3J 1P3. Tel.: +1 416 736 2100x40890, +416 736 2100x70352; fax: +1 416 736 5698.
E-mail address: kawhite@yorku.ca (K.A. White).

0042-6822/$ - see front matter © 2013 Elsevier Inc. All rights reserved.
http://dx.doi.org/10.1016/j.virol.2013.12.006

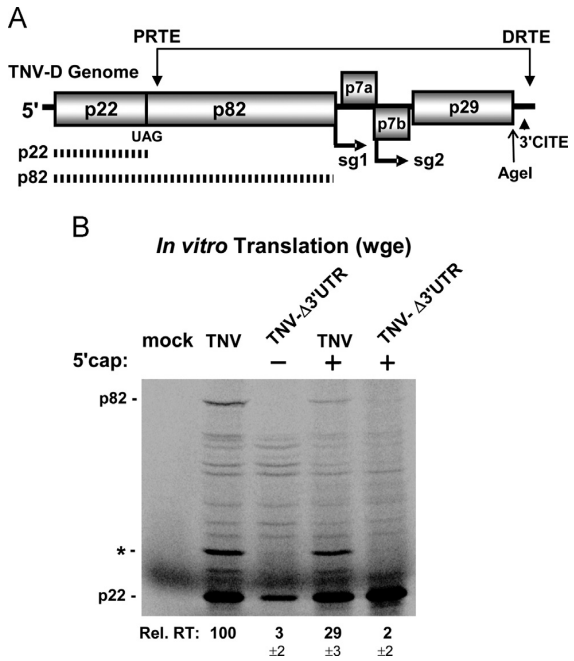

Fig. 1. Assessing the role of the 3′UTR in readthrough. (A) Schematic linear representation of the TNV-D RNA genome with boxes representing encoded proteins. p22 and its readthrough product p82 (shown by thick hatched lines) are translated directly from the genome. Initiation sites for subgenomic mRNA1 (sg1) and sg2 are indicated below the genome. The double-headed arrow above the genome connects the locations of two RNA sequences, the PRTE and DRTE, which base pair with each other to mediate readthrough. The relative positions of the 3′CITE and an AgeI restriction enzyme site are shown. (B) SDS-12%PAGE analysis of proteins translated from the TNV-D genome. Protein products in this, and all other subsequent experiments, were generated by translating 0.5 pmol of viral genomic RNA in wge for 1 h at 25 °C. The mock lane consists of a translation reaction using wge without any viral RNA added. The wild-type TNV-D genome (TNV) and a mutant TNV-D genome lacking a 3′UTR (Δ3′UTR) were tested with (+) and without (−) a 5′-cap. The positions of the viral proteins produced, p22 and p82 (RdRp), are indicated to the left and the asterisk denotes the position of p29 capsid protein. In this and subsequent experiments the corresponding means (±standard error) were determined from at least three independent experiments. Relative readthrough (Rel. RT) was calculated as the ratio of p82/p22, with that for wt TNV set as 100%.

Offei and Coutts, 1996; Molnár et al., 1997; Jiwan et al., 2011). The viral genome is neither 5′-capped nor 3′-polyadenylated and translation of viral proteins requires the activity of a 3′ cap-independent translational enhancer (3′CITE) that is located in the 3′UTR of the genome (Fig. 1A) (Shen and Miller, 2004). In addition to the 3′CITE, the 3′UTR also harbours RNA elements that are important for TNV-D genome replication (Shen and Miller, 2007).

In the present study we have investigated the readthrough process in TNV-D that mediates production of its RdRp. Our findings indicate that TNV-D requires a long-range RNA-RNA interaction for efficient translation of p82. Characterization of the readthrough signals along with comparative structural-function analyses provide novel insights into this translational recoding event.

Results

Efficient readthrough of p82 requires a 3′-proximal sequence

Translation of viral proteins from the TNV-D RNA genome was assessed using a wheat germ extract (wge) *in vitro* translation system. Translation of *in vitro* synthesized transcripts of the wt TNV-D genome yielded abundant p22 and lesser amounts of its readthrough product p82 (Fig. 1B, lane 2). The readthrough efficiency was calculated to be 2.5% ± 0.1. An additional prominent product of ~29 kDa was also observed (Fig. 1B, asterisk), which through additional analysis was determined to be the p29 coat protein that is likely expressed via an internal ribosome entry site (data not shown), as shown for some carmoviruses (Koh et al., 2003; Fernández-Miragall and Hernández, 2011). When the 3′UTR was deleted in TNV-Δ3′UTR, expression of all major products was dramatically reduced and the relative readthrough level of p82 (*i.e.* the ratio of p82/p22) was ~3% that of wt (Fig. 1B, lane 3). Adding a 5′-cap structure to TNV-Δ3′UTR led to revived p22 levels, but relative readthrough of p82 remained low at ~2% (Fig. 1B, lane 5). The presence of a 5′-cap on the wt TNV-D genome did reduce relative readthrough to ~29% of wt (Fig. 1B, lane 4), possibly due to interference with normal 3′CITE-mediated translation that may be important for efficient readthrough. However, ~29% was still ~15-fold higher than the ~2% level observed for capped TNV-Δ3′UTR. Collectively, these data suggest that the 3′UTR not only contains elements that are necessary for efficient cap-independent translation (*i.e.* a 3′CITE), as previously reported (Shen and Miller, 2004), it also contains a determinant for efficient readthrough of p82.

A long-range RNA–RNA interaction is required for readthrough

The requirement for an element in the 3′UTR of TNV-D (Fig. 1B), along with the previous observation of complementary sequences in the RNA structure 3′-adjacent to the readthrough site and a sequence in the 3′UTR (Cimino et al., 2011), suggested that readthrough production of p82 may require a long-range intra-genomic interaction. This interaction was predicted to occur between a sequence, the proximal readthrough element (PRTE), located in a bulge within an extended stem-loop structure, termed SL-PRTE, positioned 3′-proximal to the readthrough site and a sequence, the distal readthrough element (DRTE), located near the 3′-terminus of the viral genome (Figs. 1 and 2A). To test the possible involvement of the proposed interaction in readthrough, substitutions were introduced into the TNV-D genome that were predicted to disrupt (mutants TNV-2A and TNV-2B) and then restore (mutant TNV-2C) complementarity between the PRTE and DRTE (Fig. 2A). *In vitro* translation assays in wge revealed that the reduced pairing potential in mutants TNV-2A and TNV-2B lowered relative readthrough by ~10-fold, while re-establishing base pairing potential in mutant TNV-2C led to full recovery of readthrough (Fig. 2B). The effect of the mutations on virus viability was also assessed in protoplast transfections. Mutants TNV-2A and TNV-2B with reduced pairing accumulated to ~29 and ~66% the level of wt TNV-D, respectively, whereas mutant TNV-2C with restored pairing accumulated to wt levels (Fig. 2C). These results support an important role for the long-range interaction in both synthesis of p82 and viability of the viral genome.

The SL-PRTE structure is important for readthrough

The structural context of the PRTE places it within a bulge in an extended stem-loop structure, the SL-PRTE (Fig. 3A), and similar structural contexts have also been predicted for known and proposed PRTEs in all tombusvirids that utilize readthrough (Cimino et al., 2011). Comparably structured elements are also located 3′-proximal to −1 frameshift sites in BYDV and RCNMV (Barry and Miller, 2002; Tajima et al., 2011), thus similar secondary structures are required for both readthrough and frameshifting in these viruses. Despite their prevalence, the importance of the secondary structure within these RNA elements has not yet been investigated experimentally for any of these viruses. Fortunately, in the case of TNV-D, four base pairs in the lower part of SL-PRTE corresponded to opposing wobble positions (Fig. 3A), which allowed for substitutions of individual base pairs (Fig. 3B) or

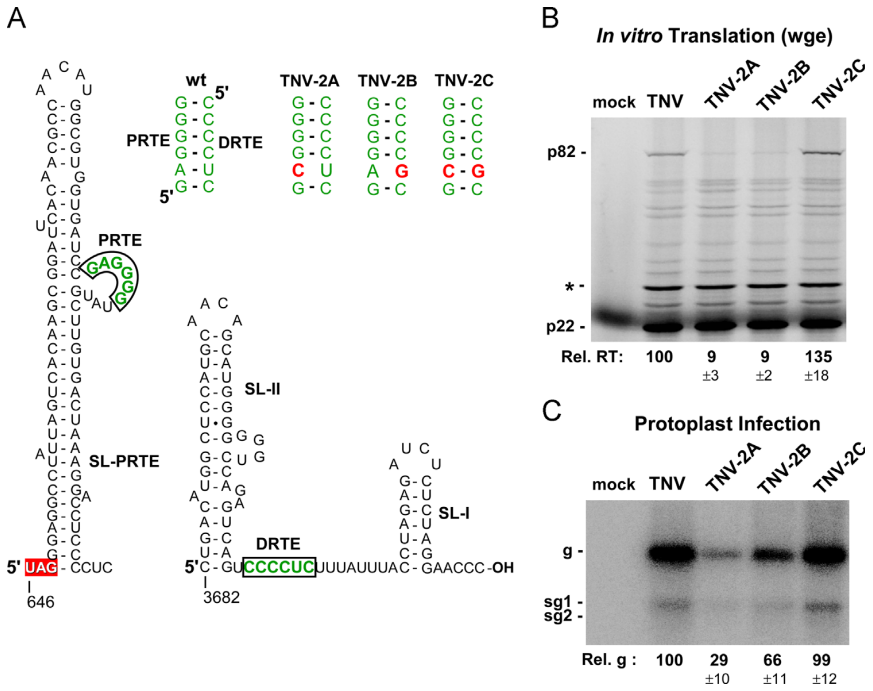

Fig. 2. Requirement for the PRTE-DRTE interaction for readthrough and genome replication. (A) Mfold-predicted RNA secondary structures of SL-PRTE and 3′-end of TNV-D, including the complementary PRTE and DRTE (green and boxed) and the stop codon highlighted by a red box. Wild-type and mutant PRTE-DRTE interactions are shown with substituted nucleotides in red. (B) *In vitro* translation analysis in wge of TNV-D genomes containing various mutations as depicted in panel A. (C) Northern blot analysis of TNV-D genomic and sg mRNA accumulation in plant protoplasts 22 h post-transfection. The viral genomes analysed are shown above their respective lanes. The positions of the genomic (g) and subgenomic RNAs (sg1, and sg2) are indicated to the left of the blot. In this and subsequent Northern blot analyses the corresponding means (± standard error) were determined from at least three independent experiments, and were normalized to the accumulation of the wild-type genomic RNA levels (Rel. g), which was set to 100%.

combinations thereof (Fig. 3C) while maintaining amino acid identities. Disruptive and restorative compensatory substitutions were introduced into individual base pairs at four different sites and mutants were tested for readthrough activity in wge and for viability in protoplast infections (Fig. 3B). For the RTS1 series mutants, RTS1-A with the CG-to-UG substitution exhibited wt levels of readthrough and genome accumulation, indicating that the UG pair was functionally equivalent. Conversely, the CA substitution at the same position in RTS1-B resulted in notable decreases in both readthrough and genome accumulation to ~12% and ~24% of wt, respectively. In RTS1-C, where Watson/Crick pairing was restored with an AU pair, greater than wt levels of both activities were observed, supporting an important role for the base pair that closes the lower half of the bulge (Fig. 3B). Testing of other individual base pairs located lower in the stem in mutant series RTS2, RTS3 and RTS4 revealed lesser effects, with no compelling correlations with predicted pairing strength (Fig. 3B). Similar results were also obtained when different combinations of the three lower pairs were targeted in tandem (series RTS2+RTS3, RTS3+RTS4 and RTS2+RTS3) (Fig. 3C). However, when all three lower pairs were simultaneously disrupted and then restored in series RTS2+RTS3+RTS4, a positive correlation between predicted base pairing strength and readthrough efficiency as well as genome viability was observed (Fig. 3C), indicating that stability of this lower stem region is important.

Stop codon identity influences readthrough

The TNV-D readthrough element is categorized as a type-III readthrough motif, which has the core consensus sequence UAGG followed by some type of higher-order RNA structure (Firth and Brierley, 2012). To determine if the TNV-D element could also support readthrough of the other two stop codons, UAA and UGA, substitutions were made to replace the wt UAG with either of these alternative codons (Fig. 4). Interestingly, both readthrough *in vitro* and genome accumulation in protoplasts occurred efficiently for TNV-UGA, which contained a UGA stop codon (Fig. 4A and B). Reverse transcription-PCR of the readthrough and flanking region in progeny genomes confirmed that the UGA codon was maintained (data not shown). In contrast, mutant TNV-UAA containing a UAA stop codon was inactive in both readthrough and genome replication (Fig. 4A and B). The ability of the RNA elements in TNV-D to mediate readthrough therefore depends on the type of stop codon present, with UAA being non-permissive.

Readthrough efficiency, but not virus viability, is rescued by a heterologous readthrough element

Previous studies demonstrated that that a readthrough defect in CIRV caused by disruption of its long-range interaction could be partially restored by introducing a TMV type-I motif (Cimino et al., 2011). To test if a comparable TNV-D defect could be rescued by the TMV element, the TMV sequence CAAUUA was inserted directly downstream of the TNV-D stop codon in the readthrough-defective mutant TNV-2A, thus creating TNV-2A+T (Fig. 5A). The insertion of the TMV element in TNV-2A+T led to greater than wt levels of readthrough *in vitro*, while a non-functional mutated form of the TMV element inserted as a control in TNV-2A+Tm had little effect (Fig. 5B). However, even though TNV-2A+T exhibited efficient readthrough *in vitro*, this genome was unable to accumulate to levels higher than those of TNV-2A in protoplast infections (Fig. 5C). In fact, the presence of the TMV element reduced the level of genome accumulation for both

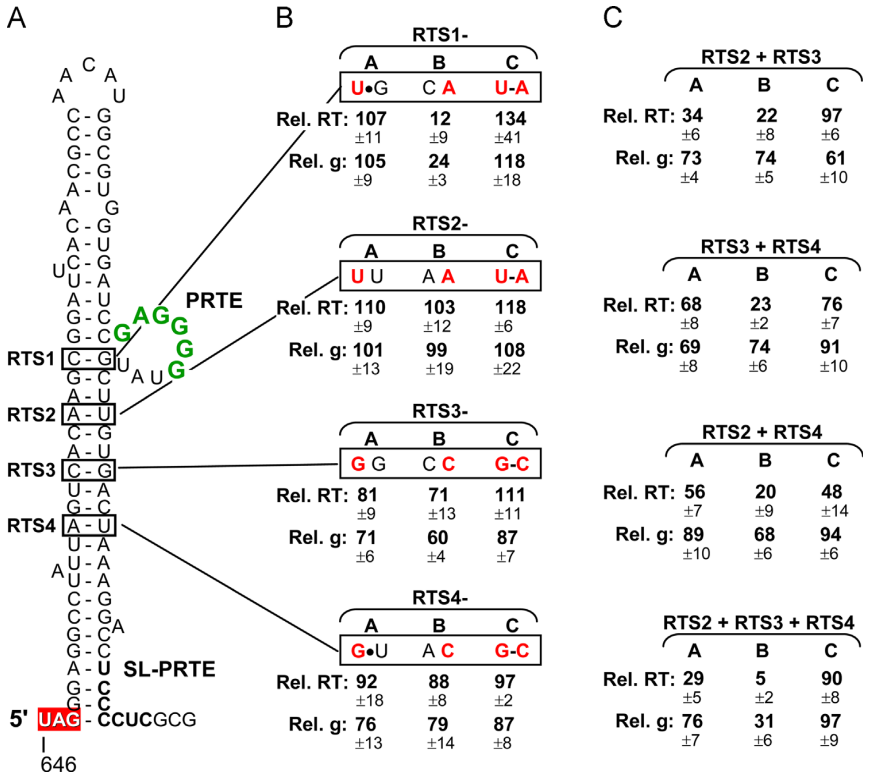

Fig. 3. Effect of SL-PRTE stability on readthrough and genome replication. (A) Mfold-predicted RNA secondary structures for SL-PRTE, with the PRTE shown in green and the stop codon highlighted by a red box. Base pairs targeted for compensatory mutational analysis, RTS1, RTS2, RTS3, and RTS4, are boxed. (B) Effects of single compensatory mutations on relative readthrough (Rel. RT) in wge and genome accumulation (Rel. g) in protoplast infections. Substituted nucleotides are red. (C) Effects of combinations of individual compensatory mutations. Two or three RTS sites were targeted simultaneously and analyzed as described above.

TNV-2A+T and TNV-2A+Tm relative to TNV-2A, indicating that both sequence insertions were detrimental to genome replication.

A readthrough element is compatible with frameshifting

As mentioned previously, the general structure of the SL-PRTE in TNV-D (Fig. 3A) is also maintained by other tombusvirids that use readthrough to express their RdRps, such as the tombusvirus CIRV (Cimino et al., 2011), as well as by the tombusvirid RCNMV (Tajima et al., 2011) and the luteovirus BYDV (Barry and Miller, 2002), which use frameshifting for RdRp expression. The existence of similar structures in two different recoding processes prompted us to test whether the RNA elements required for TNV-D readthrough were also able to facilitate frameshifting. To test this, the wt shifty heptanucleotide sequence used by BYDV for −1 frameshifting (5′–GGGUUUU), or a control non-functional version (5′–AGGCUUC), was inserted upstream of the SL-PRTE in the TNV-D genome (Figs. 6 and 7A) and, for comparison, the same modifications were also made in the CIRV genome (Figs. 6D and 7B). To accomplish this, two consecutive wt residues, the A preceding the wt stop codon for the pre-readthrough protein and the U in the UAG, were replaced with the sequence 5′-**GGGUUUU**UAG (Fig. 6A and D). This introduced the wt shifty heptanucleotide sequence (bold) and a new associated stop codon (underlined). In both viruses, the new stop codons were in-frame with respect to their pre-readthrough ORFs and the readthrough ORFs were in the −1 reading frame with respect to the new stop codons; thus, the production of either RdRp would require −1 frameshifting, instead of a readthrough event.

TNV-D genomes harbouring either a wt (TNV-fs) or mutated (TNV-fsm) form of the BYDV shifty heptanucleotide did not produce detectable p82 in wge and were defective for accumulation in protoplasts (Fig. 6B and C). For CIRV, p36 is the pre-readthrough protein (comparable to p22 in TNV-D) and p95 is the RdRp produced by readthrough of p36. In CIRV-fs, the CIRV genome with the wt shifty heptanucleotide, p95 production was detectable in wge, with a calculated *in vitro* frameshifting efficiency of 0.28% ± 0.04 (*versus* 0.8% ± 0.1 for wt CIRV readthrough), and the mutant was viable in protoplast infections (Fig. 6E and F). Both of these activities were shifty heptanucleotide-dependent, because CIRV-fsm with a mutated shifty heptanucleotide showed three-fold lower levels of p95 production *in vitro* and was not viable in protoplast infections (Fig. 6E and F). Additionally, the efficient production of p95 in wge from CIRV-fs required that its PRTE interact with its DRTE, as shown by mutants CIRV-fs-A, -B and -C (Fig. 6E), which contained compensatory mutations in the long-range interaction (Fig. 7B, box). A similar requirement for the long-range interaction was also observed in protoplast infections (Fig. 6F). Importantly, reverse transcription-PCR of the frameshift region in viable progeny genomes confirmed that the introduced frameshift signal and the flanking sequences were maintained.

Discussion

The analysis of a TNV-D genome lacking its 3′UTR revealed the presence of a determinant of translational readthrough in this region. The element responsible was identified as a 6 nt long DRTE

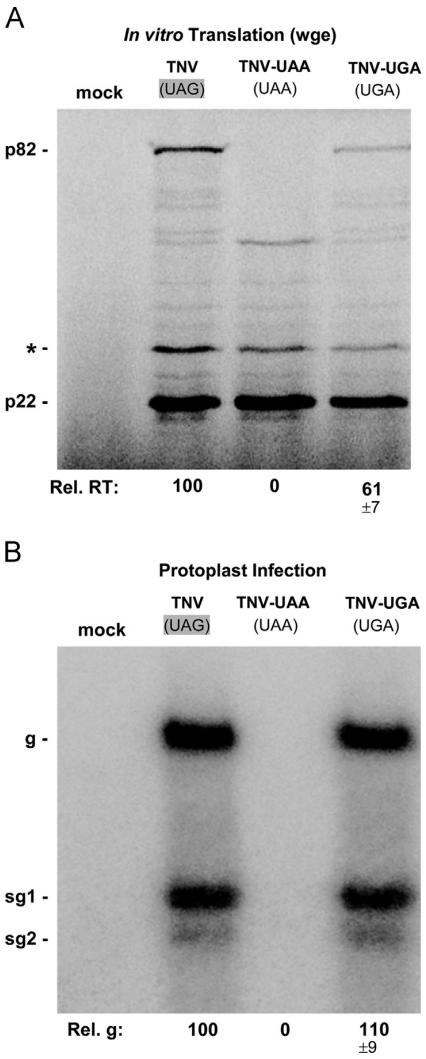

Fig. 4. Assessing the consequence of stop codon identity on readthrough and genome replication. (A) *In vitro* translation analysis in wge of TNV-D genomes containing a substitution of the p22 wild-type UAG stop codon with UAA (TNV-UAA) or UGA (TNV-UGA). The faint bands in between p22 and p82 are of unknown origin. (B) Northern blot analysis of wt and mutant TNV-D genomes in protoplasts and quantification of plus-strand viral genome accumulation.

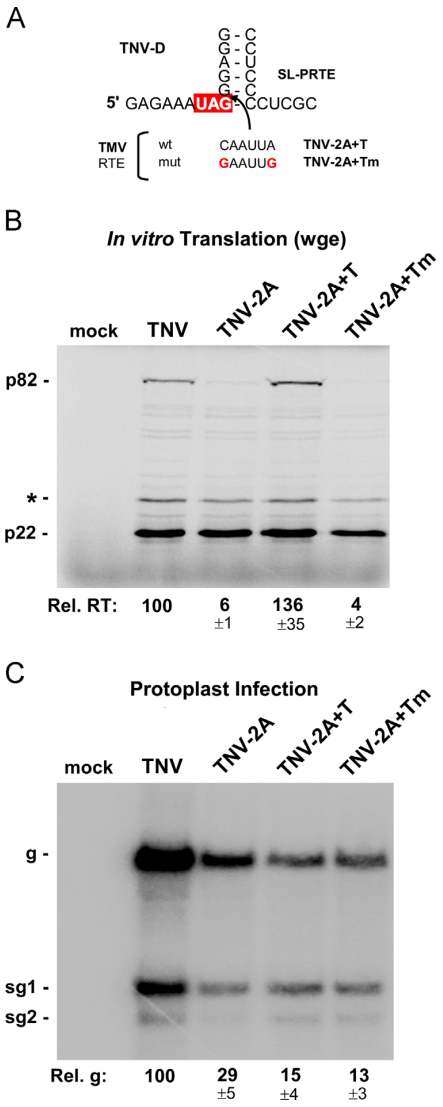

Fig. 5. Restoring readthrough with a heterologous readthrough element. (A) The lower portion of SL-PRTE in TNV-D is shown with the insertion site (arrow) of the wild-type and mutant forms of the 6 nucleotide TMV readthrough element (RTE). The wild-type and mutant forms of the TMV RTE are shown below, with mutated nucleotides in red. (B) *In vitro* translation analysis in wge of TNV-D genomes containing mutations in the PRTE-DRTE interaction (see TNV-2A in Fig. 2A) and an inserted wild-type (TNV-2A+T) or mutant (TNV-2A+Tm) TMV RTE. (C) Northern blot analysis of wt and mutant TNV-D genomes in protoplasts and quantification of plus-strand viral genome accumulation.

with complementarity to a bulge sequence in the readthrough proximal SL-PRTE. Subsequent compensatory mutational analysis showed that base pairing between these two sequences was required for efficient readthrough *in vitro* and productive genome replication in protoplasts. This represents the third genus in Tombusviridae to have this requirement and further supports the proposal that all genera of Tombusviridae that use readthrough for RdRp production require a long-range interaction between the readthrough sites and their 3′UTRs (Cimino et al., 2011). Our results with TNV-D also represent the first experimentally supported functional long-distance interaction in a necrovirus. Although long-range base pairing between the 5′UTR and 3′CITE in TNV-D was previously proposed to be important for translation initiation, no experimental evidence to support this notion has yet been provided (Shen and Miller, 2004).

The general structure of SL-PRTE in TNV-D is also predicted in corresponding regions of other tombusvirids and luteoviruses (Cimino et al., 2011; Tajima et al., 2011; Barry and Miller, 2002). The mutational analysis of the stem region of this structure in TNV-D provides the first experimental evidence that this substructure is important for readthrough. The sensitivity of the lower base pair closing the bulge to disruption suggests that a precise architecture at this site involving a base pair is required. The lower portion of the stem was also shown to be relevant; however this region was more tolerant to individual disruptions, possibly due to compensation by non-canonical pairing and/or nearest neighbour effects. However, since the triple disruption did cause notable inhibition, overall stability of the lower stem is clearly important

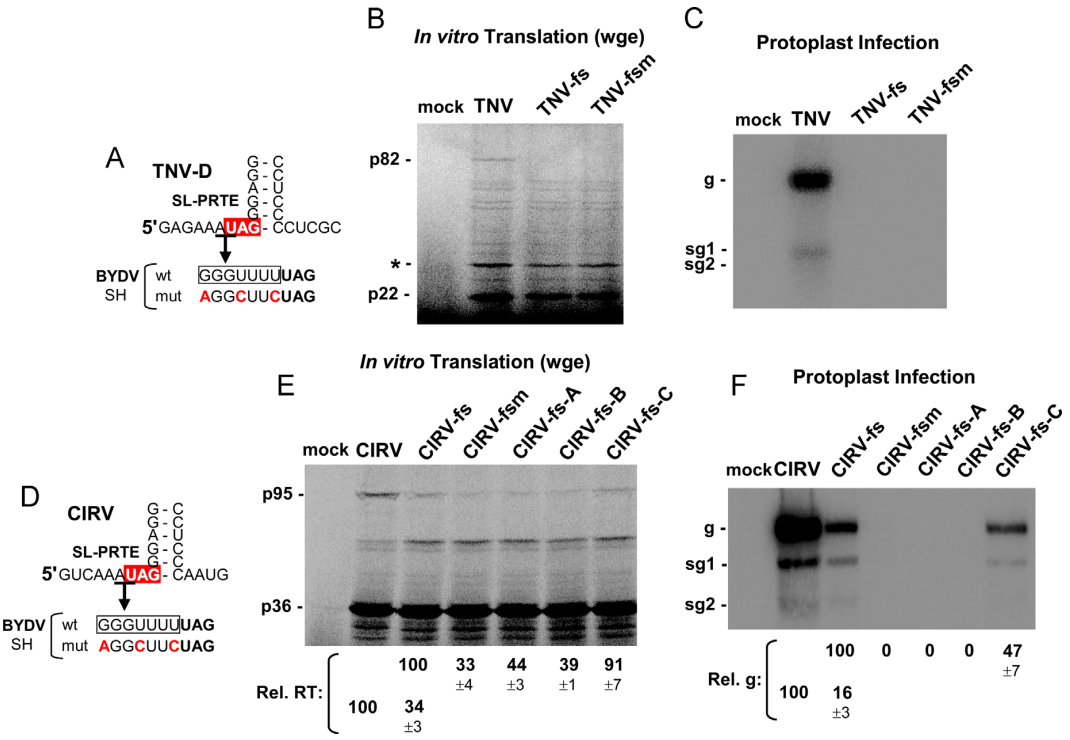

Fig. 6. Compatibility of BYDV shifty heptanucleotide with TNV-D and CIRV readthrough elements. (A) The lower portion of SL-PRTE in TNV-D is shown with the wt stop codon highlighted by a red box. The top end of the arrow shows the AU nucleotides that were replaced with either the wild-type BYDV shifty heptanucleotide (SH, boxed) or a mutant form of the BYDV SH. The nucleotides substituted in the mutant SH are in red. (B) *In vitro* translation analysis in wge of TNV-D genomes containing a wild-type BYDV SH (TNV-fs) or a mutant form of the BYDV SH (TNV-fsm). (C) Northern blot analysis of wt and mutant TNV-D genomes in protoplasts and quantification of plus-strand viral genome accumulation. (D) The lower portion of SL-PRTE in CIRV is shown with the wt stop codon highlighted by a red box. The top end of the arrow shows the AU nucleotides that were replaced with either the wild-type BYDV SH (boxed) or a mutant form. (E) *In vitro* translation analysis in wge of CIRV genomes containing a wild-type BYDV SH (CIRV-fs) or a mutant form of the BYDV SH (CIRV-fsm). Also tested were derivatives of CIRV-fs (CIRV-fs-A, -B and -C) which had compensatory mutations in the CIRV PRTE-DRTE interaction (as shown in Fig. 7B, box). (F) Northern blot analysis of wt and mutant CIRV genomes in protoplasts and quantification of plus-strand viral genome accumulation.

for readthrough function. The role of this lower stem could be to support formation of the bulge and/or it may affect ribosome function in a way that favours recoding. Since this general structure is conserved in other tombusvirids, the corresponding structures in these other viruses may also display similar structure–function requirements. It will also be interesting to see if the RNA elements involved in readthrough of the luteovirus BYDV capsid protein have comparable structural features, as this event also requires an additional RNA sequence located ~700 nt downstream of the readthrough site (Brown et al., 1996).

Based on its core consensus UAGG and 3′-proximal SL-PRTE structure, the TNV-D readthrough element is classified as a type-III readthrough motif (Firth and Brierley, 2012). Interestingly, this context was functional for *in vitro* readthrough and genome replication when the wt UAG was substituted with UGA. Similarly, the Moloney murine leukemia virus (Mo-MuLV) type-III context was also able to efficiently suppress UGA (Feng et al., 1989). For TNV-D, no activity was observed when UAG was substituted with UAA. Efficient readthrough of this stop codon occurs most commonly in type-I contexts (*i.e.* UAACAAUYA, *U*=purine, *Y*=pyrimidine) (Skuzeski et al., 1991) and to a lesser degree in type-II contexts, where UGA is usually suppressed (Beier and Grimm, 2001). Nonetheless, unlike for TNV-D, the type-III context of Mo-MuLV was able to suppress UAA in CHO hamster cells and in rabbit reticulocyte lysate supplemented with tRNAs from NIH 3T3 cells (Feng et al., 1989). Thus, some type-III contexts are able to suppress UAA. The inability of the TNV-D context to suppress UAA is likely related to some property of the TNV-D signal that prevents UAA suppressor tRNA utilization.

Previous studies with the CIRV genome revealed that inhibition caused by disruption of the PRTE-DRTE interaction could be partially rescued in wge (*i.e.* relative readthrough increased from 3% of wt to 71%) and in protoplast infections (*i.e.* genome accumulation increased from 0% to 26%) by introducing a local readthrough element derived from TMV into a readthrough-defective CIRV mutant (Cimino et al., 2011). In contrast, a similar approach attempted with TNV-D was able to restore readthrough in wge, but did not enhance replication in protoplasts. The functionality of the TMV element was confirmed *in vitro*, where the wt motif conferred efficient readthrough, while the corresponding mutated form did not. Accordingly, if p82 production was also restored in protoplasts, the inability to recover accumulation *in vivo* may be related to a different function impeded by the disrupted long-range interaction in the mutant. The most likely process to be affected would be genome replication, as the interaction involves the 3′-terminal region of the genome that contains RNA replication elements (Shen and Miller, 2007). Another contributing factor could be a defect caused by insertion of the 6 nt long TMV sequence. Although tolerated in CIRV, the introduction of this sequence in TNV-D sequence may have altered an important *cis*-acting RNA element or the two added amino acids (*i.e.* CAA UUA=Gln Leu) may have caused inhibition of p82 activity. Regardless of the nature of the defect, the results suggest that TNV-D is not amenable to the same recoding modification that is both tolerated and beneficial in CIRV.

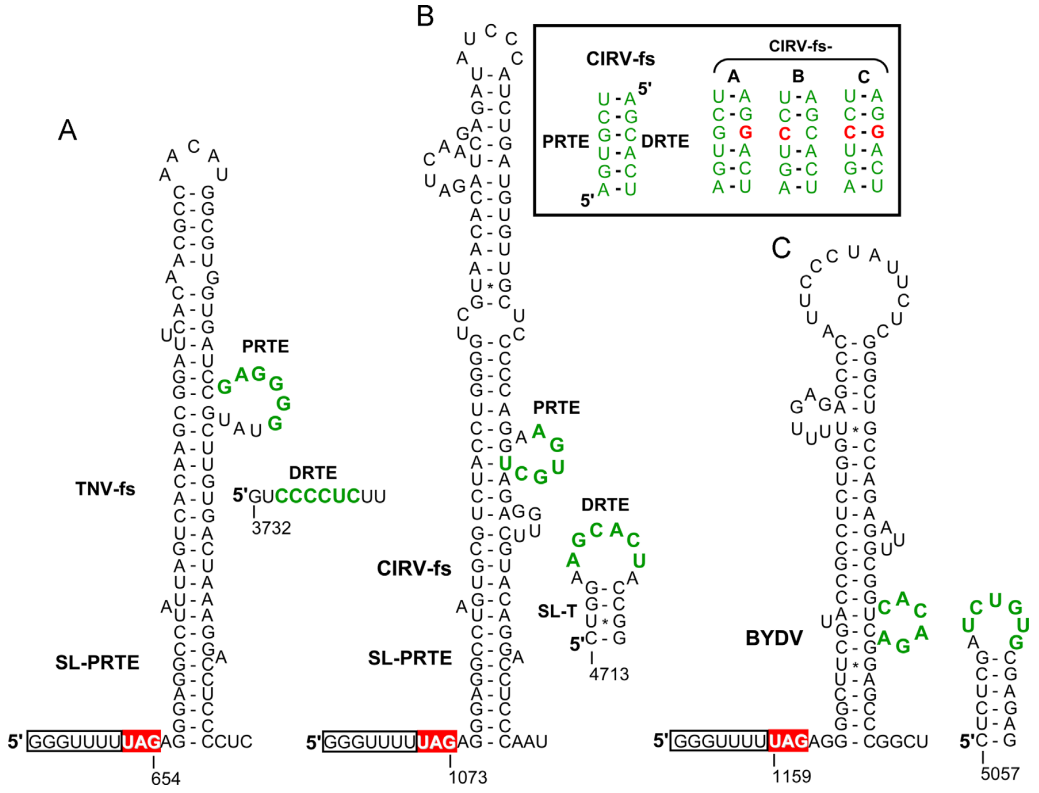

Fig. 7. Comparison of chimeric and wildtype frameshifting elements. (A) Mfold-predicted RNA secondary structure for chimeric TNV-fs showing its SL-PRTE and DRTE regions in green. (B) Mfold-predicted RNA secondary structure for chimeric CIRV-fs showing its SL-PRTE and DRTE regions. The box shows CIRV-fs PRTE-DRTE compensatory mutants with substitutions in red. (C) Predicted RNA secondary structure for BYDV showing its SL-PRTE-like and DRTE-like elements in green (Barry and Miller, 2002).

The similarity in structure of the RNA elements proximal and distal to recoding sites for viruses utilizing readthrough and frameshifting led us to test if the TNV-D or CIRV readthrough elements could mediate frameshifting. The TNV-D elements were not able to do so, while the CIRV elements were partially functional. The low but notable frameshifting and replication activities observed for CIRV demonstrate functional compatibility of its readthrough RNA structures with an alternative recoding event. With respect to the PRTE-DRTE interactions in TNV-D-fs or CIRV-fs *versus* the corresponding interaction for frameshifting in BYDV, the interaction in CIRV is more similar to that in BYDV (Fig. 7). In BYDV, the distal partner sequence (equivalent to a DRTE) is located in the terminal loop of a SL structure and its interaction with the proximal readthrough structure is predicted to involve all residues in the in the bulge (Fig. 7C). Similarly, the CIRV-fs DRTE is present in the terminal loop of a hairpin (SL-T) and the PRTE-DRTE interaction involves all but one of the residues in the bulge (Fig. 7B). In contrast, the TNV-D DRTE is predicted to be located in an ssRNA region between two SL structures (Fig. 2A) and for the PRTE-DRTE interaction three of the bulged residues are predicted to be unpaired (Fig. 7A). The greater similarity between the CIRV-fs and BYDV structural components may have contributed to the observed activity in the former. However, despite such similarities, differences between the two structures also exist. The spacing between the shifty heptanucleotide sequence and the long-range interaction within the recoding proximal structure is quite different in CIRV-fs and BYDV, and spacing is known to affect frameshifting efficiency (Lin et al., 2012). In BYDV it involves a 5 nt single-stranded spacer followed by an 8 bp stem, while in CIRV-fs the spacing involves a 4 nt spacer followed by an irregular stem of 18 bps. This difference in relative spacing did not prevent frameshifting in CIRV-fs, though it may have contributed to the reduced activity observed. The three-fold lower level of p95 produced from CIRV-fs *versus* wt CIRV could also have negatively affected its ability to replicate efficiently. Regardless, the fact that the CIRV readthrough elements were functional for frameshifting helps to explain the similarity in structure observed in nature and suggests at least some mechanistic similarities between the two processes.

Materials and methods

Plasmid construction

All TNV-D mutants were derivatives of the wt TNV-D cDNA in a pUC19 plasmid supplied by Robert Coutts, Imperial College London (Coutts et al., 1991), which was modified to have a SmaI site at its 3′-end (Jiwan et al., 2011). The full-length infectious clone of CIRV has been described previously (Rubino et al., 1995) and all CIRV mutants in this study were derived from this construct. For TNV-D or CIRV, overlapping PCR-based mutagenesis was used to introduce the different modifications into genomic clones and all mutant constructs were sequenced to ensure that only the desired changes were present. The modifications in the various mutants of the TNV-D and CIRV genome are shown in the accompanying figures.

RNA preparation

TNV-D and CIRV clones used for *in vitro* transcription were prepared by linearizing the plasmids with SmaI. TNV-Δ3′UTR, lacking the 3′UTR of the TNV-D genome, was synthesized from AgeI-linearized wt TNV-D clone (position 3764 in the genome sequence). RNA transcripts were prepared using the AmpliScribe T7-Flash Transcription Kit (Epicentre Technologies) as described previously (White and Morris, 1994). Unless specified, all transcripts were not 5′-capped. The concentrations of RNA transcripts were quantified by spectrophotometry and the quality of the transcripts was examined by agarose gel electrophoresis.

In vitro translation

In vitro transcripts were subjected to translation in nuclease-treated wheat germ extract (Promega). Translation was performed in the presence of ^{35}S-methionine as previously described (Wu and White, 1999). Reactions contained 0.5 pmol of viral genomic RNA in wge for 1 h at 25 °C. Products were separated by sodium dodecyl sulfate-polyacrylamide gel electrophoresis (SDS-PAGE) in a 12% polyacrylamide gel, and quantified by radioanalytical scanning using a PharosFX Plus Molecular Imager (Bio-Rad) and QuantityOne Software (Bio-Rad). All trials were repeated at least three times.

Protoplast infection

Cucumber cotyledon protoplasts were prepared and transfected using polyethylene glycol as described previously (White and Morris, 1994). Briefly, 3 μg of viral genomic RNAs were transfected into protoplasts and incubated for 22 h at 22 °C under constant light. Total nucleic acid extraction was performed as described previously (White and Morris, 1994) and separated in nondenaturing 2% agarose gels. Northern blotting was performed as previously described (Jiwan et al., 2011). Briefly, the nucleic acids were electro-transferred from the agarose gel to a nylon membrane and hybridized with three ^{32}P-labeled probes complementary to the 3′-end of TNV-D (PTN14, complementary to coordinates 2821–2840 of TNV-D genome; PTN8, 3520–3532; PTN10, 3643–3663). Viral genome accumulation was quantified by radioanalytical scanning using a PharosFX Plus Molecular Imager (Bio-Rad) and QuantityOne Software (Bio-Rad). All trials were repeated at least three times.

RNA secondary structure prediction

RNA secondary structures were predicted at 37 °C using Mfold version 3.6 (Mathews et al., 1999; Zuker, 2003).

Acknowledgments

We thank Robert Coutts for the infectious clone of TNV-D and members of our laboratory for reviewing the manuscript. This work was supported by NSERC.

References

Barry, J.K., Miller, W.A., 2002. A −1 ribosomal frameshift element that requires base pairing across four kilobases suggests a mechanism of regulating ribosome and replicase traffic on a viral RNA. Proc. Nat. Acad. Sci. U.S.A 99, 11133–11138.
Beier, H., Grimm, M., 2001. Misreading of termination codons in eukaryotes by natural nonsense suppressor tRNAs. Nucleic Acids Res. 29, 4767–4782.
Brown, C.M., Dinesh-Kumar, S.P., Miller, W.A., 1996. Local and distant sequences are required for efficient readthrough of the barley yellow dwarf virus PAV coat protein gene stop codon. J. Virol. 70, 5884–5892.
Cimino, P.A., Nicholson, B.L., Wu, B., Xu, W., White, K.A., 2011. Multifaceted regulation of translational readthrough by RNA replication elements in a tombusvirus. PLoS Pathog. 7 (12), e1002423.
Coutts, R.H.A., Ridgen, J.E., Slabas, A.R., Lomonossoff, G.P., Wise, P.J., 1991. The complete nucleotide sequence of tobacco necrosis virus strain D. J. Gen. Virol. 72, 1521–1529.
Fang, L., Coutts, R.H., 2013. Investigations on the tobacco necrosis virus D p60 replicase protein. PLoS One 8 (11), e80912.
Feng, Y.X., Levin, J.G., Hatfield, D.L., Schaefer, T.S., Gorelick, R.J., Rein, A., 1989. Suppression of UAA and UGA termination codons in mutant murine leukemia viruses. J. Virol. 63, 2870–2873.
Fernández-Miragall, O., Hernández, C., 2011. An internal ribosome entry site directs translation of the 3′-gene from Pelargonium flower break virus genomic RNA: implications for infectivity. PLoS One 6 (7), e22617.
Firth, A.E., Brierley, I., 2012. Non-canonical translation in RNA viruses. J. Gen. Virol. 93, 1385–1409.
Firth, A., Wills, N.M., Gesteland, R.F., Atkins, J.F., 2011. Stimulation of stop codon readthrough: frequent presence of an extended 3′ RNA structural element. Nucleic Acids Res. 39, 6679–6691.
Jiwan, S.D., Wu, B., White, K.A., 2011. Subgenomic mRNA transcription in tobacco necrosis virus. Virology 418, 1–11.
Koh, D.C., Wong, S.M., Liu, D.X., 2003. Synergism of the 3′-untranslated region and an internal ribosome entry site differentially enhances the translation of a plant virus coat protein. J. Biol. Chem 278, 20565–20573.
Lin, Z., Gilbert, R.J., Brierley, I., 2012. Spacer-length dependence of programmed −1 or −2 ribosomal frameshifting on a U6A heptamer supports a role for messenger RNA (mRNA) tension in frameshifting. Nucleic Acids Res. 40, 8674–8689.
Mathews, D.H., Sabina, J., Zuker, M., Turner, D.H., 1999. Expanded sequence dependence of thermodynamic parameters provides robust prediction of RNA secondary structure. J. Mol. Biol. 288, 911–940.
Molnár, A., Havelda, Z., Dalmay, T., Szutorisz, H., Burgyán, J., 1997. Complete nucleotide sequence of tobacco necrosis virus strain DH and genes required for RNA replication and virus movement. J. Gen. Virol. 78, 1235–1239.
Offei, S.K., Coffin, R.S., Coutts, R.H.A., 1995. The tobacco necrosis virus p7a protein is a nucleic acid-binding protein. J. Gen. Virol. 76, 1493–1496.
Offei, S.K., Coutts., R.H.A., 1996. Location of the 5′ termini of Tobacco necrosis virus strain D subgenomic mRNAs. J. Phytopathol. 144, 13–17.
Paul, C.P., Barry, J.K., Dinesh-Kumar, S.P., Brault, V., Miller, W.A., 2001. A sequence required for −1 ribosomal frameshifting located four kilobases downstream of the frameshift site. J. Mol. Biol. 310, 987–999.
Rubino, L., Burgyan, J., Russo, M., 1995. Molecular cloning and complete nucleotide sequence of carnation Italian ringspot tombusvirus genomic and defective interfering RNAs. Arch. Virol. 140, 2027–2039.
Shen, R., Miller, W.A., 2004. The 3′ untranslated region of Tobacco necrosis virus RNA contains a Barley yellow dwarf virus-like cap-independent translation element. J. Virol. 78, 4655–4664.
Shen, R., Miller, W.A., 2007. Structures required for poly(A) tail-independent translation overlap with, but are distinct from, cap-independent translation and RNA replication signals at the 3′ end of Tobacco necrosis virus RNA. Virology 358, 448–458.
Sit, T.L., Lommel, S.A., 2010. Tombusviridae, Encyclopedia of Life Sciences (ELS). John Wiley & Sons, Ltd, Chichester. http://dx.doi.org/10.1002/9780470015902.a0000756.pub2.
Skuzeski, J.M., Nichols, L.M., Gesteland, R.F., Atkins, J.F., 1991. The signal for a leaky UAG stop codon in several plant viruses includes the two downstream codons. J. Mol. Biol. 218, 365–373.
Tajima, Y., Iwakawa, H.O., Kaido, M., Mise, K., Okuno, T., 2011. A long-distance RNA–RNA interaction plays an important role in programmed −1 ribosomal frameshifting in the translation of p88 replicase protein of Red clover necrotic mosaic virus. Virology 417, 169–178.
White, K.A., Morris, T.J., 1994. Nonhomologous RNA recombination in tombusviruses: generation and evolution of defective interfering RNAs by stepwise deletions. J. Virol. 68, 14–24.
Wu, B., White, K.A., 1999. A primary determinant of cap-independent translation is located in the 3′-proxminal region of the tomato bushy stunt virus genome. J. Virol. 73, 8982–8988.
Zuker, M., 2003. Mfold web server for nucleic acid folding and hybridization prediction. Nucleic Acids Res. 31, 3406–3415.

CHAPTER 3

Atypical RNA Elements Modulate Translational Readthrough in Tobacco Necrosis Virus D

This chapter is a follow up study of **Chapter 2**. It details the impact that RNA elements proximal to the core readthrough RNA elements (RTSL, PRTE, and DRTE) have on readthrough. The major findings of this study are (i) the RNA secondary structures immediately upstream and downstream of the RTSL impact readthrough efficiency and virus viability, (ii) the proposed silencer/3'-end interaction influences readthrough production of the RdRp, and (iii) stability and the apical loop of SLII are important for optimal readthrough and virus viability. Overall, this study has identified novel elements involved in TNV-D readthrough.

This chapter is presented as a research article published in the *Journal of Virology* (Newburn and White, 2017). For this article, I designed the experiments with Dr. K. Andrew White, performed all of the experiments, analyzed the data, and wrote the first draft of the manuscript.

AMERICAN SOCIETY FOR MICROBIOLOGY | Journal of Virology®

Atypical RNA Elements Modulate Translational Readthrough in Tobacco Necrosis Virus D

Laura R. Newburn, K. Andrew White
Department of Biology, York University, Toronto, Ontario, Canada

ABSTRACT Tobacco necrosis virus, strain D (TNV-D), is a positive-strand RNA virus in the genus *Betanecrovirus* and family *Tombusviridae*. The production of its RNA-dependent RNA polymerase, p82, is achieved by translational readthrough. This process is stimulated by an RNA structure that is positioned immediately downstream of the recoding site, termed the readthrough stem-loop (RTSL), and a sequence in the 3′ untranslated region of the TNV-D genome, called the distal readthrough element (DRTE). Notably, a base pairing interaction between the RTSL and the DRTE, spanning ~3,000 nucleotides, is required for enhancement of readthrough. Here, some of the structural features of the RTSL, as well as RNA sequences and structures that flank either the RTSL or DRTE, were investigated for their involvement in translational readthrough and virus infectivity. The results revealed that (i) the RTSL-DRTE interaction cannot be functionally replaced by stabilizing the RTSL structure, (ii) a novel tertiary RNA structure positioned just 3′ to the RTSL is required for optimal translational readthrough and virus infectivity, and (iii) these same activities also rely on an RNA stem-loop located immediately upstream of the DRTE. Functional counterparts for the RTSL-proximal structure may also be present in other tombusvirids. The identification of additional distinct RNA structures that modulate readthrough suggests that regulation of this process by genomic features may be more complex than previously appreciated. Possible roles for these novel RNA elements are discussed.

IMPORTANCE The analysis of factors that affect recoding events in viruses is leading to an ever more complex picture of this important process. In this study, two new atypical RNA elements were shown to contribute to efficient translational readthrough of the TNV-D polymerase and to mediate robust viral genome accumulation in infections. One of the structures, located close to the recoding site, could have functional equivalents in related genera, while the other structure, positioned 3′ proximally in the viral genome, is likely limited to betanecroviruses. Irrespective of their prevalence, the identification of these novel RNA elements adds to the current repertoire of viral genome-based modulators of translational readthrough and provides a notable example of the complexity of regulation of this process.

KEYWORDS plant virus, RNA virus, recoding, readthrough, frameshifting, RNA structure, *Tombusviridae*, tombusvirus, necrovirus, carmovirus

Received 19 December 2016 **Accepted** 27 January 2017

Accepted manuscript posted online 1 February 2017

Citation Newburn LR, White KA. 2017. Atypical RNA elements modulate translational readthrough in tobacco necrosis virus D. J Virol 91:e02443-16. https://doi.org/10.1128/JVI.02443-16.

Editor Anne E. Simon, University of Maryland

Address correspondence to K. Andrew White, kawhite@yorku.ca.

RNA plant viruses expand their coding capability by employing a variety of expression strategies. Recoding mechanisms, such as translational frameshifting and readthrough, provide a means to produce distinct proteins using the same initiation site (1). In translational frameshifting, the ribosome shifts frames before encountering its customary stop codon, often resulting in a C-terminally extended protein. Translational readthrough also produces elongated proteins; however, this process involves the normal stop codon being decoded by a near cognate tRNA, thereby allowing for

C-terminal polypeptide extension (1). Many different factors, such as RNA sequences and higher-order RNA structures (1–11), RNA remodeling (12), and viral (13, 14) or host (15, 16) proteins, have been implicated in regulating recoding in eukaryotic viruses. Among these, the RNA elements that modulate translational readthrough in plus-strand RNA viruses have been the focus of many studies (1, 9).

Members of family *Tombusviridae* are plus-sense RNA viruses that express their RNA-dependent RNA polymerase (RdRp) by either −1 frameshifting or readthrough (17). In both cases, there is an extended stem-loop (SL) RNA structure located immediately downstream of the slippery sequence or stop codon that is required for efficient recoding (5, 6, 12, 18, 19). In addition, for maximal recoding to occur, a bulge in this RNA structure must base pair, via a long-range RNA-RNA interaction, with a sequence located 3′ proximally in the viral genome (5, 6, 18, 19). It has been proposed that this RNA-based communication with the 3′ end also assists in coordinating the directionally opposing processes of translation of the RdRp and minus-strand genome synthesis (5, 18, 19).

Tobacco necrosis virus, strain D (TNV-D), is a member of the family *Tombusviridae* (17), and the type member of the genus *Betanecrovirus* (20). Currently, three members of this genus have been sequenced: TNV-D (21), beet black scorch virus (BBSV) (22), and leek white stripe virus (LWSV) (23). These viruses possess monopartite, single-stranded, ~3.8-kb plus-sense RNA genomes that lack both a 5′ cap and a 3′ poly(A) tail. Instead, they use a 3′-cap-independent translational enhancer (3′CITE) located in their 3′ untranslated regions (3′ UTRs) to recruit eukaryotic translation initiation factors (24–26). The TNV-D genome encodes five open reading frames (Fig. 1A) (21). Accessory replication protein p22 and the p82 RdRp share the same initiation codon, the latter being a readthrough product of the former (Fig. 1A). Readthrough in TNV-D, as for most tombusvirids, requires an extended RNA secondary structure, the readthrough stem-loop (RTSL) (Fig. 1B), located just 3′ to the p22 stop codon, which must interact with sequences in the 3′ UTR, via proximal and distal readthrough elements (PRTE and DRTE, respectively) (Fig. 1A) (6). Other 3′-proximal proteins, involved in virus movement (p7a and p7b) and packaging (p29, capsid protein), are translated from two subgenomic (sg) mRNAs that are transcribed during infections (27–31). A small amount of p29 capsid protein is also translated *in vitro* from the full-length TNV-D genome via a putative internal ribosome entry site (30). The relevance of this occurrence is currently unknown; however, a similar activity in another tombusvirid, the pelargonium flower break virus (genus *Carmovirus*), was shown to be important for efficient infection of plant hosts (32).

In this study, we investigated the RTSL and whether RNA sequences and structures that flank the known regulators of readthrough in TNV-D genome, i.e., RTSL and DRTE, could modulate the production of the p82 RdRp. Our results identified additional RNA structures, proximal and distal to the readthrough site, that are required for optimal readthrough in cell extracts and efficient viral genome accumulation in protoplasts. These findings expand the current documented assortment of RNA-based regulators and show that readthrough can be modulated by multiple discrete RNA elements.

RESULTS

The PRTE is critical for efficient readthrough and virus viability. To assess the importance of the size of the PRTE-containing bulge, viral genomic mutants containing deletions in multiples of three nucleotides were tested for their ability to produce p82 in wheat germ extract and to accumulate in protoplast transfections (Fig. 1B). The triplet nucleotide deletions were designed to precisely remove complete amino acids in p82 (i.e., methionine, glycine, and arginine). Removal of 3 or 6 nucleotides (nt) from the bulge in mutants Δ3 and Δ6, respectively, decreased translational readthrough to ~10% that of wild type (wt), and eliminated genome accumulation in protoplasts (Fig. 1C and D, left panels). Although the Δ3 construct contained the complete PRTE, the 5′-proximal guanosine in the PRTE was predicted by Mfold to pair with the adjoining stem (Fig. 1B), and this could reduce its accessibility to the DRTE. To investigate this

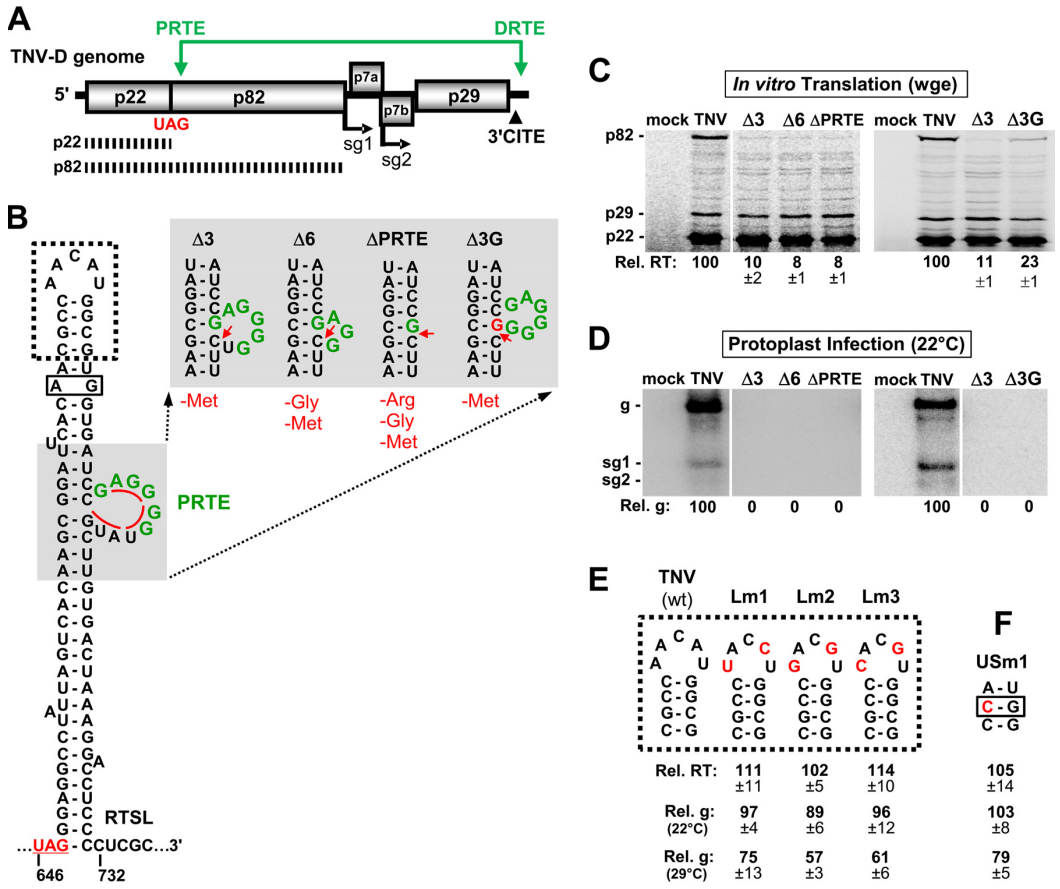

FIG 1 The TNV-D genome and mutational analysis of the RTSL. (A) Linear representation of TNV-D RNA genome with encoded proteins represented as gray boxes. Initiation sites for subgenomic (sg) mRNA1 and -2 are indicated below the genome, as well as the relative position of the 3′ cap-independent translational enhancer (3′CITE). Hatched black lines represent p22 protein and its readthrough product p82. Green double-headed arrows denote the long-range base-pairing interaction between the proximal readthrough element (PRTE) and distal readthrough element (DRTE). (B) Mfold-predicted RNA secondary structure of the readthrough stem-loop (RTSL) with the p22 stop codon in red and the PRTE in green. The gray boxes show wt and mutant forms of the PRTE bulge. Red arrows indicate the position of deleted nucleotides, with the corresponding amino acid deletions shown below and indicated by red lines on the RNA structure. (C) *In vitro* translation assay of TNV-D genomic RNA in wheat germ extract. The names of the TNV-D mutants are listed above their respective lanes, and the identities of the protein products (p82, p29, and p22) are shown on the left. The mock lane consists of a reaction performed with no viral RNA, and TNV represents a reaction completed with wt TNV-D genome RNA. Relative readthrough (Rel. RT) was calculated as the ratio of p82/p22, with that for wt TNV set as 100%. The corresponding means (± the standard errors where applicable) were calculated based on at least three independent assays. (D) Northern blot analysis of TNV-D RNA accumulation in plant protoplasts incubated for 22 h at 22°C. Shown above each lane is the name of the viral genome analyzed. The positions of the viral genome (g) and sg mRNAs (sg1 and sg2) are indicated to the left of the blot. The relative genome levels (Rel. g) are provided below, with the corresponding means (± the standard error, where applicable) calculated from at least three independent protoplast infections. (E and F) Substitutions in the apical loop and upper stem of RTSL are shown as red nucleotides. Relative readthrough and genome levels are provided below each mutant.

idea, a silent substitution of U to G was made in the nucleotide just 3′ to the PRTE, creating Δ3G (Fig. 1B). In this mutant, the introduced G was predicted to pair with the stem, thus allowing for presentation of the entire PRTE in the bulge. For Δ3G, there was an ~2-fold increase in p82 accumulation levels over Δ3, suggesting that accessibility was enhanced; however, replication in protoplasts was not rescued (Fig. 1C and D, right panels). Complete deletion of the 9-nt bulge in mutant ΔPRTE, which generated an uninterrupted portion of helix in RTSL and a more stable RTSL (i.e., ΔG for wt RTSL = −50.22 kcal/mol and ΔPRTE RTSL = −57.64 kcal/mol, at 30°C), also yielded low levels of p82 production (~8%) and no genome replication (Fig. 1C and D). Thus, all deletions in the PRTE bulge dramatically reduced p82 translation *in vitro* and eliminated genome accumulation in infections.

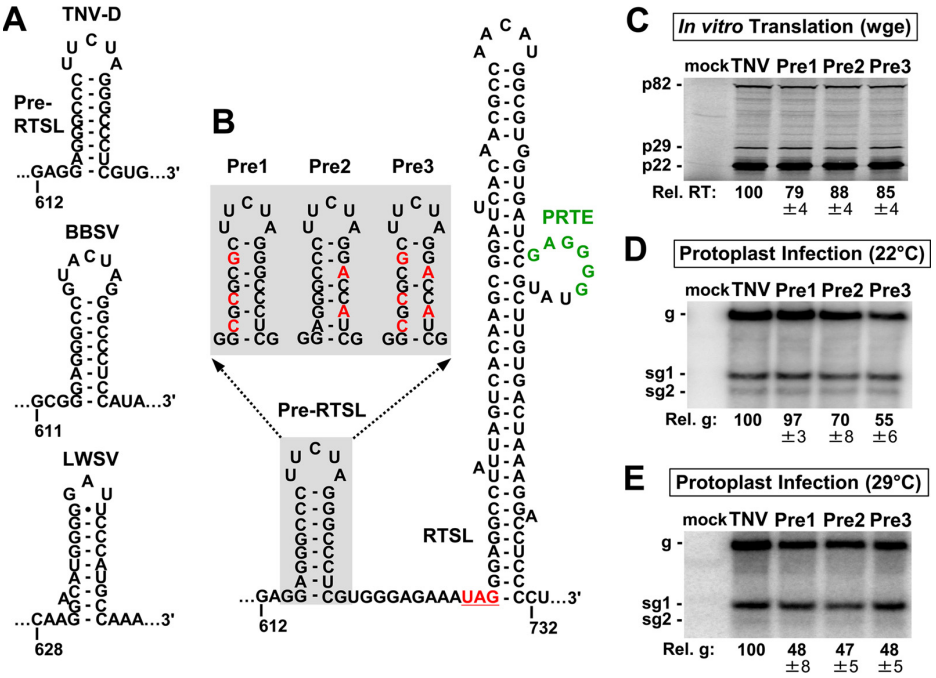

FIG 2 Mutational analysis of Pre-RTSL. (A) Mfold-predicted secondary structure of Pre-RTSL element in betanecroviruses TNV-D, beet black scorch virus (BBSV), and leek white stripe virus (LWSV). The bottom of the stems for TNV-D and BBSV are separated from their cognate UAG stop codons by 10-nt spacers, whereas this spacer length is 3 nt in LWSV. (B) TNV-D Pre-RTSL and RTSL structures. Pre-RTSL mutants are shown in the gray box with substituted nucleotides in red. (C) *In vitro* translation analysis of Pre-RTSL mutants. (D and E) Northern blot analysis of protoplast infections with Pre-RTSL mutants.

Structural features of the upper portion of the RTSL moderately affect viral genome levels but not readthrough. A previous study confirmed the importance of the stability of the RTSL stem for efficient readthrough (6). However, the potential role of other structural features in the RTSL, such as its apical loop and an AG mismatch in its stem, was not investigated (Fig. 1B). Substitutions in the apical loop that maintained the p82 amino acid sequence in mutants Lm1, Lm2, and Lm3 did not notably affect either readthrough or infectivity levels at 22°C (Fig. 1E). Elevating the incubation temperature of protoplast infections, which also increases the stringency of base pairing, can sometimes reveal defective phenotypes (33, 34). Testing the terminal loop mutants at the elevated temperature of 29°C resulted in decreases in genome levels to ~57 to 75% that of the wt (Fig. 1E).

TNV-D, BBSV, and LWSV all contain a single mismatch in the upper portion of their RTSLs. However, only the AG mismatch in TNV-D (Fig. 1B) could potentially be replaced with a CG canonical pair without altering the p82 amino acid sequence; nonetheless, the virus does not implement this option. When the above-mentioned substitution was introduced into mutant USm1, wt levels were observed for readthrough and genome accumulation at 22°C, but at 29°C the genome levels dipped by ~20% (Fig. 1F).

A conserved RNA hairpin upstream of the RTSL affects readthrough minimally and facilitates viral genome accumulation. To further explore RNA elements that could be involved in the readthrough production of p82, the region upstream of the RTSL was examined. A small GC-rich stem-loop structure, here termed Pre-RTSL, was identified 10 nt upstream of the p22 stop codon. Comparable RNA hairpins are also present in other members of the genus *Betanecrovirus* (Fig. 2A), and similarly positioned stem-loops are predicted in all tombusvirids (12). Silent mutations designed to disrupt the stem of Pre-RTSL in mutants Pre1 through Pre3, (Fig. 2B) reduced readthrough by ~10 to 20% (Fig. 2C). In protoplasts incubated at 22°C, there were various degrees of genome accumulation, ranging from ~55 to 97%, whereas at 29°C the level of all

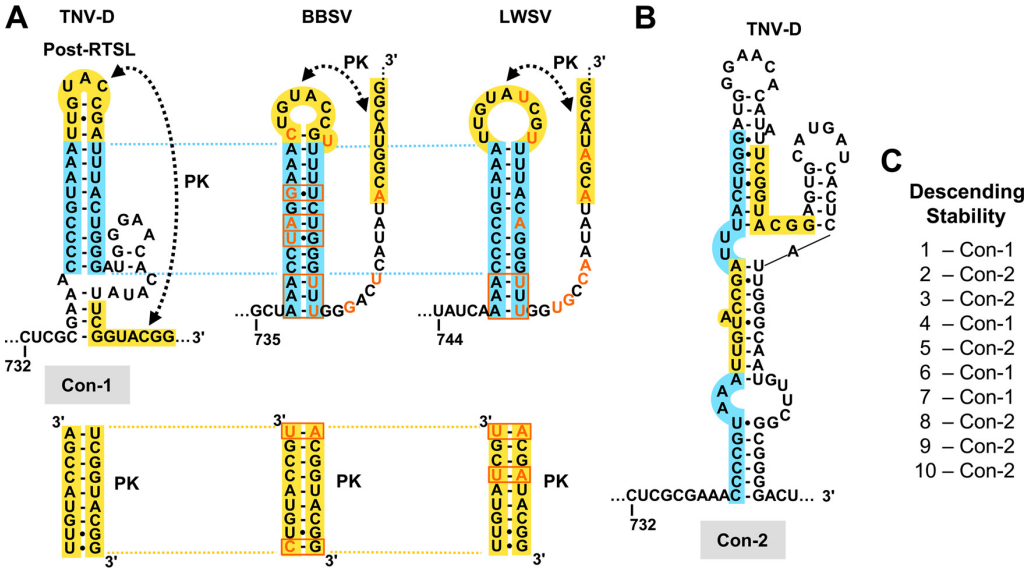

FIG 3 Comparative structural analysis of the Post-RTSL element in betanecroviruses. (A) Mfold-predicted structures for conformation 1 (Con-1) of the Post-RTSL for TNV-D, BBSV, and LWSV. Conserved stems and pseudoknots (PKs) are highlighted, respectively, in blue and yellow. Naturally occurring substitutions in BBSV and LWSV are shown in orange, and those that maintain base pairing are boxed. (B) Mfold-predicted structure for Con-2 of the Post-RTSL in TNV-D. The positions of nucleotides involved in the conserved stem and PK of Con-1 are highlighted in blue and yellow, respectively. (C) Mfold predictions of Con-1 or Con-2 for wt TNV-D genome. Number 1 in the list corresponds to the predicted most stable (or optimal) structure, while those below represent predicted suboptimal structures listed in order of decreasing stabilities.

mutants was reduced by half (Fig. 2D and E). These results suggest a relatively minor role for Pre-RTSL in readthrough under our *in vitro* conditions, but a noteworthy role during infections.

RNA structures downstream of the RTSL. In TNV-D, there is a predicted tertiary RNA structure, here termed Post-RTSL (or Con-1), located immediately downstream of the RTSL (Fig. 3A). Compared to corresponding segments in other betanecrovirus genomes, regions of conservation included a base-paired stem structure (blue), and a potential pseudoknot (PK) forming interaction (yellow). The stems in BBSV and LWSV are extended by three base pairs and contain substitutions that maintain the helices (Fig. 3A, upper panel). The PK interaction is also well conserved and, notably, includes covarying base pairs (Fig. 3A, lower panel). In TNV-D, but not the other betanecroviruses, this region can adopt an alternate fold, Con-2 (Fig. 3B), which was predicted in 6 of the top 10 most thermodynamically stable structures when the complete TNV-D genome was analyzed by Mfold (Fig. 3C). Thus, either or both structures could be functionally relevant in TNV-D.

To further clarify the formation of Con-1 and/or Con-2, *in vitro* selective 2′-hydroxyl acylation analyzed by primer extension (SHAPE) analysis was performed on transcripts of the full-length TNV-D genome. In SHAPE probing, nucleotides that are flexible are more readily modified and are predicted to correspond to single-stranded residues (35). All residues in regions 1 and 3 (blue), corresponding to the stem of Con-1, exhibited low flexibility (Fig. 4A), a finding consistent with the formation of this stem (Fig. 4B). Regions 2 and 5 (yellow), which mapped to the proposed pseudoknot of Con-1, exhibited lower levels of flexibility at the 3′ end of region 2 and the 5′ end of region 5, compared to the rest of the sequences in these two regions (Fig. 4A). This suggests that, under the assay conditions, the proposed pseudoknot may be partially formed and less stable. The presence of highly reactive residues within predicted double-stranded regions in Con-2 and of poorly reactive nucleotides in proposed single-stranded regions (Fig. 4C) indicates that Con-2 is likely not a dominant structure in solution. Accordingly, both

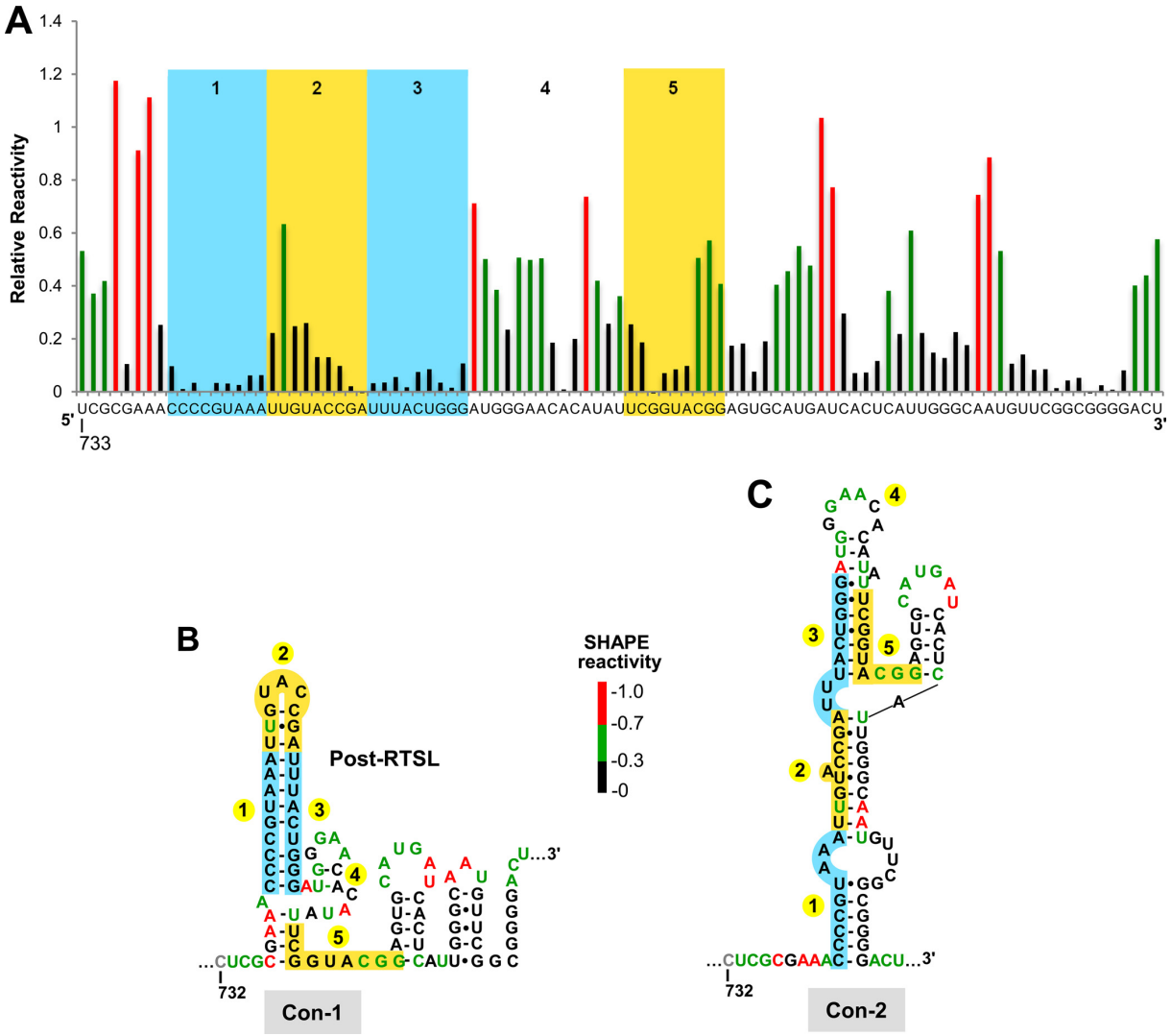

FIG 4 SHAPE analysis of the Post-RTS element. (A) The relative reactivity of each nucleotide is plotted graphically, where red, green, and black bars represent highly reactive, moderately reactive, and poorly reactive residues, respectively. Regions of the graph corresponding to the stem and pseudoknot of Con-1 are highlighted in blue and yellow, respectively, and numbered. (B) Mfold-predicted structure of Con-1 with color-coded stem and PK. Nucleotides in red, green, and black convey relative SHAPE reactivity (see key). (C) Corresponding Mfold-predicted secondary structure for Con-2, color-coded as described in panel B.

comparative structural analysis (Fig. 3) and chemical probing (Fig. 4) more strongly support Post-RTSL forming Con-1.

Con-1 of Post-RTSL is important for readthrough and virus viability. To determine whether the formation of the stem portion of Con-1 was important for p82 production, compensatory mutational analysis was used to disrupt and then restore one of the base pairs in the helix (Fig. 5A). The downstream substitution in mutants 1B and 1C resulted in a conservative amino acid change of threonine to serine; however, this same replacement is present naturally in BBSV. Neither the *in vitro* translation assay nor protoplast infections incubated at 22°C showed compelling deviations from the wt of either p82 or genome levels, respectively (Fig. 5B and C). However, when the protoplast incubation temperature was raised to 29°C, both disruptive mutants showed a decline in genomes to ~50 to 60% of the wt, and the restorative mutant resulted the in recovery of accumulation to ~86% (Fig. 5D). Thus, the stem of Con-1 appears to contribute to virus viability.

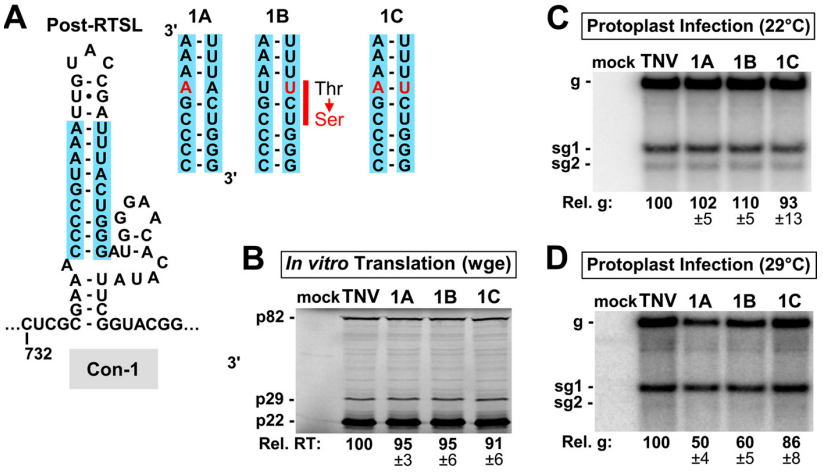

FIG 5 Mutational analysis of the Post-RTSL Con-1 stem. (A) Wt and mutant stem interactions are shown with nucleotide substitutions in red. The nucleotide substitution in mutants 1B and 1C results in an amino acid change from threonine to serine in the p82 product. (B) *In vitro* translation analysis of pseudoknot mutants. (C and D) Northern blot analysis of protoplast infections with Pre-RTSL mutants.

To investigate the importance of the proposed Con-1 pseudoknot formation, three base pairs were targeted with silent compensatory mutations in PKA, PKB, and PKC (Fig. 6A). In wheat germ extract, the disruptive mutants resulted in a decline in readthrough to ~52 and ~57%, and the regenerative mutant resulted in a recovery of p82 production to ~99% (Fig. 6B). In protoplasts incubated at 22°C there was no decline in genome accumulation for all mutants (Fig. 6C), but at 29°C the levels

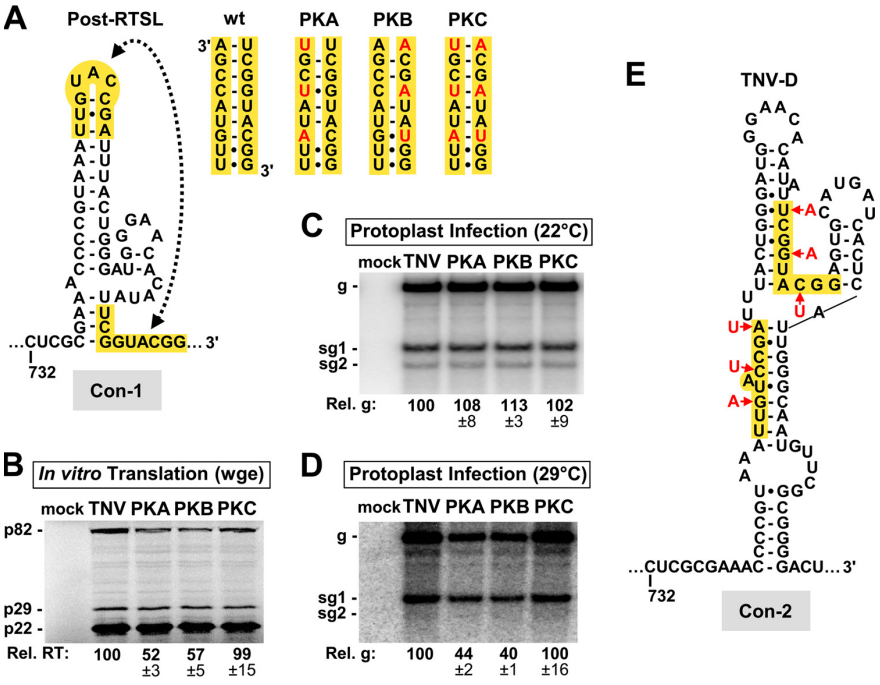

FIG 6 Mutational analysis of the Post-RTSL Con-1 pseudoknot. (A) Wt and mutant pseudoknot interactions are highlighted in yellow with compensatory mutations indicated in red. (B) *In vitro* translation analysis of pseudoknot mutants. (C and D) Northern blot analysis of protoplast infections with pseudoknot mutants. (E) Substitutions from mutant PKC mapped onto Con-2.

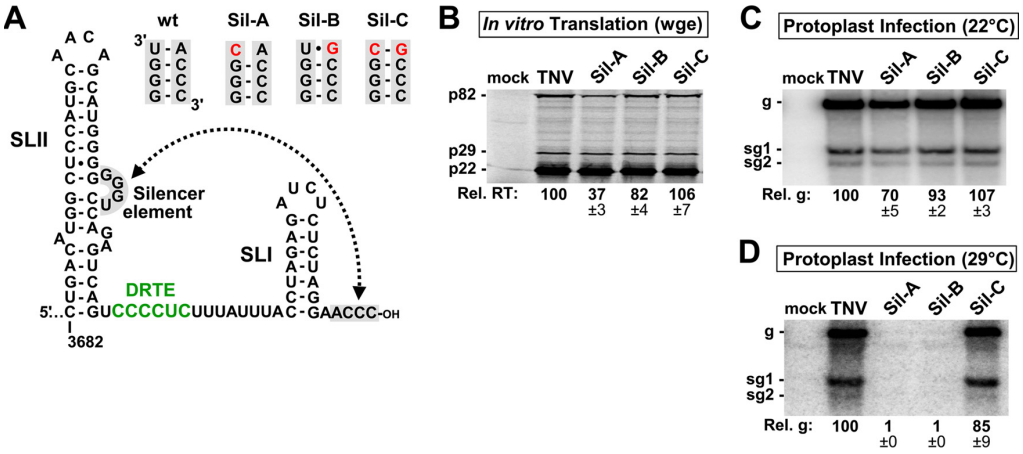

FIG 7 Mutational analysis of the silencer/3′-end interaction. (A) Predicted secondary structure of the 3′ UTR of TNV-D with the silencer/3′-end interaction highlighted in gray and the DRTE sequence in green. Wt and mutant base pairing interactions for the interaction are shown, with nucleotide replacements in red. (B) *In vitro* translation analysis of silencer/3′-end mutants. (C and D) Northern blot analysis of protoplast infections with silencer/3′-end mutants.

correlated well with those observed for readthrough (Fig. 6D). Mapping the substitutions in PKC, which yielded wt performance, onto Con-2, revealed that the changes would destabilize the predicted structure (Fig. 6E). Accordingly, Con-1 of Post-RTSL appears to be the functionally relevant structure.

The silencer/3′-end interaction modulates readthrough and genome accumulation. The 3′-terminal nucleotides in tombusvirid genomes are complementary to a nearby upstream sequence, termed the silencer element (36). Silencer/3′-end interactions have been shown to be important for viral genome replication in several family members, including tombusviruses (34, 37), carmoviruses (38), and aureusviruses (39). TNV-D has a predicted silencer/3′-end interaction (Fig. 7A); however, its functional importance has not been assessed. This 3′-proximal region is also relevant to translational readthrough since the sequence that intervenes the silencer/3′-end interaction includes the DRTE, which must pair with the PRTE for efficient p82 production (Fig. 7A) (6). Consequently, the silencer/3′-end interaction could influence the presentation or accessibility of the DRTE.

To address this possibility, compensatory mutations were introduced at the UA base pair in the silencer/3′-end interaction (Fig. 7A). Replacement with a CG base pair was chosen, because these residues are present at corresponding positions in the BBSV genome. The CA mismatch in Sil-A produced lower levels of p82 (~37%) and reduced genome accumulation in protoplasts incubated at 22°C (~70%), while milder negative effects were seen for Sil-B containing the UG wobble base pair (Fig. 7B and C). The presence of a canonical CG base pair in Sil-C restored both activities to wt levels (Fig. 7B and C). Increasing protoplast incubation temperature to 29°C resulted in negligible genome levels for Sil-A and Sil-B (Fig. 7D), which were recovered to ~85% of the wt level in Sil-C. Therefore, the silencer/3′-end interaction modulates readthrough and is crucial for genome accumulation.

The apical loop of SLII facilitates readthrough and genome accumulation. Two stem-loop structures, SLI and SLII, flank the DRTE (Fig. 8A). To investigate their possible effects on readthrough and genome levels, the terminal loop sequences in SLI and SLII were replaced with superstable tetranucleotide loops, GAAA (Fig. 8A). When the loop of SLI was replaced, readthrough and replication levels remained close to those for wt (Fig. 8B and C). In contrast, loop replacement in SLII led to a significant decrease in readthrough (~15%) and genome (~30%) levels at 22°C (Fig. 8B and C). To confirm the latter result, the SLII terminal loop (AACA) was replaced with a different class of superstable tetra-loop (UUCG) or a modified loop sequence (GACG) (Fig. 8D). In both

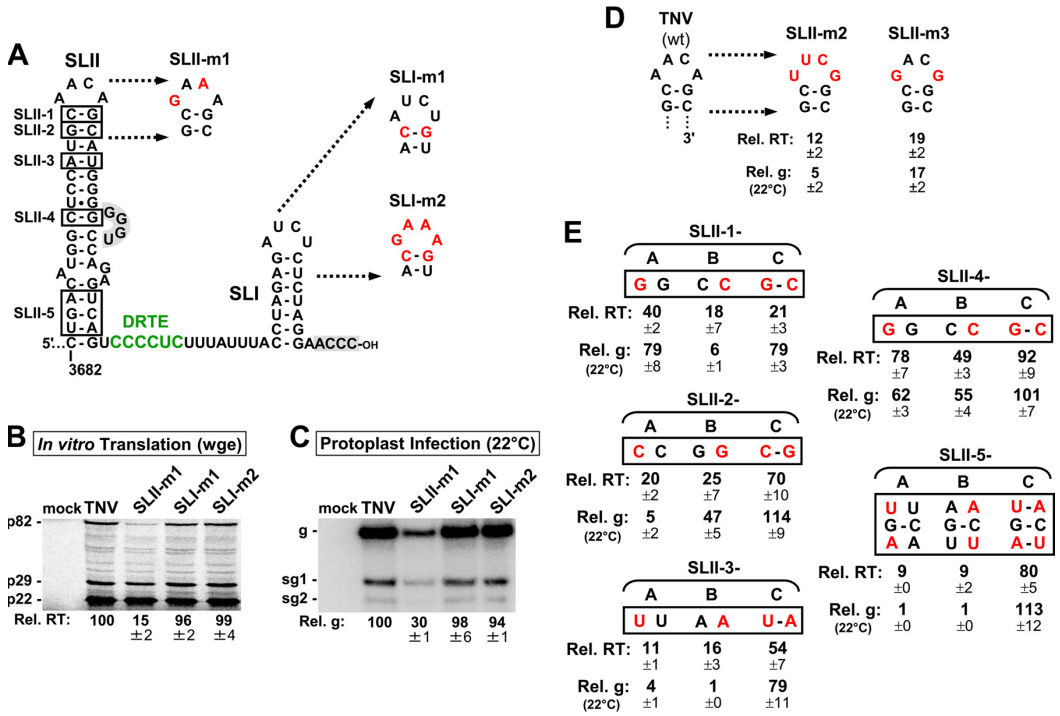

FIG 8 Mutational analysis of SLI and SLII in the 3′ UTR. (A) Base pairs in SLII targeted with compensatory mutations are boxed in black. Nucleotide substitutions in apical loops are shown in red. GNRA-type tetraloops are more stable when closed by a CG base pair. SLI-m1 is a control to determine the effect of changing the wt GC closing base pair to CG. (B) *In vitro* translation analysis of SLII and SLI apical loop mutants. (C) Northern blot analysis of protoplast infections of SLII and SLI apical loop mutants. (D) Analysis of additional SLII apical loop mutants. Relative readthrough and genome levels are provided below each mutant. (E) Analysis of sets of compensatory mutants in SLII. The position for each mutant set in SLII is indicated in panel A.

cases, there was a decrease in p82 production and genome accumulation to below 20% of wt, reinforcing the functional relevance of the loop. Strikingly, these strong phenotypes were observed at the less stringent 22°C incubation temperature of protoplasts, further underscoring the significance of this structural element.

Due to the critical role of the terminal loop in SLII, the possible influence of its immediate context was examined using a series of compensatory mutations targeting base pairs in the upper (SLII-1, -2, and -3 series), middle (SLII-4 series), and lower (SLII-5 series) regions of the stem in SLII (Fig. 8E). All disruptive mutations in the upper portion of the stem had various negative effects that were partially rescued upon restoration of the base pairs; the exception being SLII-1C, where the regenerative GC pair did not lead to recovered readthrough (Fig. 8E). Assessment of the middle and lower stem regions (SLII-4 and -5 series) also supported the importance of stem stability in regions for both readthrough and genome accumulation (Fig. 8E). Accordingly, the entire SLII structure is relevant to the activities that were monitored.

One possible mode of function for the terminal loop of SLII is to interact via base pairing with a complementary sequence elsewhere in the TNV-D genome. Indeed, there is ample precedence for intragenomic interactions modulating various activities among tombusvirids (26, 40) and other plus-strand RNA viruses (7, 41, 42). Several candidate partner sequences for the terminal loop of SLII were selected for analysis based on their: (i) conservation between TNV-D, BBSV, and LWSV; (ii) potential to extend base pairing beyond the AACA loop sequence; and (iii) proximity to previously characterized functional regions of the genome (Fig. 9A). Most of the putative partner interactions investigated involved canonical base pairing (Fig. 9B); however, two did not (Fig. 9C). In all cases, silent modifications to the candidate partner sequence did not notably

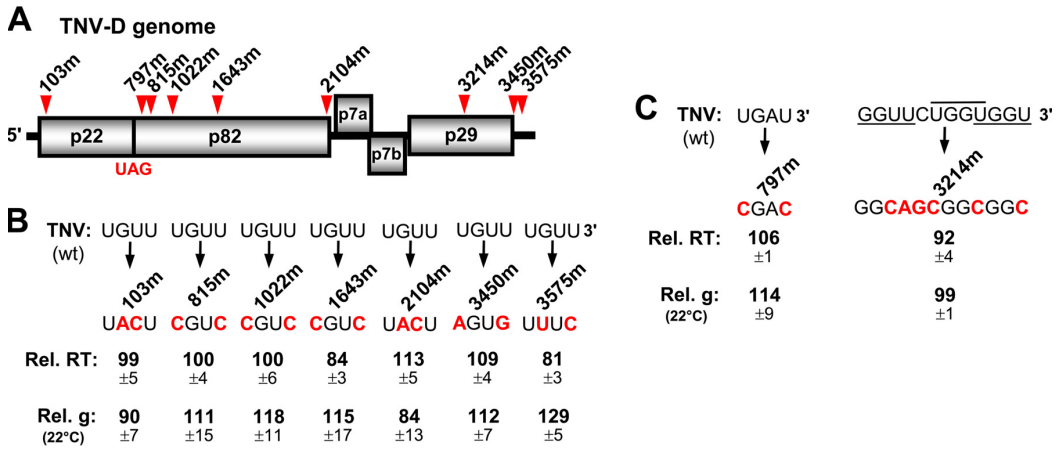

FIG 9 Testing potential base pairing partners of SLII. (A) Cartoon representation of the TNV-D genome with the relative positions of substitutions. Mutant names indicate the TNV genome coordinate for the first nucleotide position of each potential pairing interaction. (B) Substitutions introduced into potential canonical base pairing partners of SLII loop are shown in red. The effects of the substitutions on relative readthrough and relative genome accumulation are shown below each mutant. (C) Analysis of substitutions introduced into potential noncanonical base pairing partners of SLII loop. Lines above and below the sequence define areas of potential base pairing with ACAA.

affect either readthrough or genome accumulation, thereby ruling out their possible involvement in the activity associated with the terminal loop in SLII (Fig. 9B and C).

DISCUSSION

Translational readthrough represents an important gene expression strategy utilized by different classes of viruses (9). Our analysis of TNV-D suggests that RNA elements beyond those previously identified can markedly influence this process and the robustness of viral infections. These features and their possible roles in translational readthrough and virus reproduction are discussed below.

RTSL. The RTSL in TNV-D contains a PRTE that interacts with the 3′-proximal DRTE to enhance readthrough production of p82 (Fig. 1A and B) (6). Currently, how this and similar interactions in other tombusvirids (5, 12) promote readthrough is unknown. One possibility is that binding of the DRTE to the PRTE-containing bulge in RTSL stabilizes the RTSL helix. This is a reasonable option, because the stability of RNA structures 3′ proximal to readthrough sites, including that in TNV-D (6), is known to positively correlate with readthrough efficiency (1). However, our results indicated that deletion of the bulge in mutant ΔPRTE, which would stabilize the RTSL helix, inhibited readthrough activity (Fig. 1C). This suggests that the PRTE-DRTE interaction does more than simply stabilize the RTSL. Instead, the specific structure formed by the interaction could be important for function, or the interaction could recruit other required 3′-proximal RNA elements or their associated proteins. The readthrough defects observed *in vitro* in mutants with deletions in the PRTE-bulge could be responsible for the corresponding lack of infectivity in protoplasts (Fig. 1D), but it is also possible that the deletion of encoded amino acids rendered the RdRp inactive.

The upper region of the TNV-D RTSL was also investigated for function. In turnip crinkle virus (TCV) (genus *Carmovirus*, family *Tombusviridae*), an apical portion of its RTSL is essential for efficient readthrough, because it forms a local pseudoknot with the 3′ end of the RTSL (12). When the upper portion of the TNV-D RTSL was investigated, the results indicated that neither the terminal loop nor a base pair mismatch affected readthrough; although moderate reductions in genome accumulation were observed at 29°C (Fig. 1E and F). Therefore, unlike in TCV, the upper region of the RTSL in TNV-D does not appear to play a major role in readthrough under our assay conditions.

Pre-RTSL. GC-rich RNA hairpins are predicted just 5′ of frameshift and readthrough sites in tombusvirids (12); however, they do not share any noteworthy sequence

identity and their positions relative to their cognate stop codons vary, i.e., ~0 to 10 nt (unpublished data). Functional RNA hairpins immediately upstream of recoding sites have been described and studied previously. The RNA hairpin in pea enation mosaic virus (genus *Umbravirus*, family *Tombusviridae*) does not influence frameshifting in the wt context, but can act as an inhibitor when tested in a modified viral context (11). Conversely, the upstream hairpin in barley yellow dwarf virus (genus *Luteovirus*, family *Luteoviridae*, but related to tombusvirids) (43) was found to enhance frameshifting (18). In a third example, severe acute respiratory syndrome coronavirus, the upstream hairpin downregulated frameshifting activity (10). Thus, the effects of such RNA structures on frameshifting can vary significantly.

For readthrough, disruption of the upstream hairpin present in TCV did not affect readthrough *in vitro*; however, genome accumulation was reduced in infections to 28% that of wt (12). Our results with Pre-RTSL in TNV-D are similar to those for TCV in that infectivity was reduced (~48% of wt), but, in contrast, readthrough levels were also negatively affected, albeit to a lesser degree (79 to 88% of wt) (Fig. 2). Consequently, the TNV-D Pre-RTSL appears to moderately affect readthrough under our *in vitro* assay conditions. The variability in distance of upstream tombusvirid hairpins from their stop codons suggests that, if some of them also function in readthrough, precise spacing may not be important. Also, since sequence identity is not conserved among the different hairpins, the formation of a stable helix is likely to be a key feature for their function. Theoretically, the Pre-RTSL could influence ribosome readthrough activity (i) when the ribosome first encounters the RNA structure, which may stall it, (ii) if the structure reforms when the ribosome is engaging the stop codon, and/or (iii) if the structure functions as an "insulator" that sequesters proximal sequence to guard against their interference with proper folding of the RTSL. Additional studies will be required to determine the role of these conserved structures in readthrough and/or other aspects of virus replication.

Post-RTSL. Unexpectedly, an RNA element located just 3′ to the RTSL was found to be important for efficient readthrough *in vitro*. SHAPE, mutational, and comparative RNA structural analyses were all consistent with Con-1 being the functional structure of the Post-RTSL. The Post-RTSL is predicted to form a pseudoknot structure that is located just 9 nts downstream from the base of the RTSL. This would position it close to ribosomes engaging the stop codon and could allow for the structure, or possible associated proteins, to interact with the ribosome or release factors and cause increased readthrough. Alternatively, as considered for the Pre-RTSL, the Post-RTSL could act as a type of structural insulator to promote proper folding of the RTSL.

As a distinct local structure, positioned immediately downstream from the RTSL, the Post-RTSL represents a novel type of readthrough-modulating element. In TBSV, a similarly positioned (i.e., 3 nt from the RTSL), but structurally different local RNA secondary structure was shown to contribute to efficient genome accumulation (44); however, its influence on translation or readthrough was not assessed. Likewise, aureusviruses have a distinct conserved local secondary structure 4 to 6 nt downstream from their RTSL that has not been functionally characterized (unpublished). The Post-RTSLs in these three genera do not share any obvious structural similarities, but they all reside in RdRp coding regions, and the RdRps of betanecroviruses are most closely related to those of tombusviruses and aureusviruses (20). Thus, although the structures have taken different evolutionary paths, they may maintain their original function which, based on our results with TNV-D, may be, in part, to facilitate readthrough.

3′ UTR. The 3′-proximal ~80 nt of the TNV-D genome harbors RNA elements important for both genome replication and readthrough (6, 25). Our findings show that the silencer/3′-end interaction is critical for genome accumulation in protoplast infections (Fig. 7D), which is the first demonstration of this for a betanecrovirus and consistent with results from other studies showing its importance for tombusvirid genome replication (36–39). The same interaction also modestly modulated readthrough under our assay conditions (Fig. 7B). In contrast, the loop of SLII in the

3′-proximal region was found to be a major contributor to readthrough efficiency because three different loop modifications led to an average reduction in readthrough of ~7-fold (Fig. 8B and D) and a corresponding average drop in genome accumulation of ~6-fold (Fig. 8C and D). Collectively, these results suggest that the identity of the nucleotides in the loop, AACA, is important for its function. In contrast, data from compensatory mutational analysis of SLII indicated that base pairing of the stem region, not sequence identity, is more important (Fig. 8E). Although most of the stem may act to properly present the loop sequence, the inability to recover readthrough activity in compensatory mutant SLII-1C suggests a possible identity-dependent role for the wt CG closing base pair (Fig. 8E).

One way that the AACA loop sequence could function is by interacting with a complementary sequence proximal to SLII, the RTSL, or other regions of the viral genome. Accordingly, possible base pairing partner sequences were selected and assessed by introducing substitutions into them that were predicted to disrupt potential interactions with AACA (Fig. 9). In all cases, no major effects on either readthrough or genome accumulation in infections were observed. It is, however, possible that the AACA sequence has a base pairing partner sequence other than those tested. Conversely, the sequence could engage other genomic sequences through noncanonical interactions or bind to a required protein factor. Also of significance is that when the PRTE-DRTE interaction is formed, it positions SLII proximal to the readthrough site, which would allow for it or any bound cargo to engage the ribosome or translation release factors. Interestingly, in the two other sequenced betanecroviruses, LWSV and BBSV, the corresponding SLII loop sequences are cAACAg and cUCCUAUg, respectively (loop sequences are capitalized). Hence, the sequence in LWSV is identical to that in TNV-D, whereas the one in BBSV is markedly different in both size and nucleotide content. It remains to be determined whether either of these sequences is able to function in a manner similar to that observed for TNV-D.

MATERIALS AND METHODS

Plasmid construction. All TNV-D clones created for this study were derived from wild-type (wt) TNV-D cDNA in a pUC19 plasmid, supplied by Robert Coutts (21), which was modified to introduce a SmaI site at the viral 3′ terminus (31). Standard PCR-based site-directed mutagenesis was used to create TNV-D mutants, using a Velocity DNA polymerase PCR kit (Bioline). Sequencing confirmed the correctness of all mutant constructs and the changes introduced into the TNV-D genome are shown in the accompanying figures.

Preparation of viral RNAs. Uncapped *in vitro* transcripts of SmaI-linearized TNV-D constructs were produced using the AmpliScribe T7-Flash transcription kit (Epicentre Technologies) as described previously (45). RNA transcript concentrations were quantified by spectrophotometry, and the quality of transcripts was verified by agarose gel electrophoresis.

RNA secondary structure prediction. RNA secondary structures were predicted at 37°C using Mfold version 3.6 using default settings (46, 47).

***In vitro* SHAPE RNA structure probing.** Selective 2′-hydroxyl acylation analyzed by primer extension (SHAPE) was performed as previously described (5). Briefly, full-length *in vitro* transcribed TNV-D genomic RNA was refolded, treated with 1-methyl-7-nitroisatoic anhydride, and then subjected to reverse transcription using Superscript IV reverse transcriptase (Invitrogen). Fluorescently labeled primers complementary to TNV-D nt 1079 to 1108 were used to evaluate the region of interest. Raw fluorescence intensity data were analyzed using ShapeFinder (48). The top 10 peak intensities were averaged, and all raw nucleotide reactivities were divided by this average. The average relative reactivities from two *in vitro* SHAPE experiments were plotted graphically and mapped onto Mfold-predicted conformations.

***In vitro* translation.** The levels of protein accumulation were measured by incubating RNA transcripts in nuclease-treated wheat germ extract (Promega). Uncapped viral genomic RNA (0.5 pmol) was incubated in the extract for 1 h at 25°C in the presence of [^{35}S]methionine, as described previously (6). Products were separated by sodium dodecyl sulfate-polyacrylamide gel electrophoresis in a 12% polyacrylamide gel. Viral proteins produced were detected using a Typhoon TRIO+ variable mode imager (GE Healthcare) and quantified using QuantityOne software (Bio-Rad). All trials were repeated at least three times, and the averages were calculated with the standard errors.

Protoplast infection. Cucumber cotyledon protoplasts were prepared and transfected with uncapped *in vitro* transcribed viral genomic RNA (45). Specifically, 3×10^5 protoplasts were transfected with 3 μg of viral genomic RNA and incubated under constant light for 22 h at either 22 or 29°C. The total nucleic acids were extracted as described previously (45) and separated in nondenaturing 2% agarose gels. Viral RNAs were detected via Northern blotting using three ^{32}P-radiolabeled probes complementary to the 3′ end of TNV-D: nt 2821 to 2840, 3520 to 3532, and 3643 to 3663 (31). Viral RNA accumulation

was monitored using a Typhoon TRIO+ variable mode imager and quantified using QuantityOne software. All trials were repeated at least three times, and averages were calculated with the standard errors.

ACKNOWLEDGMENTS

We thank members of our laboratory for reviewing the manuscript and Robert Coutts for providing the TNV-D clone.

This research was funded by an NSERC Discovery Grant. L.R.N. was supported by an NSERC Graduate Scholarship.

REFERENCES

1. Firth AE, Brierley I. 2012. Noncanonical translation in RNA viruses. J Gen Virol 93(Pt 7):1385–1409. https://doi.org/10.1099/vir.0.042499-0.
2. Harrell L, Melcher U, Atkins JF. 2002. Predominance of six different hexanucleotide recoding signals 3′ of readthrough stop codons. Nucleic Acids Res 30:2011–2017. https://doi.org/10.1093/nar/30.9.2011.
3. Skuzeski JM, Nichols LM, Gesteland RF, Atkins JF. 1991. The signal for a leaky UAG stop codon in several plant viruses includes the two downstream codons. J Mol Biol 218:365–373. https://doi.org/10.1016/0022-2836(91)90718-L.
4. Urban C, Zerfass K, Fingerhut C, Beier H. 1996. UGA suppression by tRNACmCATrp occurs in diverse virus RNAs due to a limited influence of the codon context. Nucleic Acids Res 24:3424–3430. https://doi.org/10.1093/nar/24.17.3424.
5. Cimino PA, Nicholson BL, Wu B, Xu W, White KA. 2011. Multifaceted regulation of translational readthrough by RNA replication elements in a tombusvirus. PLoS Pathog 7:e1002423. https://doi.org/10.1371/journal.ppat.1002423.
6. Newburn LR, Nicholson BL, Yosefi M, Cimino PA, White KA. 2014. Translational readthrough in Tobacco necrosis virus-D Virology 450-451: 258–265. https://doi.org/10.1016/j.virol.2013.12.006.
7. Newburn LR, White KA. 2015. *Cis*-acting RNA elements in positive-strand RNA plant virus genomes. Virology 479-480:434–443. https://doi.org/10.1016/j.virol.2015.02.032.
8. Firth AE, Wills NM, Gesteland RF, Atkins JF. 2011. Stimulation of stop codon readthrough: frequent presence of an extended 3′ RNA structural element. Nucleic Acids Res 39:6679–6691. https://doi.org/10.1093/nar/gkr224.
9. Beier H, Grimm M. 2001. Misreading of termination codons in eukaryotes by natural nonsense suppressor tRNAs. Nucleic Acids Res 29:4767–4782. https://doi.org/10.1093/nar/29.23.4767.
10. Cho C, Lin S, Chou M, Hsu H, Chang K. 2013. Regulation of programmed ribosomal frameshifting by cotranslational refolding RNA hairpins. PLoS One 8:e62283. https://doi.org/10.1371/journal.pone.0062283.
11. Gao F, Simon AE. 2016. Multiple cis-acting elements modulate programmed −1 ribosomal frameshifting in Pea enation mosaic virus. Nucleic Acids Res 44:878–895. https://doi.org/10.1093/nar/gkv1241.
12. Kuhlmann MM, Chattopadhyay M, Stupina VA, Gao F, Simon AE. 2016. An RNA element that facilitates programmed ribosomal readthrough in turnip crinkle virus adopts multiple conformations. J Virol 90:8575–8591. https://doi.org/10.1128/JVI.01129-16.
13. Orlova M, Yueh A, Leunge J, Goff SP. 2003. Reverse transcriptase of Moloney murine leukemia virus binds to eukaryotic release factor 1 to modulate suppression of translational termination. Cell 115:319–331. https://doi.org/10.1016/S0092-8674(03)00805-5.
14. Li Y, Treffers EE, Napthine S, Tas A, Zhu L, Sun Z, Bell S, Mark BL, van Veelen PA, van Hemert MJ, Firth AE, Brierley I, Snijder EJ, Fang Y. 2014. Transactivation of programmed ribosomal frameshifting by a viral protein. Proc Natl Acad Sci U S A 111:E2172–E2181. https://doi.org/10.1073/pnas.1321930111.
15. Beznosková P, Wagner S, Jansen ME, von der Haar T, Valášek LS. 2015. Translation initiation factor eIF3 promotes programmed stop codon readthrough. Nucleic Acids Res 43:5099–5111. https://doi.org/10.1093/nar/gkv421.
16. Napthine S, Treffers EE, Bell S, Goodfellow I, Fang Y, Firth AE, Snijder EJ, Brierley I. 2016. A novel role for poly(C) binding proteins in programmed ribosomal frameshifting. Nucleic Acids Res 44:5491–5503. https://doi.org/10.1093/nar/gkw480.
17. Sit TL, Lommel SA. 2010. Tombusviridae, p 1–9. In Encyclopedia of life sciences. John Wiley & Sons, Ltd., Chichester, United Kingdom.
18. Barry JK, Miller WA. 2002. A −1 ribosomal frameshift element that requires base pairing across four kilobases suggests a mechanism of regulating ribosome and replicase traffic on a viral RNA. Proc Natl Acad Sci U S A 99:11133–11138. https://doi.org/10.1073/pnas.162223099.
19. Tajima Y, Iwakawa HO, Kaido M, Mise K, Okuno T. 2011. A long-distance RNA– RNA interaction plays an important role in programmed −1 ribosomal frameshifting in the translation of p88 replicase protein of Red clover necrotic mosaic virus. Virology 417:169–178. https://doi.org/10.1016/j.virol.2011.05.012.
20. Rochon D, Lommel SA, Martelli GP, Rubino L, Russo M. 2012. Tombusviridae, p 1111–1138. *In* King AMQ, Adams MJ, Carstens EB, Lefkowitz EJ (ed), Virus taxonom, ninth report of the international committee on taxonomy of viruses. Elsevier/Academic Press, London, United Kingdom.
21. Coutts RH, Rigden JE, Slabas AR, Lomonossoff GP, Wise PJ. 1991. The complete nucleotide sequence of tobacco necrosis virus strain D. J Gen Virol 72(Pt 7):1521–1529. https://doi.org/10.1099/0022-1317-72-7-1521.
22. Cao Y, Cai Z, Ding Q, Li D, Han C, Yu J, Lui Y. 2002. The complete nucleotide sequence of Beet black scorch virus (BBSV), a new member of the genus *Necrovirus*. Arch Virol 147:2431–2435. https://doi.org/10.1007/s00705-002-0896-1.
23. Lot H, Rubino L, Delecolle B, Jacquemond M, Tuturo C, Russo M. 1996. Characterization, nucleotide sequence and genome organization of Leek white stripe virus, a putative new species of the genus *Necrovirus*. Arch Virol 141:2375–2386. https://doi.org/10.1007/BF01718638.
24. Shen R, Miller WA. 2004. The 3′ untranslated region of Tobacco necrosis virus RNA contains and Barley yellow dwarf virus-like cap-independent translation element. J Virol 78:4655–4664. https://doi.org/10.1128/JVI.78.9.4655-4664.2004.
25. Shen R, Miller WA. 2007. Structures required for poly(A) tail-independent translation overlap with, but are distinct from, cap-independent translation and RNA replication signals at the 3′ end of Tobacco necrosis virus RNA. Virology 358:448–458. https://doi.org/10.1016/j.virol.2006.08.054.
26. Simon AE, Miller WA. 2013. 3′ cap-independent translation enhancers of plant viruses. Annu Rev Microbiol 67:21–42. https://doi.org/10.1146/annurev-micro-092412-155609.
27. Offei SK, Coffin RS, Coutts RH. 1995. The Tobacco necrosis virus p7a protein is a nucleic acid-binding protein. J Gen Virol 76(Pt 6):1493–1496. https://doi.org/10.1099/0022-1317-76-6-1493.
28. Offei SK, Coutts RH. 1996. Location of the 5′ termini of Tobacco necrosis virus strain D subgenomic mRNAs. J Phytopathol 144:13–17. https://doi.org/10.1111/j.1439-0434.1996.tb01481.x.
29. Molnár A, Havelda Z, Dalmay T, Szutorisz H, Burgyán J. 1997. Complete nucleotide sequence of tobacco necrosis virus strain DH and genes required for RNA replication and virus movement. J Gen Virol 78: 1235–1239. https://doi.org/10.1099/0022-1317-78-6-1235.
30. Chkuaseli T, Newburn LR, Bakhshinyan D, White KA. 2015. Protein expression strategies in Tobacco necrosis virus-D. Virology 486:54–62. https://doi.org/10.1016/j.virol.2015.08.032.
31. Jiwan SD, Wu B, White KA. 2011. Subgenomic mRNA transcription in tobacco necrosis virus. Virology 418:1–11. https://doi.org/10.1016/j.virol.2011.07.005.
32. Fernández-Miragall O, Hernández C. 2011. An internal ribosome entry site directs translation of the 3′-gene from Pelargonium flower break virus genomic RNA: implications for infectivity. PLoS One 6:e22617. https://doi.org/10.1371/journal.pone.0022617.
33. Monkewich S, Lin H, Fabian MR, Xu W, Na H, Ray D, Chernysheva OA, Nagy PD, White KA. 2005. The p92 polymerase coding region contains an internal RNA element required at an early step in Tombusvirus

genome replication. J Virol 79:4848–4858. https://doi.org/10.1128/JVI.79.8.4848-4858.2005.
34. Na H, Fabian MR, White KA. 2006. Conformational organization of the 3′ untranslated region in the tomato bushy stunt virus genome. RNA 12:2199–2210. https://doi.org/10.1261/rna.238606.
35. Low JT, Weeks KM. 2010. SHAPE-directed RNA secondary structure prediction. Methods 52:150–158. https://doi.org/10.1016/j.ymeth.2010.06.007.
36. Na H, White KA. 2006. Structure and prevalence of replication silencer-3′ terminus RNA interactions in *Tombusviridae*. Virology 345:305–316. https://doi.org/10.1016/j.virol.2005.09.008.
37. Pogany J, Fabian MR, White KA, Nagy PD. 2003. A replication silencer element in a plus-strand RNA virus. EMBO J 22:5602–5611. https://doi.org/10.1093/emboj/cdg523.
38. Zhang J, Zhang G, Guo R, Shapiro BA, Simon AE. 2006. A pseudoknot in a preactive form of a viral RNA is part of a structural switch activating minus-strand synthesis. J Virol 80:9181–9191. https://doi.org/10.1128/JVI.00295-06.
39. Lee PK, White KA. 2014. Construction and characterization of an aureusvirus defective RNA. Virology 452-453:67–74. https://doi.org/10.1016/j.virol.2013.12.033.
40. Miller WA, White KA. 2006. Long-distance RNA-RNA interactions in plant virus gene expression and replication. Annu Rev Phytopathol 44:447–467. https://doi.org/10.1146/annurev.phyto.44.070505.143353.
41. Nicholson BL, White KA. 2014. Functional long-range RNA-RNA interactions in positive-strand RNA viruses. Nat Rev Microbiol 12:493–504. https://doi.org/10.1038/nrmicro3288.
42. Nicholson BL, White KA. 2015. Exploring the architecture of viral RNA genomes. Curr Opin Virol 12:66–74. https://doi.org/10.1016/j.coviro.2015.03.018.
43. Miller WA, Liu S, Beckett R. 2002. Barley yellow dwarf virus: *Luteoviridae* or *Tombusviridae*? Mol Plant Pathol 3:177–183. https://doi.org/10.1046/j.1364-3703.2002.00112.x.
44. Wu B, Grigull J, Ore MO, Morin S, White KA. 2013. Global organization of a positive-strand RNA virus genome. PLoS Pathog 9:e1003363. https://doi.org/10.1371/journal.ppat.1003363.
45. White KA, Morris TJ. 1994. Nonhomologous RNA recombination in tombusviruses: generation and evolution of defective interfering RNAs by stepwise deletions. J Virol 68:14–24.
46. Mathews DH, Sabina J, Zuker M, Turner DH. 1999. Expanded sequence dependence of thermodynamic parameters provides robust prediction of RNA secondary structure. J Mol Biol 288:911–940. https://doi.org/10.1006/jmbi.1999.2700.
47. Zuker M. 2003. Mfold web server for Nucleic acid folding and hybridization prediction. Nucleic Acids Res 31:3406–3415. https://doi.org/10.1093/nar/gkg595.
48. Vasa SM, Guex N, Wilkinson KA, Weeks KM, Giddings MC. 2008. ShapeFinder: a software system for high-throughput quantitative analysis of nucleic acid reactivity information resolved by capillary electrophoresis. RNA 14:1979–1990. https://doi.org/10.1261/rna.1166808.

CHAPTER 4

Investigation of Novel RNA Elements in the 3'UTR of Tobacco Necrosis Virus-D

This chapter investigated previously uncharacterized RNA elements in the 3'UTR of TNV-D. This study confirms the involvement of the proposed UL-DL interaction in promoting TNV-D readthrough. SLX, SLY and the intervening sequence between them were also investigated with varying importance. Most importantly, this study demonstrates that SLX is important for efficient genome accumulation. Overall this study has been important in identifying novel regulatory elements in the 5'-portion of the 3'UTR

This chapter is presented as a research article published in *Viruses* (Newburn et al., 2020). For this article, I designed the experiments with Dr. K. Andrew White, performed approximately 90% of the experiments, analyzed the data, and wrote the first draft of the manuscript. Dr. Baodong Wu contributed the constructs used for Figure 2 and provided data for Figure 2B.

Article

Investigation of Novel RNA Elements in the 3′UTR of Tobacco Necrosis Virus-D

Laura R. Newburn, Baodong Wu and K. Andrew White *

Department of Biology, York University, Toronto, ON M3J 1P3, Canada; lnewburn@yorku.ca (L.R.N.); baodongw@gmail.com (B.W.)
* Correspondence: kawhite@yorku.ca

Received: 17 July 2020; Accepted: 4 August 2020; Published: 6 August 2020

Abstract: RNA elements in the untranslated regions of plus-strand RNA viruses can control a variety of viral processes including translation, replication, packaging, and subgenomic mRNA production. The 3′ untranslated region (3′UTR) of Tobacco necrosis virus strain D (TNV-D; genus *Betanecrovirus*, family *Tombusviridae*) contains several well studied regulatory RNA elements. Here, we explore a previously unexamined region of the viral 3′UTR, the sequence located upstream of the 3′-cap independent translation enhancer (3′CITE). Our results indicate that (i) a long-range RNA–RNA interaction between an internal RNA element and the 3′UTR facilitates translational readthrough, and may also promote viral RNA synthesis; (ii) a conserved RNA hairpin, SLX, is required for efficient genome accumulation; and (iii) an adenine-rich region upstream of the 3′CITE is dispensable, but can modulate genome accumulation. These findings identified novel regulatory RNA elements in the 3′UTR of the TNV-D genome that are important for virus survival.

Keywords: plant virus; RNA virus; 3′UTR; recoding; readthrough; cap-independent translation; RNA structure; tombusviridae; betanecrovirus

1. Introduction

Tobacco necrosis virus strain D (TNV-D), and other plus-strand RNA plant viruses contain RNA elements throughout their genomes that regulate different viral processes [1–8]. Although some regulatory elements can reside in coding regions, most are located in non-coding regions, where they do not have to maintain compatibility with viral open reading frames (ORFs). Consequently, many such RNA sequences and structures are present in the 5′ and 3′ untranslated regions (UTRs) of viral genomes.

TNV-D is a plus-sense RNA plant virus in the family *Tombusviridae*, and is the type-member of the genus *Betanecrovirus,* which also includes Beet black scorch virus (BBSV) [9]. The genome of TNV-D is 3.8 kb in length and contains five open reading frames (ORFs) (Figure 1A) [10]. Proteins that are produced directly from the viral genome include the accessory RNA replication protein (p22), and the RNA-dependent RNA polymerase (RdRp; p82), produced via readthrough of the p22 stop codon [11,12]. Movement proteins p7a and p7b are translated from subgenomic (sg) mRNA1, and coat protein (CP; p29) is produced from sg mRNA2 [13].

Different regions of the 3′UTR of the TNV-D genome are involved in various viral processes, including translation initiation, translational readthrough, and RNA replication. The last 80 nt of the 3′UTR contains two stem–loop (SL) structures, SL-II and SL-I, that are separated by 15 nts. A base-pairing interaction between the 3′-terminal 4 nts and a bulge in SLII is important for efficient RNA synthesis, and likely protects the 3′-end of the genome from exonucleases (Figure 1C, black circles) [2,7]. Just 3′ to SLII resides the distal readthrough element (DRTE) (Figure 1C, green), a 6 nt long segment that activates readthrough of p82 by forming a long-range RNA–RNA interaction with its partner sequence, the proximal readthrough element (PRTE) (Figure 1A, top) [1]. The PRTE is a bulged sequence located

within an extended SL structure, the readthrough SL (RTSL), that is positioned just downstream of the p22 UAG stop codon (Figure 1A). The PRTE–DRTE interaction is the only reported long-range RNA–RNA interaction known to occur in betanecroviruses [1].

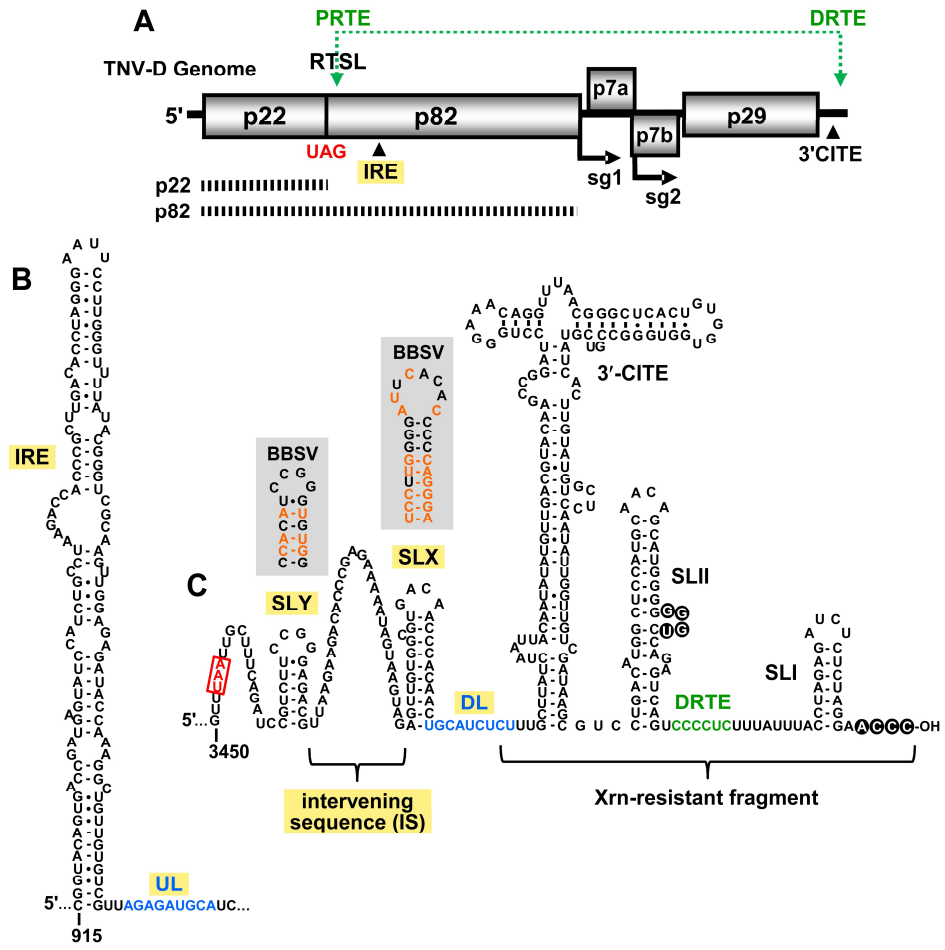

Figure 1. Tobacco necrosis virus strain D (TNV-D) genome and the predicted RNA secondary structures. (**A**) A cartoon representation of the TNV-D genome with the encoded proteins represented by grey boxes. The UAG stop codon for p22 is indicated in red. Subgenomic mRNA1 and 2 initiation sites (sg1 and sg2) are shown below the genome. The location of the 3′ cap independent translational enhancer (3′CITE) and the internal replication element (IRE) are also shown. The black dashed bars below the genome correspond to the p22 protein and the p82 readthrough product. The green double-headed arrow shows a long-range RNA–RNA interaction between the proximal readthrough element (PRTE; located within the readthrough stem–loop, RTSL) and the distal readthrough element (DRTE; in the 3′UTR) that is necessary for efficient readthrough. (**B**) Mfold-predicted RNA secondary structure of the TNV-D internal replication element (IRE), located within the coding region of p82. The 3′-adjacent upstream linker (UL) sequence is shown in blue. (**C**) Predicted RNA secondary structure of the 3′UTR in the TNV-D genome based on comparative structural analysis, compensatory mutational analysis, and structure probing data [2,5–7]. The UAA stop codon of the p29 capsid protein is boxed and highlighted in red, and the portion of the 3′UTR that accumulates as an Xrn-resistant fragment in infections is delineated. The 3′CITE and relevant stem–loop (SL) structures are labelled, as are the intervening sequence (IS), downstream linker (DL; blue) and DRTE (green). The grey boxes show the corresponding secondary structures of SLX and SLY for Beet black scorch virus (BBSV), with orange nucleotides representing the sequence changes when compared with TNV-D.

The translation of TNV-D and its two sg mRNAs is mediated by a BTE-type 3′-cap independent translation enhancer (3′CITE) [3,6,7]. This 3′CITE is located in the central region of the 3′UTR (Figure 1C), and is responsible for recruiting the translational machinery to the 5′-uncapped and 3′-non-adenylated viral mRNAs. The mechanism by which the 3′-recruited translation factors gain access to the 5′-end of these viral messages is unknown [3]. During infections, an Xrn-resistant fragment accumulates, which corresponds to a 3′-proximal portion of the 3′UTR, including the 3′CITE (Figure 1C) [14]. The precise role of this 3′-terminal viral RNA fragment is unclear, but its presence appears to confer viral fitness [14].

In this study, we investigated the importance of RNA elements present in the previously unexplored 5′-portion of the 3′UTR of TNV-D. Our results provide evidence for a second long-range RNA–RNA interaction in the TNV-D genome that is important for viral RNA accumulation and translational readthrough. We also uncovered a conserved RNA hairpin, SLX, that is involved in supporting efficient viral replication. These findings further our understanding of RNA-based regulatory elements in betanecroviruses.

2. Materials and Methods

2.1. Plasmid Construction

Constructs for this study were derivatives of wild-type (wt) TNV-D cDNA in a pUC19 plasmid, provided by Robert Coutts [10], which was modified to include a SmaI cut site at the 3′-terminus of the viral cDNA. Overlapping and standard PCR-based mutagenesis was used to introduce modifications to the TNV-D clones, using the Q5 High-Fidelity DNA Polymerase kit (NEB). The inclusion of only desired alterations was confirmed through sequencing. Changes introduced to the TNV-D genome are shown in the accompanying figures.

2.2. Preparation of Viral RNAs

Uncapped in vitro RNA transcripts were synthesized from SmaI-linearized TNV-D plasmids using the T7-FlashScribeTranscription Kit (CELLSCRIPT), as previously described [15]. RNA transcript concentration and quality were verified through spectrophotometry and agarose gel electrophoresis, respectively.

2.3. RNA Secondary Structure Prediction

TNV-D RNA secondary structures were predicted at 37 °C using the default settings of *Mfold* version 3.6 [16,17].

2.4. In Vitro Translation Assay

As described previously, 0.5 pmol of uncapped in vitro-generated viral genomic RNA transcripts were incubated in a nuclease-treated wheat germ extract (Promega, Madison, WI, USA) in the presence of ^{35}S-methionine for 1 h at 25 °C [1,2]. The protein products were separated by sodium dodecyl sulfate-polyacrylamide gel electrophoresis in a 12% resolving gel. Viral proteins produced were detected by radio-analytical scanning using a Typhoon imager (GE Healthcare, Chicago, IL, USA) and quantified using QuantityOne software (Bio-Rad, Hercules, CA, USA). All trials were completed at least three times. Averages with standard errors are shown in the accompanying figures.

2.5. Protoplast Infections

Cucumber cotyledon protoplasts were prepared and transfected with uncapped in vitro-generated viral genomic RNA transcripts as described previously [18]. Briefly, 3 µg of viral genomic RNA was transfected into protoplasts using polyethylene glycol and incubated under constant light for 22 h at 22 or 29 °C, as indicated in each figure. Total nucleic acid extraction was performed as described previously [18], and separated in non-denaturing 2% agarose gels. The nucleic acids

were electro-transferred from the agarose gel to a nylon membrane and viral RNAs were detected through Northern blotting using ^{32}P-radiolabeled probes designed to hybridize to the 3′UTR of TNV-D. Since the constructs used in this study had altered 3′UTR sequences, different probes were used to avoid overlap with the positions of the modifications. For the upstream linker (UL)–downstream linker (DL) modifications (Figure 2), three oligonucleotide probes were used; pTN14 (complementary to nt 2821–2840), pTN8 (complementary to nt 3512–3531), and pTN10 (complementary to nt 3643–3663). For the SLX and SLY modifications (Figures 3–5), two probes were used; pTN14 and pTN10. For all intervening sequence modifications (Figure 6), two probes were used; pTN14 and pL205 (complementary to nt 3568–3588). Viral RNA accumulation was monitored using a Typhoon imager (GE Healthcare) and quantified with QuantityOne software (Bio-Rad). All trials were completed three times, and averages with standard errors are shown in the accompanying figures.

3. Results

3.1. A Long-Range RNA–RNA Interaction Promotes Genome Accumulation and Translational Readthrough

Several members of the family *Tombusviridae*, including TNV-D, utilize an internal replication element (IRE) located in the readthrough portion of their RdRp ORFs (Figure 1A), which forms an extended RNA stem–loop structure (Figure 1B) [4]. In tombusviruses, the IRE (termed RII-SL) is bound by dimers of the auxiliary replication protein p33, which corresponds to p22 in TNV-D [19–21]. In Tomato bushy stunt virus (TBSV), the sequence 3′-adjacent to the base of the RII-SL structure, termed the upstream linker (UL), engages in a long-range base pairing interaction with a sequence in the genomic 3′UTR, called the downstream linker (DL) [22]. This interaction positions RII-SL proximal to another important replication structure, RIV, located at the 3′ end of the genome. The bipartite RII-SL/RIV structure forms an RNA platform on which the RNA replication complex assembles [22]. Accordingly, the UL–DL interaction is required for tombusvirus RNA synthesis and accumulation in infections. The UL–DL interaction also promotes efficient readthrough-based production of the RdRp [23].

Analysis of the sequence 3′-adjacent to the IRE in the TNV-D genome and sequences within the 3′UTR revealed a possible base-pairing interaction similar to the UL–DL interaction in tombusviruses. A 9 nt-long UL sequence immediately downstream of the IRE was found to be complementary to a DL segment positioned just upstream of the 3′CITE (Figure 1B,C respectively, blue nucleotides). To functionally assess the putative UL–DL interaction, the partner sequences were subjected to compensatory mutational analysis in which complementarity was disrupted and then restored. Two sets of mutants were generated, each of which targeted a different base pair (Figure 2A). Both of the substitutions introduced into the UL sequence in mutants U5 and U6 resulted in single amino acid changes in the RdRp (Figure 2A), however, neither residue is highly conserved in members of *Tombusviridae* [24]. Initially, viral replication was assessed in protoplast infections incubated at 22 °C for 22 hr (Figure 2B). While one set of mutations (U6, D6, and UD6) did not show a correlative trend (Figure 2B, lower panel), the other set (U5, D5, and UD5) exhibited a dependence on complementarity between the partner sequences (Figure 2B, upper panel). At a higher incubation temperature of 29 °C, where the requirement for base pairing stability is more stringent, both sets of mutants showed a clear requisite for the UL–DL interaction (Figure 2C).

When the same genomic mutants were tested in in vitro translation assays, the production of the viral auxiliary replication protein p22 was moderately affected, whereas the efficiency of readthrough-production of p82 correlated positively with complementarity (Figure 2D). These results indicate that the UL–DL interaction is functionally important for both viral genome accumulation in protoplasts, and translational readthrough in vitro.

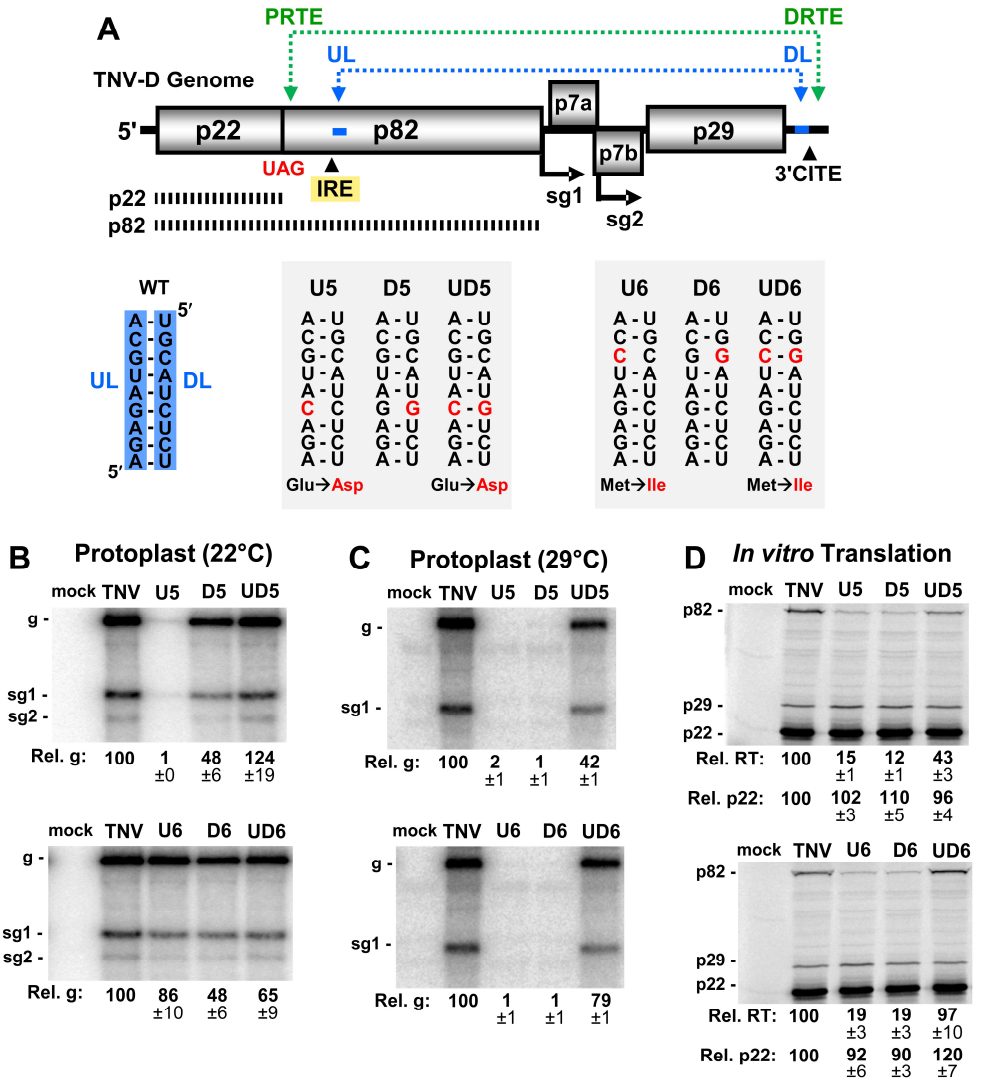

Figure 2. Analysis of the upstream linker (UL) and downstream linker (DL) interaction. (**A**) Cartoon representation of the TNV-D genome with the UL–DL interaction shown by a blue double-headed arrow. Wild-type nucleotide sequences of the UL–DL interaction are highlighted in blue, and nucleotide substitutions in mutants are shown in red, with corresponding amino acid changes below. (**B** and **C**) Northern blot analyses of TNV-D RNA accumulation in cucumber cotyledon protoplasts incubated for 22 h at either (**B**) 22 °C or (**C**) 29 °C. Above each lane is the name of the viral genome analyzed, with the positions of the viral genome (g) and subgenomic mRNAs (sg1 and sg2) denoted to the left of the blot. In this and subsequent experiments, the relative genome levels (Rel. g) of mutant genomes were determined by relative comparison to that of wt TNV-D (set at 100%) and are shown below each lane, as determined from three independent experiments (±standard error). (**D**) In vitro translation assay of TNV-D genomic RNA incubated in wheat germ extract. Viral constructs tested are noted above their respective lanes, and the identities of the protein products (p82, p29, and p22) are shown on the left. Relative readthrough (Rel. RT) was calculated as the ratio of p82/p22, with that for the wild-type genome set as 100%. Relative p22 levels (Rel. p22) were determined by direct comparison of wt (100%) versus mutant levels. The corresponding means (±standard errors) were calculated based on three independent assays.

3.2. SLY Affects Translation In Vitro but not Viral RNA Accumulation in Protoplasts

Two SL structures, SLX and SLY, separated by a 32 nt A-rich intervening sequence (IS), were predicted upstream of the DL sequence (Figure 1C). The relevance of these SLs in TNV-D was supported by corresponding SLs at equivalent positions in genus-member BBSV, which contained numerous co-varying base pairs within the stems (Figure 1C, shaded boxes). The SLY terminal loops in both viruses were identical, whereas those in SLX were unique (Figure 1C).

The function of SLY was examined by introducing modifications into its loop or stem regions. The terminal loop of SLY was replaced by an ultra-stable tetraloop, UNCG, in genome mutant Ym1 (Figure 3A). The in vitro translation of Ym1 yielded decreased levels of p22, to ~39% of wt, while readthrough efficiency was elevated by a third (Figure 3B, left panel). When the stem of SLY was disrupted in YmA and YmB, p22 production fell to ~33–48% of wt, and recovered partially (~66%) in the compensatory mutant YmC (Figure 3B, right panel), while all three mutants exhibited moderately decreased readthrough-based production of p82 (Figure 3B). When assessed in protoplast infections, all SLY mutants showed comparatively modest increases or decreases in genome levels (Figure 3C,D). Accordingly, the more pronounced negative effects of the SLY alterations on translation initiation in vitro were not correspondingly evident in protoplast infections.

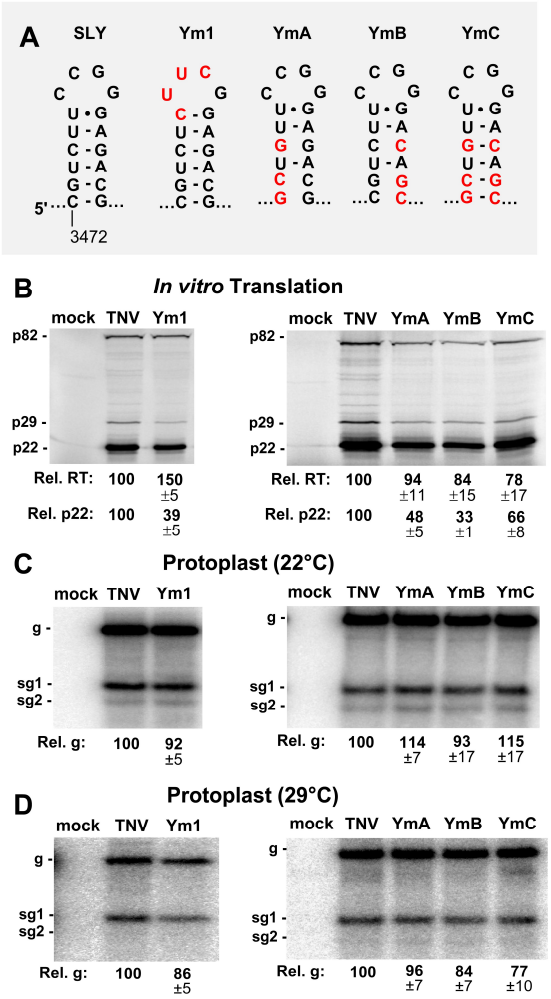

Figure 3. Mutational analysis of the SLY. (**A**) Wild-type and mutant SLYs, with substituted nucleotides in red. (**B**) In vitro translation analysis of the SLY mutants in panel A. (**C** and **D**) Northern blot analysis of the protoplast infections with SLY mutants at (**C**) 22 °C and (**D**) 29 °C.

3.3. SLX Is Important for Viral RNA Accumulation in Protoplast Infections

SLX is predicted to contain a 4 nt terminal loop and a single nucleotide C bulge. Initially, the closing base pair of the terminal loop was altered from a UA to a CG in mutant Xm0, to introduce an optimal context for both UNCG and GNRA-type ultra-stable tetraloops (Figure 4A). For Xm0, and when the loop substitutions were added in Xm1 and Xm2, moderate decreases in p22 translation were observed (Figure 4B). Similarly, the deletion of the C bulge in XΔC did not notably influence translation levels, however, all of the mutations appeared to modestly enhance readthrough (Figure 4B). When these genome mutants were assessed in protoplast infections incubated at 22 °C, accumulation levels were considerably reduced in all cases, to ~10–20% of wt, and the inhibition was exacerbated when the incubation temperature was increased to 29 °C (Figure 4C,D). Accordingly, the loop and bulge in SLX are important for viral RNA accumulation.

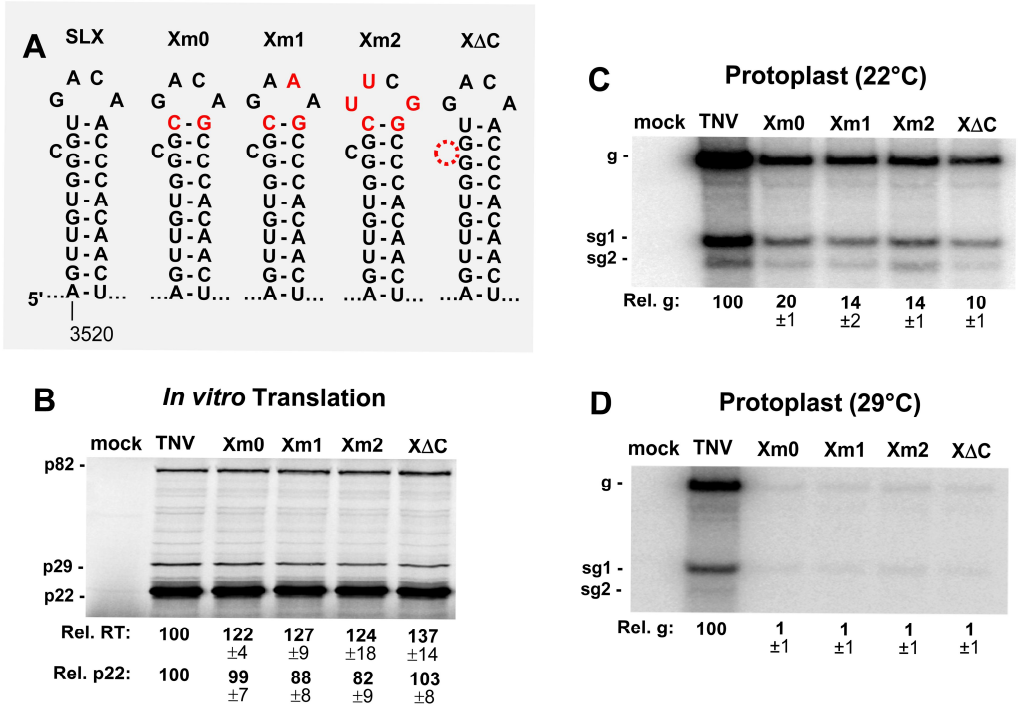

Figure 4. Mutational analysis of the loop and bulge of SLX. (**A**) Wild-type and mutant SLXs, with substituted nucleotides in red. (**B**) In vitro translation analysis of the SLX mutants. (**C** and **D**) Northern blot analysis of the protoplast infections with SLX mutants at (**C**) 22 °C and (**D**) 29 °C.

To investigate the functional relevance of the stem of SLX, compensatory mutations were introduced into this region (Figure 5A). In vitro translation assays showed elevated levels of readthrough (Figure 5B), similar to the loop mutants (Figure 4B). The production of p22 was modestly affected, with the exception of XmA, which showed about a 50% reduction (Figure 5B). When these constructs were tested for genome accumulation in protoplast infections incubated at 22 °C, genome accumulation decreased for all mutants to ~60–71% of wt (Figure 5C). However, when the incubation temperature was raised to 29 °C, a clear defect in genome accumulation was evident for XmA and XmB containing destabilized stems (~6% and ~10% of wt, respectively), with the compensatory mutant XmC showing recovery to ~64% (Figure 5C,D). Collectively, the results implicate all parts of SLX as being important for viral genome accumulation, with the upper region containing the loop and bulge being most functionally relevant.

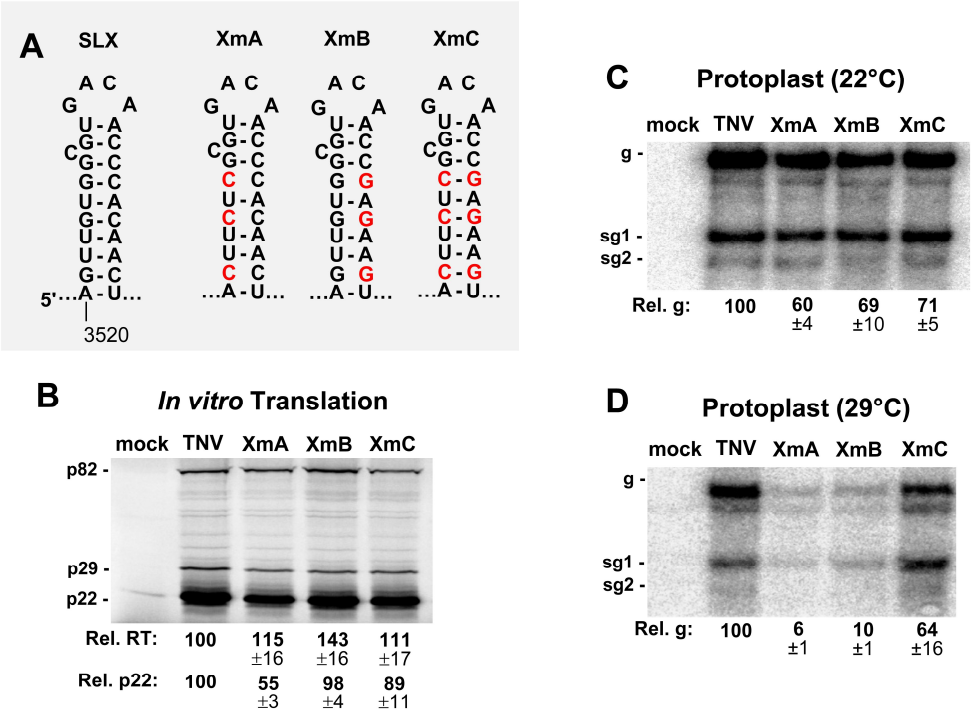

Figure 5. Mutational analysis of the stem of SLX. (**A**) Wild-type and mutant SLXs, with substituted nucleotides in red. (**B**) In vitro translation analysis of the SLX mutants. (**C** and **D**) Northern blot analysis of the protoplast infections with SLX mutants at (**C**) 22 °C and (**D**) 29 °C.

3.4. The Intervening Sequence (IS) between SLX and SLY Is not Vital for Viral Translation or Infection

The intervening sequence (IS) between SLX and SLY is an A-rich segment with 16 of the 32 nucleotides being adenylates (Figure 1C). In Red clover necrotic mosaic virus (RCNMV) RNA1, an A-rich sequence is bound by poly-A binding protein (PABP) and, along with its 3'CITE, is critically important for facilitating translation of RCNMV RNA1 [25]. TNV-D has the same class of 3'CITE as RCNMV RNA1, termed BTE [6], and thus may also have a requirement for PABP recruitment. To test if the A-rich IS in TNV-D was important for viral function, sequential deletions of 14, 24, and 29 nucleotides were created in this segment (Figure 6A). When tested for in vitro translation, the effects were generally moderate (Figure 6B). Protoplast infections incubated at 22 °C yielded near wt levels of genome accumulation (Figure 6C), while at 29 °C, defects in genome accumulation, to ~76% and ~61% of wt, were observed when 24 or 29 nucleotides were deleted, respectively (Figure 6D).

To assess the importance of the IS independent of its length, substitutions were made that decreased (341) or increased (345) adenylate content, or shuffled (343) the wt sequence (Figure 6E). All changes resulted in increased translational readthrough by ~40–50%, and varying negative effects on translation initiation (~52–96% of wt) (Figure 6F). In protoplast infections at 22 °C, viral RNA accumulation was near wt (Figure 6G), however, at 29 °C, the effect was modestly negative for 341 and 343 (~78% and ~73%, respectively), but notably inhibitory for the A-enriched 345 (~18%) (Figure 6H). Overall, with the exception of mutant 345, the IS appears to moderately influence both translation in vitro and viral RNA accumulation in protoplast infections.

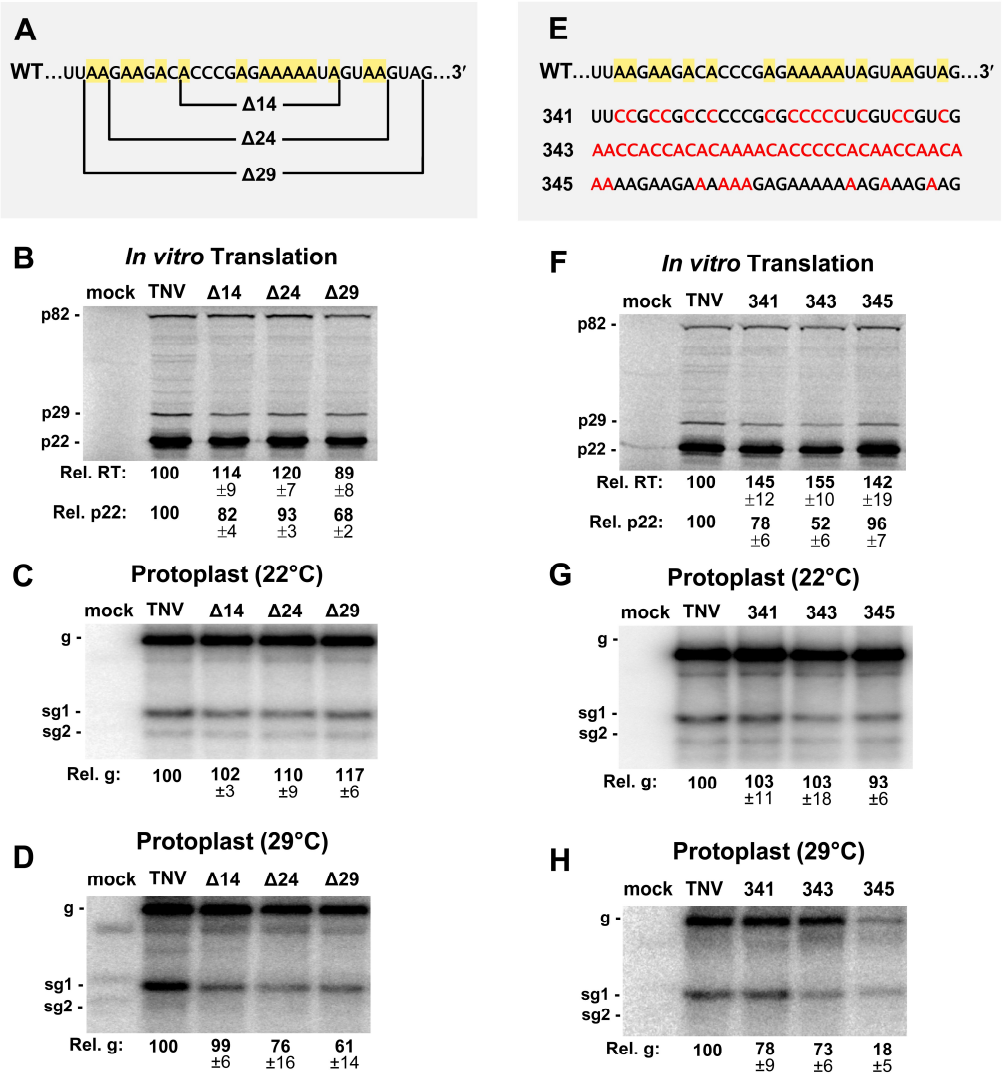

Figure 6. Mutational analysis of the intervening sequence (IS). (**A**) Deletions made in the 32 nucleotide long IS region (Δ14, Δ24, Δ29). Adenylate residues are highlighted in yellow in the wt sequence. (**B**) In vitro translation analysis of the IS mutants in panel A. (**C** and **D**) Northern blot analysis of protoplast infections with deletion mutants in panel A at (**C**) 22 °C and (**D**) 29 °C. (**E**) Substitutions in the IS are shown in red (341, 343, 345) and adenylate residues are highlighted in yellow in the wt sequence. (**F**) In vitro translation analysis of IS mutants in panel E. (**G** and **H**) Northern blot analysis of protoplast infections with deletion mutants in panel E at (**G**) 22 °C and (**H**) 29 °C.

4. Discussion

The 3′UTRs of plus-strand RNA viruses have long been known to harbor regulatory RNA elements important for controlling viral processes [2,26]. Our analysis of unexplored regions within the 3′UTR of the TNV-D genome revealed novel elements important for viral function. These RNA elements and their possible roles in viral translation and replication are discussed below.

Our results have identified a UL–DL interaction in the TNV-D genome that unites its IRE with the 3′UTR (Figure 2). In tombusviruses, the corresponding UL–DL interaction forms an IRE-3′UTR RNA platform that mediates RNA replicase complex assembly [21,22]. Aureusviruses also have a similar requirement for an equivalent UL–DL interaction [27], which is not surprising, as they encode orthologous viral proteins in similar positions as tombusviruses, and are the genera most

closely related to tombusviruses [28]. In contrast, betanecroviruses, like TNV-D, have genomes that are chimeric in origin, having accessory replication protein (p22) and RdRp (p82) related to counterparts in tombusviruses, and movement and capsid proteins orthologous to those in carmoviruses [9]. However, even with these differences, TNV-D retained the requirement for a UL–DL interaction. This suggests that although TNV-D encodes distinct carmovirus-like proteins in the 3′-half of its genome, its tombusvirus-like RNA replication proteins dictate the requirement of an IRE–3′UTR interaction which, as shown for tombusviruses [21,22], may facilitate RNA replicase complex assembly for TNV-D. Whether other tombusvirids with IREs [4] also employ long-range RNA-based communication with their 3′UTRs remains to be explored.

Readthrough in TNV-D relies on an essential PRTE–DRTE interaction (Figure 2A) [1]. However, its UL–DL interaction was also found to be necessary for optimal readthrough production of the RdRp in in vitro translation assays (Figure 2D), as was observed for tombusviruses [23]. In tombusviruses, the readthrough-promoting role of the UL–DL was also shown to be required during protoplast infections, as demonstrated using a defective interfering (DI) RNA reporter assay [23]. Corresponding in vivo confirmation was not possible with TNV-D, because no naturally-occurring or artificially-engineered DI RNAs exist for this virus. Thus, only in vitro data support a role for TNV-D's UL–DL interaction in readthrough. If this interaction does indeed enhance readthrough during infections, it would likely do so by promoting and/or stabilizing the PRTE–DRTE interaction, due to the proximity of the two interactions (Figure 2A).

Tombusvirus genomes do not contain any functionally important secondary structures in the region immediately upstream from their DL sequences. In contrast, TNV-D is predicted to contain two conserved hairpins in this location. SLY is the first predicted RNA secondary structure downstream of the p29 stop codon in the TNV-D genome (Figure 1C). Modifications in SLY that altered its loop or disrupted its stem primarily led to reduced translation initiation in in vitro assays (Figure 3B). However, protoplast infections indicated relatively minor inhibitory effects on viral RNA accumulation, suggesting a negligible role for SLY in vivo (Figure 3C,D). Nonetheless, the conservation of SLY in TNV-D and BBSV (Figure 1C) implies that it likely does confer a selective advantage to these viruses, however, this benefit may not be discernable under our experimental conditions.

SLX is also conserved in both betanecroviruses (Figure 1C). Modifications in its loop, bulge, or stem regions increased readthrough variably in translation assays, along with mostly minor negative effects on translation initiation (Figures 5B and 6B). Unlike for SLY, mutants of SLX exhibited readily observable phenotypes when assessed in protoplast infections (Figure 5C,D and Figure 6C,D). The bulge and loop mutations were highly inhibitory to viral RNA accumulation, but stem stability also contributed, albeit less notably. These results implicate the upper region of SLX as the key feature conferring function, with the stem likely acting in a supporting role to optimally present the upper structural features. Accordingly, to confer its function, the loop/bulge region of SLX likely interacts with either a viral or host protein or another region of the viral RNA. A search for complementary sequences to the loop/bulge region in the TNV-D genome did not yield any compelling candidates, thus, the latter possibility seems less likely. Therefore, the more probable role for SLX is in interacting with a protein factor that acts to facilitate viral RNA accumulation.

Some tombusvirids, in addition to their 3′CITE, require an interaction with PABP to enhance translation [25]. In the case of RCNMV RNA-1, an adenine-rich sequence located 5′-proximal to its 3′CITE binds to PABP and assists in the recruitment of translation initiation factors [25]. The similar positioning of the A-rich IS upstream of the 3′CITE in TNV-D suggested that it could function in a similar capacity. Variable effects on both translation initiation (~52–96%) and readthrough (~89–155%) were observed when sections of the IS were deleted or replaced (Figure 6B,F). However, major decreases in protein synthesis were expected if it played a critical role in translation initiation. In protoplast infections, moderate viral RNA inhibition was observed for most mutants (73–99%), but only at 29 °C (Figure 6C,D,G,H). The most adverse effects were seen for the largest deletion (Δ29, 61%) and the A-enriched mutant (345, 18%) (Figure 6D,H). The former result suggests that the IS may be important for

the optimal spacing of other RNA elements, while the latter observation indicates that certain sequences and/or nucleotide content can be very detrimental to genome accumulation during infections.

5. Conclusions

This study provides an initial assessment of the functional relevance of RNA elements in the upstream third of TNV-D's 3'UTR. The results revealed the presence of RNA elements that were either similar to other tombusvirids (UL–DL interaction) or unique to the betanecrovirus genus (SLX and SLY). Among the four RNA elements investigated, SLX and the DL (along with its partner, the UL) were most functionally relevant. The UL–DL interaction promotes readthrough, and may facilitate RNA replicase complex assembly (as demonstrated in tombusviruses [21,22]), while the unknown essential role of SLX in mediating viral RNA accumulation will be the focus of future studies.

Author Contributions: Conceptualization, L.R.N. and K.A.W.; methodology, L.R.N., B.W. and K.A.W.; writing—original draft preparation, L.R.N.; writing—review and editing, K.A.W.; supervision and project administration, K.A.W.; funding acquisition, K.A.W. All authors have read and agreed to the published version of the manuscript.

Funding: This study was supported by a grant from the Natural Sciences and Engineering Council (NSERC) of Canada to K.A.W. L.R.N. was supported by an NSERC Graduate Scholarship and a Queen Elizabeth II Scholarship in Science and Technology from the Government of Ontario.

Acknowledgments: We thank members of our laboratory for reviewing the manuscript and Robert Coutts for providing the TNV-D clone.

Conflicts of Interest: The authors declare no conflicts of interest.

References

1. Newburn, L.R.; Nicholson, B.L.; Yosefi, M.; Cimino, P.A.; White, K.A. Translational readthrough in tobacco necrosis virus-D. *Virology* **2014**, *450*, 258–265. [CrossRef] [PubMed]
2. Newburn, L.R.; White, K.A. Atypical RNA elements modulate translational readthrough in tobacco necrosis virus D. *J. Virol.* **2017**, *91*. [CrossRef] [PubMed]
3. Chkuaseli, T.; Newburn, L.R.; Bakhshinyan, D.; White, K.A. Protein expression strategies in Tobacco necrosis virus-D. *Virology* **2015**, *486*, 54–62. [CrossRef] [PubMed]
4. Nicholson, B.L.; Lee, P.K.; White, K.A. Internal RNA replication elements are prevalent in Tombusviridae. *Front. Microbiol.* **2012**, *3*, 279. [CrossRef] [PubMed]
5. Kraft, J.J.; Treder, K.; Peterson, M.S.; Miller, W.A. Cation-dependent folding of 3' cap-independent translation elements facilitates interaction of a 17-nucleotide conserved sequence with eIF4G. *Nucleic Acids Res.* **2013**, *41*, 3398–3413. [CrossRef] [PubMed]
6. Shen, R.; Miller, W.A. The 3' untranslated region of tobacco necrosis virus RNA contains a barley yellow dwarf virus-like cap-independent translation element. *J. Virol.* **2004**, *78*, 4655–4664. [CrossRef] [PubMed]
7. Shen, R.; Miller, W.A. Structures required for poly(A) tail-independent translation overlap with, but are distinct from, cap-independent translation and RNA replication signals at the 3' end of Tobacco necrosis virus RNA. *Virology* **2007**, *358*, 448–458. [CrossRef]
8. Newburn, L.R.; White, K.A. Cis-acting RNA elements in positive-strand RNA plant virus genomes. *Virology* **2015**, *479*, 434–443. [CrossRef]
9. Sit, T.L.; Lommel, S.A. Tombusviridae. In *Encyclopedia of Life Sciences*; John Wiley & Sons: Chichester, UK, 2010; pp. 1–9.
10. Coutts, R.H.A.; Rigden, J.E.; Slabas, A.R.; Lomonossoff, G.P.; Wise, P.J. The complete nucleotide sequence of tobacco necrosis virus strain D. *J. Gen. Virol.* **1991**, *72*, 1521–1529. [CrossRef]
11. Molnár, A.; Havelda, Z.; Dalmay, T.; Szutorisz, H.; Burgyán, J. Complete nucleotide sequence of tobacco necrosis virus strain DH and genes required for RNA replication and virus movement. *J. Gen. Virol.* **1997**, *78*, 1235–1239. [CrossRef]
12. Fang, L.; Coutts, R.H. Investigations on the tobacco necrosis virus D p60 replicase protein. *PLoS ONE* **2013**, *8*, e80912. [CrossRef]

13. Offei, S.K.; Coutts, R.H.A. Location of the 5′ termini of tobacco necrosis virus strain D subgenomic mRNAs. *J. Phytopathol.* **1996**, *144*, 13–17. [CrossRef]
14. Gunawardene, C.D.; Newburn, L.R.; White, K.A. A 212-nt long RNA structure in the tobacco necrosis virus-D RNA genome is resistant to Xrn degradation. *Nucleic Acids Res.* **2019**, *47*, 9329–9342. [CrossRef]
15. Newburn, L.R.; White, K.A. A trans-activator-like structure in RCNMV RNA1 evokes the origin of the trans-activator in RNA. *PLoS Pathog.* **2020**, *16*, e1008271. [CrossRef] [PubMed]
16. Mathews, D.H.; Sabina, J.; Zuker, M.; Turner, D.H. Expanded sequence dependence of thermodynamic parameters provides robust prediction of RNA secondary structure. *J. Mol. Biol.* **1999**, *288*, 911–940. [CrossRef] [PubMed]
17. Zuker, M. Mfold web server for nucleic acid folding and hybridization prediction. *Nucleic Acids Res.* **2003**, *31*, 3406–3415. [CrossRef] [PubMed]
18. White, K.A.; Morris, T.J. Nonhomologous RNA recombination in tombusviruses: Generation and evolution of defective interfering RNAs by stepwise deletions. *J. Virol.* **1994**, *68*, 14–24. [CrossRef]
19. Monkewich, S.; Lin, H.X.; Fabian, M.R.; Xu, W.; Na, H.; Debashish, R.; Chernysheva, O.A.; Nagy, P.D.; White, K.A. The p92 polymerase coding region contains an internal RNA element required at an early step in tombusvirus genome replication. *J. Virol.* **2005**, *79*, 4848–4858. [CrossRef] [PubMed]
20. Pogany, J.; White, K.A.; Nagy, P.D. Specific binding of tombusvirus replication protein p33 to an internal replication element in the viral RNA Is essential for replication. *J. Virol.* **2005**, *79*, 4859–4869. [CrossRef]
21. Pathak, K.B.; Pogany, J.; Xu, K.; White, K.A.; Nagy, P.D. Defining the roles of cis-acting RNA elements in tombusvirus replicase assembly in vitro. *J. Virol.* **2012**, *86*, 156–171. [CrossRef]
22. Wu, B.; Pogany, J.; Na, H.; Nicholson, B.L.; Nagy, P.D.; White, K.A. A discontinuous RNA platform mediates RNA virus replication: Building an integrated model for RNA-based regulation of viral processes. *PLoS Pathog.* **2009**, *5*, e1000323. [CrossRef] [PubMed]
23. Cimino, P.A.; Nicholson, B.L.; Wu, B.; Xu, W.; White, K.A. Multifaceted regulation of translational readthrough by RNA replication elements in a tombusvirus. *PLoS Pathog.* **2011**, *7*, e1002423. [CrossRef] [PubMed]
24. Gunawardene, C.D.; Jaluba, K.; White, K.A. Conserved motifs in a tombusvirus polymerase modulate genome replication, subgenomic transcription, and amplification of defective interfering RNAs. *J. Virol.* **2015**, *89*, 3236–3246. [CrossRef] [PubMed]
25. Iwakawa, H.O.; Tajima, Y.; Taniguchi, T.; Kaido, M.; Mise, K.; Tomari, Y.; Taniguchi, H.; Okuno, T. Poly(A)-binding protein facilitates translation of an uncapped/nonpolyadenylated viral RNA by binding to the 3′ untranslated region. *J. Virol.* **2012**, *86*, 7836–7849. [CrossRef]
26. Chkuaseli, T.; White, K.A. Intragenomic long-distance RNA-RNA interactions in plus-strand RNA plant viruses. *Front. Microbiol.* **2018**, *9*, 529. [CrossRef] [PubMed]
27. Lee, P.K.; White, K.A. Construction and characterization of an aureusvirus defective RNA. *Virology* **2014**, *452*, 67–74. [CrossRef]
28. Rubino, L.; Russo, M.; Martelli, G.P. Sequence analysis of pothos latent virus genomic RNA. *J. Gen. Virol.* **1995**, *76*, 2835–2839. [CrossRef]

CHAPTER 5

Discussion

Analysis of type III translational readthrough is important for understanding how this particular gene expression strategy functions. This dissertation has focused on the characterization of RNA sequences, structures, and long-range RNA-RNA interactions within TNV-D that are functionally relevant for readthrough production of the viral RdRp. The results from this work have identified several sections of the viral genome that are of particular importance for efficient readthrough. These include, the region 5'-proximal to the p22 stop codon, the section immediately downstream of the readthrough site, and the 3'UTR. Moreover, during readthrough, theses regions are brought together by dual long-range intragenomic RNA-RNA interactions. Collectively, the major findings of this study indicate that:

1. Several features of the RTSL are important for promoting efficient readthrough, including:
    (i) base pair stability of the RTSL, particularly regions proximal to the PRTE,
    (ii) the size of the PRTE bulge, and
    (iii) the type/context of the stop codon.
2. Additional RNA structures flanking the RTSL, the Pre- and Post-RTSL, are necessary for optimal readthrough activity.

3. A long-range RNA-RNA interaction between the PRTE and DRTE in the 3'UTR is necessary for TNV-D readthrough, and this interaction cannot be replaced by enhanced stabilization of the RTSL, suggesting that proximal positioning of the 3'UTR with the readthrough site is required.
4. Local structures/interactions within the 3'UTR, including SLII, and the silencer/3'-end interaction, are needed for readthrough and virus viability.
5. A second long-range RNA-RNA interaction between the UL and DL in the TNV-D genome, which likely reinforces the PRTE-DRTE interaction, is also important for promoting readthrough and virus viability.

Accordingly, readthrough in TNV-D is a complex process that relies on numerous local RNA elements/interactions, as well as long-distance interactions. These findings provide insights into this process in TNV-D, and may also be relevant to programmed recoding events in other systems. Discussed below, in section **5.1**, is a potential mechanism for readthrough in TNV-D that integrates the information in this dissertation, along with relevant information from other studies.

5.1 A Potential Mechanism of Readthrough in TNV-D

A common theme amongst members of the virus family *Tombusviridae* is their requirement for a complex series of intragenomic interactions that act to regulate different viral processes (Chkuaseli and White, 2018; Chkuaseli and White, 2020). Similarly, for TNV-D, a detailed investigation of different viral RNA elements has revealed that type III readthrough in this viral genome is far more complicated than previously appreciated (Cimino et al., 2011).

Below I propose a potential readthrough mechanism for TNV-D that aims to unite the individual results presented in **Chapters 2, 3,** and **4** (**Figure 7**).

5.1.1 Initial State of the Infecting TNV-D Genome.

Following uncoating, to initiate an infection in a host cell, the infecting TNV-D genome must act as an mRNA for translation of the auxiliary replication protein p22 and direct readthrough for the production of the p82 RdRp (**Figure 7i**). These occurrences are essential for subsequent RdRp-mediated events: *e.g.* replication of the viral genome and sg mRNA transcription, leading to further gene expression (Jiwan et al., 2011; Fang and Coutts, 2013). The local and global RNA structure of the viral genome is relevant to both translation initiation and readthrough. Through the analyses of the TNV-D genome RNA secondary structure using a combination of computer-based structure prediction, covariation analysis, solution structure probing, and mutational analyses, several RNA structures and interactions were identified that are functionally relevant for promoting readthrough (Newburn et al., 2014; Chkuaseli et al., 2015; Newburn and White, 2017; Newburn et al., 2020). These structures include localized RNA elements including the RTSL, Pre-RTSL, Post-RTSL, SLII, and BTE, as well as two long-range RNA-RNA interactions, the PRTE-DRTE, and UL-DL.

5.1.2 Translation of the Pre-Readthrough Product – p22

The step prior to readthrough involves translation initiation at the 5'-end of the genome. In TNV-D, eIF4G, a subunit in the eIF4F complex, binds to the upper region of the 3'CITE (Kraft et al., 2013) and is relocated to the 5'-end of the virus through an unknown mechanism (**Figure 7ii**; note, eIFs and ribosome subunits are not shown to allow for unobstructed views of the relevant RNA structures and long-range interactions) (Chkuaseli et al., 2015). When positioned near the

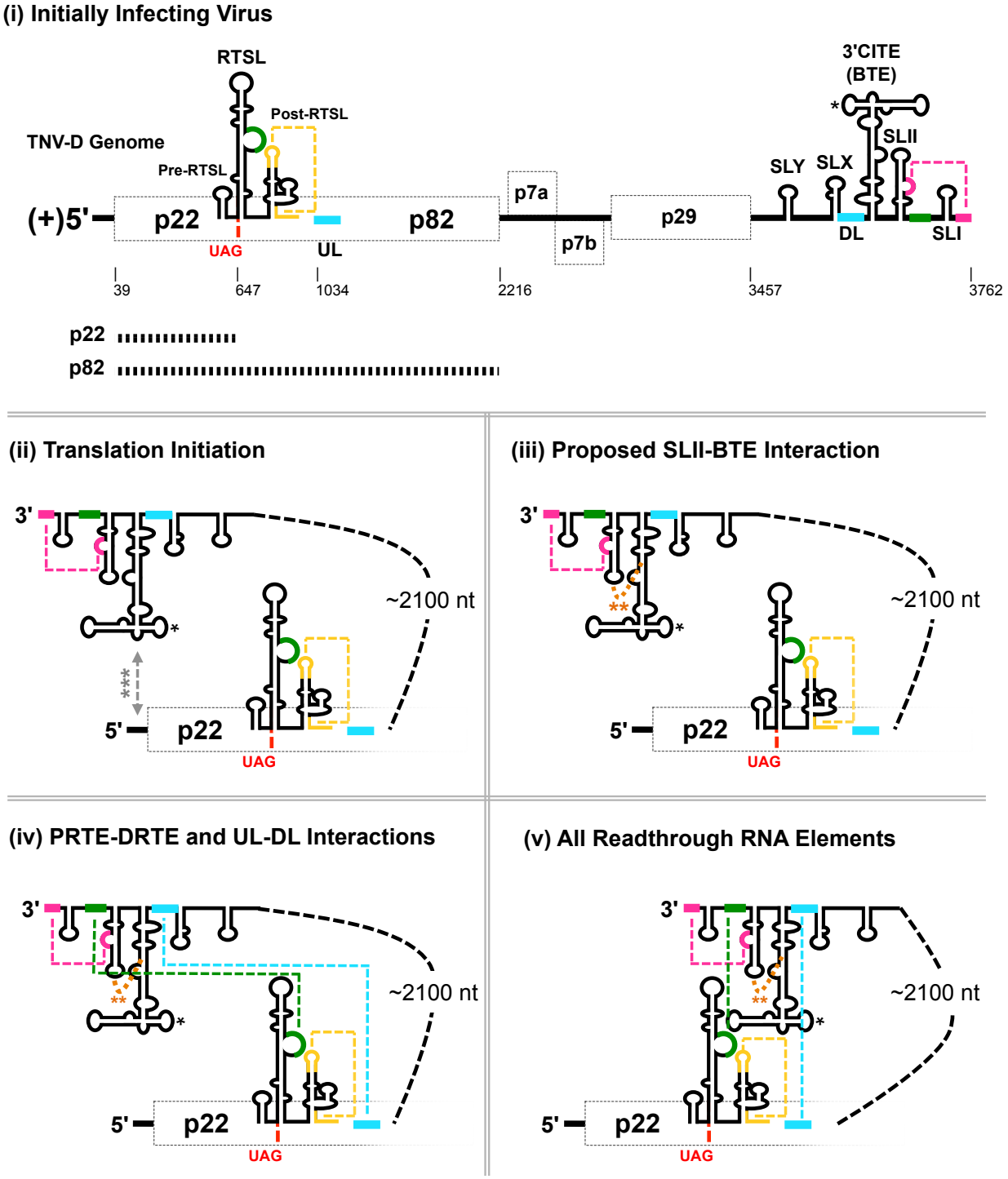

Figure 7. A proposed model for RNA-mediated readthrough regulation in TNV-D. (i) A schematic representation of the TNV-D genome along with RNA secondary and tertiary structures relevant to readthrough. * denotes the 17 nucleotide BTE consensus sequence. Also shown are the silencer/3'end interaction (pink) and post-RTSL pseudoknot structure (gold). **(ii)** Translation initiation showing repositioning of the 3'-proximal BTE next to the 5'-end of the viral genome, via an unknown mechanism (grey arrow and ***). **(iii)** Proposed SLII-BTE interaction required for readthrough (orange and **). **(iv)** The two long-range interactions, PRTE-DRTE (green) and UL-DL (cyan), necessary for readthrough. **(v)** Overview of all of the RNA elements and long-range interactions needed for readthrough. See text for additional details.

5'-end of the genome, the eIFs recruit the 43S small ribosomal subunit to the message, where it scans toward the p22 start codon. The 43S traffic along the 5'UTR of the genome is predicted to disrupt the unknown form of communication between the eIF4F-bound 3'CITE and the 5'-end. However, the association could reengage once the 43S finishes traversing this region. Upon encountering the p22 start codon, the large subunit would join, and translation would initiate, proceeding until the ribosome reaches the p22 stop codon. At the termination codon, the translating ribosome may bind either eRFs and terminate, or a near-cognate tRNA and proceed. Based on *in vitro* translation assays with the TNV-D genome, it is estimated that ribosomes at the p22 stop codon engage eRFs ~97.5% of the time, while ~2.5% of the time readthrough production of p82 occurs (Newburn et al., 2014). It is presumed that these ratios reflect relative levels during infections, however the precise ratio of p22 and p82 in infections is not known, as antibodies against p22 are not available.

5.1.3 TNV-D Readthrough

Multiple RNA elements in the TNV-D genome influence readthrough efficiency. The most direct way to modulate this event would be to alter the utilization of eRFs and near-cognate tRNAs by the ribosome in favour of the latter. This could be achieved be either interfering with the recognition of eRFs or by enhancing the use of near-cognate tRNAs. In either case, the ribosomes structure and conformation could influence its binding to these different factors. Since the RNA elements that influence readthrough efficiency are located near the termination codon (RTSL, Pre-RTSL and Post-RTSL), or are recruited to a position near the termination codon (BTE, and SLII), it is possible that they are able to regulate which factor is preferred by interacting directly with the ribosome (or a factor). The local RTSL, considered to be a major

component of the regulatory system, could function to stall the ribosome at the stop codon by blocking the RNA entrance tunnel to the ribosome with its structure. In this stalled position, the Pre-RTSL and the Post-RTSL may also be able to interact with the ribosome directly or indirectly (i.e. via a bound protein), in a way that causes decreased eRF recruitment or increased near-cognate tRNA binding.

It is also important to remember that RTSL activity requires an interaction between its PRTE bulge and the DRTE sequence in the 3'UTR of the genome (Newburn et al., 2014). Although it is possible that this interaction acts to stabilize the RTSL, deleting the PRTE bulge to create a perfect helix that is predicted to make the RTSL more stable, resulted in severely decreased readthrough (Newburn and White, 2017). This suggests that the PRTE-DRTE interaction plays a different functional role, which could be related to repositioning the 3'-end of the genome near the stop codon. RNA elements in the 3'UTR, besides the DRTE, are required for efficient readthrough. The BTE itself is crucial, because readthrough efficiency dropped dramatically when the BTE was deleted and translation initiation at the p22/82 start codon was instead facilitated by capping the BTE-less genome (Chkuaseli et al., 2015). It was determined that although readthrough levels decreased for this capped-BTE-less genome, translation of p22 remained at near wild type levels, indicating that some feature of the BTE, which is independent of its translation initiation promoting activity, is needed for efficient readthrough.

Other 3'-proximal RNA elements that promote readthrough include SLII, and the local silencer/3'-end interaction (Newburn and White, 2017). The silencer/3'-end interaction is believed to provide protection to the 3'-end of the genome from 3'-to-5' exonuclease digestion by pairing the 3'-terminus with the silencer bulge in SLII (Newburn and White, 2017). However, independent of this function, it also seems to contribute to readthrough, as disruption of this

interaction did not greatly affect translation initiation, but did reduce production of p82 (Newburn and White, 2017). This activity may be linked to SLII, because both the stability of its stem and the nucleotide identity of its terminal loop are important for robust readthrough (Newburn and White, 2017). Interestingly, when the terminal loop of SLII was replaced with a super-stable tetranucleotide loop, solution structure analysis indicated that a region near the base of the BTE exhibited increased flexibility (Gunawardene et al., 2019). This suggests that the terminal loop of SLII and a basal region of the BTE interact (**Figure 7iii**), and since both are required for efficient readthrough, this interaction could be important for their readthrough-promoting activity. Potential base pairing interactions between these two structures in the implicated regions were investigated, but were inconclusive (Newburn and White, 2017; LRN, Chaminda Gunawardene, unpublished data). This leaves open the possibility that the contact between the two regions may occur through a non-canonical interaction. It remains to be determined if the RNA elements in the 3'UTR facilitate readthrough by directly interacting with the ribosome/eRFs or, alternatively, by delivering a bound bridging protein to that region.

In addition to the long-range PRTE-DRTE interaction, a second long-range interaction, UL-DL, is also important for readthrough efficiency (Newburn et al., 2020). The proposed role of this latter interaction is to facilitate and/or stabilize the formation of the PRTE-DRTE interaction (Newburn et al., 2020). Notably, the DL sequence is located immediately 5'-proximal to the base of the BTE, which also places it close to SLII (**Figure 7iv**). This opens the possibility that the interaction between the BTE and SLII may be related to controlling the accessibility of the DL and DRTE for interacting with the UL and PRTE, respectively (**Figure 7iv**). What is clear from these analyses is that a diverse array of RNA elements and interactions are collectively involved in modulating readthrough (**Figure 7v**). It is possible that together the elements provide better

control over the amount of the replication proteins produced, or offer different ways to control how much and when readthrough occurs. Whatever the mode of action, it is expected that this sophisticated regulatory system ensures that optimal amounts of p22 and p82 are provided for successful virus infection.

5.2 Advantages of Using Readthrough as a Gene Expression Strategy

Throughout the viral life cycle, several viral proteins are produced in varying quantities, and the gene expression strategy used can dictate the quantity of production. In recoding events, such as frameshifting and readthrough, the C-terminally extended protein is produced at a lower frequency than the pre-recoding product. The benefit of recoding versus another overlapping ORF translation method is that the C-terminally extended product will share the same amino acid sequence as the pre-recoding product. In the case of TNV-D, the pre-readthrough product, p22, is believed to be responsible for creating virus-induced membrane spherules in host organelles (where viral RNA replication occurs), as has been shown for other members of *Tombusviridae* (Scholthof et al., 1995; McCartney et al., 2005; Turner et al., 2004; Rochon et al; 2014). In these membrane invaginations, oligomerization of p22, which contains a membrane-anchor domain, would induce and cover the inside of spherules, serving as the structure scaffold. Similarly, the N-terminal domain of the p82 RdRp shares this membrane integration function, therefore it too would become part of the spherules, but in lower amounts (due to its less efficient readthrough mode of production). Thus, readthrough provides a way to integrate both structural p22 and enzymatic p82 into membrane-bound virus replication structures at their required stoichiometry.

In other viruses, readthrough is used in the production of other viral proteins. In BYDV, a readthrough product of the capsid protein is translated at reduced levels and incorporated into the

viral capsid (Dinesh-Kumar et al., 1992; Chay et al., 1996). In this case, the C-terminal extension contains a domain that is able to bind to aphid mouthparts, which is important for aphid transmission from plant to plant (Chay et al., 1996). Like with the auxiliary replication and RdRp proteins, the capsid protein readthrough product is produced in smaller amounts and a only few molecules are incorporated per virus particle, which is all that is required for efficient aphid transmission (Chay et al., 1996).

5.3 Advantages of Maintaining Readthrough Elements in the 3'UTR

In both type I and type II readthrough, regulatory RNA elements exist proximal to the readthrough sites. This is a compact and efficient use of limited space in viral genomes, though exceptions exist for type II (Firth et al., 2011). Conversely, type III readthrough elements require long-distance RNA-RNA communication between the readthrough site and a distal region, such as the 3'UTR (Cimino et al., 2011). One explanation for this requirement may be that this long-distance interaction acts as a quality control check to ensure that only viral genomes containing presumably intact 3'-ends are able to produce the RdRp readthrough product.

Another possible role for communication with the 3'UTR is to coordinate translation and replication, since it is necessary to prevent these mutually-exclusive processes from occurring at the same time; i.e. translation in the 5'-to-3' direction and minus-strand synthesis in the 3'-to-5' direction. The long-range readthrough interaction with the 3'UTR could potentially inhibit minus-strand synthesis that initiates at the 3'-end of the genome. Indeed, this has been shown to occur in the tombusvirus CIRV (Cimino et al., 2011).

5.4 Readthrough in Higher Organisms

Eukaryotic protein synthesis follows a nearly universal set of decoding rules. However, stop codon readthrough has been implicated as a translation strategy utilized in yeast, fruit flies, and higher mammals. These readthrough signals typically involve local primary sequences such as UAGCARNBA, UGACUAG, or UAGCAGACUCCCG motifs (Namy et al., 2001; Anzalone et al., 2019; Loughran et al., 2014), similar to the requirements of type I readthrough. Local secondary RNA structures, generally present 9-25 nucleotides downstream of the stop codon, have also been implicated in promoting eukaryotic readthrough (Anzalone et al., 2019, Firth et al., 2011; Hudson et al., 2021), akin to the requirements of type II readthrough.

Often, the function of these readthrough products is unknown. Such as the *Drosophila melanogaster kelch* gene, which appears to use a type II-like readthrough element that relies on a local stem loop present 31 nucleotides downstream of the ORF1 UGA stop codon (Hudson et al., 2021). While the 76kDa ORF1 Kelch protein is important for maintaining actin organization in ovarian ring canals (Xue and Cooley, 1993), the exact function of the C-terminal extended 160KDa Kelch protein remains unclear, as the pre-readthrough 76kDa product was sufficient for function (Robinson and Cooley, 1997).

In some cases through, the function of the readthrough product has been determined, such as the mammalian *aquaporin-4* (AQP4) gene, and to some degree the *Drosophila headcase* (*hdc*) gene. The pre-readthrough product, AQP4, is a eukaryotic integral membrane protein that conducts water through the cell membrane (Loughran et al., 2014). The readthrough extension product appears to utilize a type I-like readthrough context, where the UGA stop codon is immediately followed by an essential CUAG motif (Loughran et al., 2014). The readthrough product, AQP4ex, is extended by 29 amino acids compared to AQP4. AQP4ex is important for

anchoring AQP4 in the central nervous system perivascular membranes, because without AQP4ex expression, AQP4 does not localize correctly (Palazzo et al., 2020).

In the case of *hdc*, a type II-like readthrough context consisting of a 79 nucleotide stem loop structure 3 nucleotides downstream of the UAA stop codon directs readthrough production of the 125kDa product versus the pre-readthrough 70kDa product (Steneberg et al., 1998). While the precise function of the 125kDa readthrough product is unknown, unlike Kelch, the readthrough product is required for proper function of the pre-readthrough product, which is involved in adult head structure development (Steneberg et al., 1998; Weaver and White, 1995).

5.5 The Challenge of Targeting Readthrough as an Antiviral Strategy

Many agriculturally important crops are vulnerable to plant virus infection. Viral infection leads to reduced crop yield and/or losses, resulting in economic and ecological harm (Patil, 2020). In *Tombusviridae*, readthrough is used to produce the RdRp in all genera, apart from *Dianthovirus*, which uses frameshifting (White, 2020). If RdRp production were to be blocked by inhibiting the function of its regulatory RNA elements, the virus would not be able to replicate its genome, and the viral lifecycle would not progress. Although this represents a potential way to inhibit virus accumulation, specific targeting of regulatory RNA elements is usually achieved using small chemicals that interact with the RNA, and most drugs that have been identified increase readthrough (Karijolich and Yu, 2014; Nagel-Wolfrum et al., 2016). Besides the challenge of screening chemical libraries to identify a molecule that would specifically inhibit type III readthrough of TNV-D, there would also be a problem in delivering it to plants in sufficient amounts in the field, and the possibility of potential toxicity, to both the plants and consumers of the plant product. Such drugs, like the one identified that inhibits -1 frameshift

RdRp production in *Severe acute respiratory syndrome coronavirus-2* (Kelly et al., 2020), are therefore better suited for treatment of mammals, where targeted administration of the drug to infected individuals is much more feasible.

5.6 Future studies

While this dissertation has improved upon the knowledge of the readthrough requirements of TNV-D, there are still additional areas of TNV-D readthrough to investigate such as the potential involvement of a protein factor(s). Furthermore, this work identified a novel element, SLX, that is worthy of additional investigation.

5.6.1 Possible Involvement of a 3'-bound Protein Factor(s) in Readthrough

The hypothesis that the long-range RNA-RNA base pairing interaction between the 3'UTR of TNV-D and the RTSL repositions a 3'end-bound protein factor to the readthrough site via the PRTE-DRTE interaction should be investigated. My previous studies have implicated the 3'UTR as a possible site for binding of such a protein. In the future, an RNA affinity-binding assay could be used (Windbichler and Schroeder, 2006). The 3'UTR or subregions would be used as bait to identify binding proteins from wheat germ extract. It is also possible that the PRTE-DRTE interaction might be necessary to promote protein binding. Thus, if the initial binding assay failed, the bait RNA could be modified to include the 3'UTR co-incubated with the RTSL in wheat germ extract to mimic the PRTE-DRTE interaction. Any bound proteins would be eluted, separated by sodium dodecyl polyacrylamide gel electrophoresis, and identified by mass spectrometry (Aebersold and Mann, 2003). The RNA binding specificity of any proteins identified would then be confirmed via an electrophoretic mobility shift assays. Finally, the

protein would be tested for functional relevance by adding it back to wheat germ extract, which would be predicted to enhance readthrough *in vitro* (Gaille, 2007; Nicholson et al., 2013)

5.6.2 TNV-D Replication Studies on SLX

The knowledge of TNV-D replication elements is largely based on other *Tombusviridae* studies, particularly those of TBSV (Chkuaseli and White, 2018). However, the TBSV 3'UTR does not contain an RNA element analogous to the TNV-D SLX, making this element unique. As the upper portion of SLX appears to be the important component (Newburn et al., 2020), investigations as to whether it interacts with a replication promoting protein or another RNA sequence should be investigated. To identify a possible protein partner, a methodology similar to that described in **5.6.1** for the 3'UTR should be carried out. In terms of an RNA partner, previous genome-wide attempts to locate compelling base pairing candidates for SLX were unsuccessful (LRN, unpublished). Performing solution structure analysis could be informative, as similar studies of modifications to the loop of SLII revealed corresponding structural changes in the lower stem region of the BTE (Gunawardene et al., 2019). Thus, structure-probing analysis, such as selective 2'-hydroxyl acylation analyzed by primer extension (Wilkinson et al., 2006) could be carried out with wild type and mutant SLX to determine if SLX modifications affect the structure of surrounding RNA regions.

One limitation to studies involving TNV-D is the inability to effectively separate viral RNA replication from other viral functions, such as translation. Therefore, the availability of a non-coding viral RNA replicon would be of great use. Defective interfering (DI) RNAs are sub-viral RNAs composed of non-contiguous RNA segments from a viral genome (White and Morris, 1999). These non-contiguous RNA segments specifically contain replication-associated

structures/sequences. Thus, the DI RNAs are able to replicate, but rely on the presence of a helper virus to supply replication proteins *in trans* (White and Morris, 1999). Previous attempts to create an artificial TNV-D based DI RNA were unsuccessful (Pui Kei K. Lee, unpublished), however the replicons constructed did not include SLX, which we now know is important for replication. Accordingly, future attempts to create a non-coding TNV-D replicon should include SLX. Successful construction of a functional replicon would provide a powerful tool for future TNV-D replication studies.

5.7 Final Thoughts

This research has shed additional light on the variety of RNA elements involved in TNV-D readthrough, and this information will be of assistance in understanding and further characterizing type III readthrough elements in both viruses and eukaryotes.

5.8 References

Aebersold R, Mann M. 2003. Mass spectrometry-based proteomics. *Nature*. **422**(6928): 198-207. doi: 10.1038/nature01511.

Anzalone AV, Zairis S, Lin AJ, Rabadan R, Cornish VW. 2019. Interrogation of Eukaryotic Stop Codon Readthrough Signals by *in Vitro* RNA Selection. *Biochemistry*. **58**(8): 1167-1178. doi: 10.1021/acs.biochem.8b01280.

Chay CA, Gunasinge UB, Dinesh-Kumar SP, Miller WA, Gray SM. 1996. Aphid Transmission and Systemic Plant Infection Determinants of Barley Yellow Dwarf Luteovirus-PAV are Contained in the Coat Protein Readthrough Domain and 17-kDa Protein, Respectively. *Virology*. **219**(1): 57-65. doi: 10.1006/viro.1996.0222.

Chkuaseli T, Newburn LR, Bakhshinyan D, White KA. 2015. Protein expression strategies in Tobacco necrosis virus-D. *Virology*. **486**: 54-62. doi: 10.1016/j.virol.2015.08.032.

Chkuaseli T, White KA. 2018. Intragenomic Long-Distance RNA-RNA Interactions in Plus-Strand RNA Plant Viruses. *Front Microbiol*. **9**:529. doi: 10.3389/fmicb.2018.00529.

Chkuaseli T, White KA. 2020. Activation of viral transcription by stepwise largescale folding of an RNA virus genome. *Nucleic Acids Res.* **48**(16): 9285-9300. doi: 10.1093/nar/gkaa675.

Cimino PA, Nicholson BL, Wu B, Xu W, White KA. 2011. Multifaceted Regulation of Translational Readthrough by RNA Replication Elements in a Tombusvirus. *PLoS Pathog.* **7**(12):e1002423. doi: 10.1371/journal.ppat.1002423.

Dinesh-Kumar SP, Brault V, Miller WA. 1992. Precise mapping and *in Vitro* Translation of a Trifunctional Subgenomic RNA of Barley Yellow Dwarf Virus. *Virology*. **187**(2): 711-22. doi: 10.1016/0042-6822(92)90474-4.

Fang L, Coutts RHA. 2013. Investigations on the *Tobacco Necrosis Virus* D p60 Replicase Protein. *PLoS One*. **8**(11): e80912. doi: 10.1371/journal.pone.0080912.

Firth AE, Wills NM, Gesteland RF, Atkins JF. 2011. Stimulation of stop codon readthrough: frequent presence of an extended 3' RNA structural element. *Nucleic Acids Res*. **39**(15): 6679-91. doi: 10.1093/nar/gkr224.

Gallie DR. 2007. Use of *In Vitro* Translation Extract Depleted in Specific Initiation Factors for the Investigation of Translational Regulation. *Methods Enzymol*. **429**: 35-51. doi: 10.1016/S0076-6879(07)29003-2.

Gunawardene CD, Newburn LR, White KA. 2019. A 212-nt long RNA structure in the Tobacco necrosis virus-D RNA genome is resistant to Xrn degradation. *Nucleic Acids Res.* **47**(17): 9329-42. doi: 10.1093/nar/gkz668.

Hudson AM, Loughran G, Szabo NL, Wills NM, Atkins JF, Cooley L. 2021. Tissue-specific dynamic codon redefinition in Drosophila. *Proc Natl Acad Sci USA*. **118**(5): e2012793118. doi: 10.1073/pnas.2012793118.

Jiwan SD, Wu B, White KA. 2011. Subgenomic mRNA transcription in tobacco necrosis virus. *Virology*. **418**(1): 1-11. doi: 10.1016/j.virol.2011.07.005.

Karijolich J, Yu YT. 2014. Therapeutic suppression of premature termination codons: Mechanisms and clinical considerations (Review). *Int J Mol Med*. **34**(2): 355-62. doi: 10.3892/ijmm.2014.1809.

Kelly JA, Olson AN, Neupane K, Munshi S, San Emeterio J, Pollack L, Woodside MT, Dinman JD. 2020. Structural and functional conservation of the programmed -1 ribosomal frameshift signal of SARS coronavirus 2 (SARS-CoV-2). *J Biol Chem*. **295**(31): 10741-8. doi: 10.1074/jbc.AC120.013449.

Kraft JJ, Treder K, Peterson MS, Miller WA. 2013. Cation-dependent folding of 3' cap-independent translation elements facilitates interaction of a 17-nucleotide conserved sequence with eIF4G. *Nucleic Acids Res*. **41**(5): 3398-413. doi: 10.1093/nar/gkt026.

Loughran G, Chou MY, Ivanov IP, Jungreis I, Kellis M, Kiran AM, Baranov PV, Atkins JF. 2014. Evidence of efficient stop codon readthrough in four mammalian genes. *Nucleic Acids Res*. **42**(14): 8928-38. doi: 10.1093/nar/gku608.

McCartney AW, Greenwood JS, Fabian MR, White KA, Mullen RT. 2005. Localization of the Tomato Bushy Stunt Virus Replication Protein p33 Reveals a Peroxisome-to- Endoplasmic Reticulum Sorting Pathway. *Plant Cell*. **17**: 3513-31. doi: 10.1105/tpc.105.036350.

Nagel-Wolfrum K, Möller F, Penner I, Baasov T, Wolfrum U. 2016. Targeting Nonsense Mutations in Diseases with Translational Read-Through-Inducing Drugs (TRIDs). *BioDrugs*. **30**(2):49-74. doi: 10.1007/s40259-016-0157-6. PMID: 26886021.

Namy O, Hatin I, Rousset JP. 2001. Impact of the six nucleotides downstream of the stop codon on translation termination. *EMBO Rep*. **2**(9): 787-93. doi: 10.1093/embo-reports/kve176.

Newburn LR, Nicholson BL, Yosefi M, Cimino PA, White KA. 2014. Translational readthrough in Tobacco necrosis virus-D. *Virology*. **450-451**: 258-65. doi: 10.1016/j.virol.2013.12.006.

Newburn LR, White KA. 2017. Atypical RNA Elements Modulate Translational Readthrough in Tobacco Necrosis Virus D. *J Virol.* **91**(8): e02443-16. doi: 10.1128/JVI.02443-16.

Newburn LR, Wu B, White KA. 2020. Investigation of Novel RNA Elements in the 3'UTR of Tobacco Necrosis Virus-D. *Viruses*. **12**(8): 856. doi: 10.3390/v12080856.

Nicholson BL, Zaslaver O, Mayberry LK, Browning KS, White KA. 2013. Tombusvirus Y-shaped Translational Enhancer Forms a Complex with eIF4F and Can Be Functionally Replaced by Heterologous Translational Enhancers. *J Virol*. **87**(3): 1872-83. doi: 10.1128/JVI.02711-12.

Palazzo C, Abbrescia P, Valente O, Nicchia GP, Banitalebi S, Amiry-Moghaddam M, Trojano M, Frigeri A. 2020. Tissue Distribution of the Readthrough Isoform of AQP4 Reveals a Dual Role of AQP4ex Limited to CNS. *Int J Mol Sci*. **21**(4): 1531. doi: 10.3390/ijms21041531.

Patil BL. 2020. Plant Viral Diseases: Economic Implications. In: *Reference Module in Life Sciences.* doi: 10.1016/b978-0-12-809633-8.21307-1.

Robinson DN, Cooley L. 1997. *Drosophila* Kelch is an Oligomeric Ring Canal Actin Organizer. *J Cell Biol*. **138**(4): 799-810. doi: 10.1083/jcb.138.4.799.

Rochon D, Singh B, Reade R, Theilmann J, Ghoshal K, Alam SB, Maghodia A. 2014. The p33 auxiliary replicase protein of Cucumber necrosis virus targets peroxisomes and infection induces *de novo* peroxisome formation from the endoplasmic reticulum. *Virology*. **452-453**: 133-42. doi: 10.1016/j.virol.2013.12.035.

Scholthof KB, Scholthof HB, Jackson AO. 1995. The Tomato Bushy Stunt Virus Replicase Proteins Are Coordinately Expressed and Membrane Associated. *Virology*. 208(1): 365-9. doi: 10.1006/viro.1995.1162.

Steneberg P, Englund C, Kronhamn J, Weaver TA, Samakovlis C. 1998. Translational readthrough in the *hdc* mRNA generates a novel branching inhibitor in the *Drosophila* trachea. *Genes Dev*. **12**(7): 956-67. doi: 10.1101/gad.12.7.956.

Turner KA, Sit TL, Callaway AS, Allen NS, Lommel SA. 2004. Red clover necrotic mosaic virus replication proteins accumulate at the endoplasmic reticulum. *Virology*. **320**(2): 276-90. doi: 10.1016/j.virol.2003.12.006.

Weaver TA, White RA. 1995. *headcase*, an imaginal specific gene required for adult morphogenesis in *Drosophila melanogaster*. *Development*. **121**(12): 4149-60.

White KA. 2020. Tombusvius-Like Viruses (Tombusviridae). In: *Reference Module in Life Sciences, Elsevier.* doi: 10.1016/B978-0-12-809633-8.21260-0.

White KA, Morris TJ. 1999. Defective and Defective Interfering RNAs of Monopartite Plus-strand RNA Plant Viruses. *Curr Top Microbiol Immunol*. **239**:1-17. doi: 10.1007/978-3-662-09796-0_1.

Wilkinson KA, Merino EJ, Weeks KM. 2006. Selective 2'-hydroxyl acylation analyzed by primer extension (SHAPE): quantitative RNA structure analysis at single nucleotide resolution. *Nat Protoc*. **1**(3): 1610-6. doi: 10.1038/nprot.2006.249.

Windbichler N, Schroeder R. 2006. Isolation of specific RNA-binding proteins using the streptomycin-binding RNA aptamer. *Nat Protoc*. **1**(2): 637-40. doi: 10.1038/nprot.2006.95.

Xue F, Cooley L. 1993. *kelch* Encodes a Component of Intercellular Bridges in Drosophila Egg Chambers. *Cell*. **72**(5): 681-93. doi: 10.1016/0092-8674(93)90397-9.

APPENDICES

Appendix A – Additional Research Contributions

Chkuaseli T, **Newburn LR**, Bakhshinyan D, White KA. 2015. Protein expression strategies in Tobacco necrosis virus-D. *Virology*. **486**: 54-62. doi: 10.1016/j.virol.2015.08.032.

Gunawardene CD, **Newburn LR**, White KA. 2019. A 212-nt long RNA structure in the Tobacco necrosis virus-D RNA genome is resistant to Xrn degradation. *Nucleic Acids Res.* **47**(17): 9329-42. doi: 10.1093/nar/gkz668.

Newburn LR, White KA. 2020. A *trans*-activator-like structure in RCNMV RNA1 evokes the origin of the *trans*-activator in RNA2. *PLoS Pathog*. **16**(1): e1008271. doi: 10.1371/journal.ppat.1008271.

Appendix B – Copyright Permission

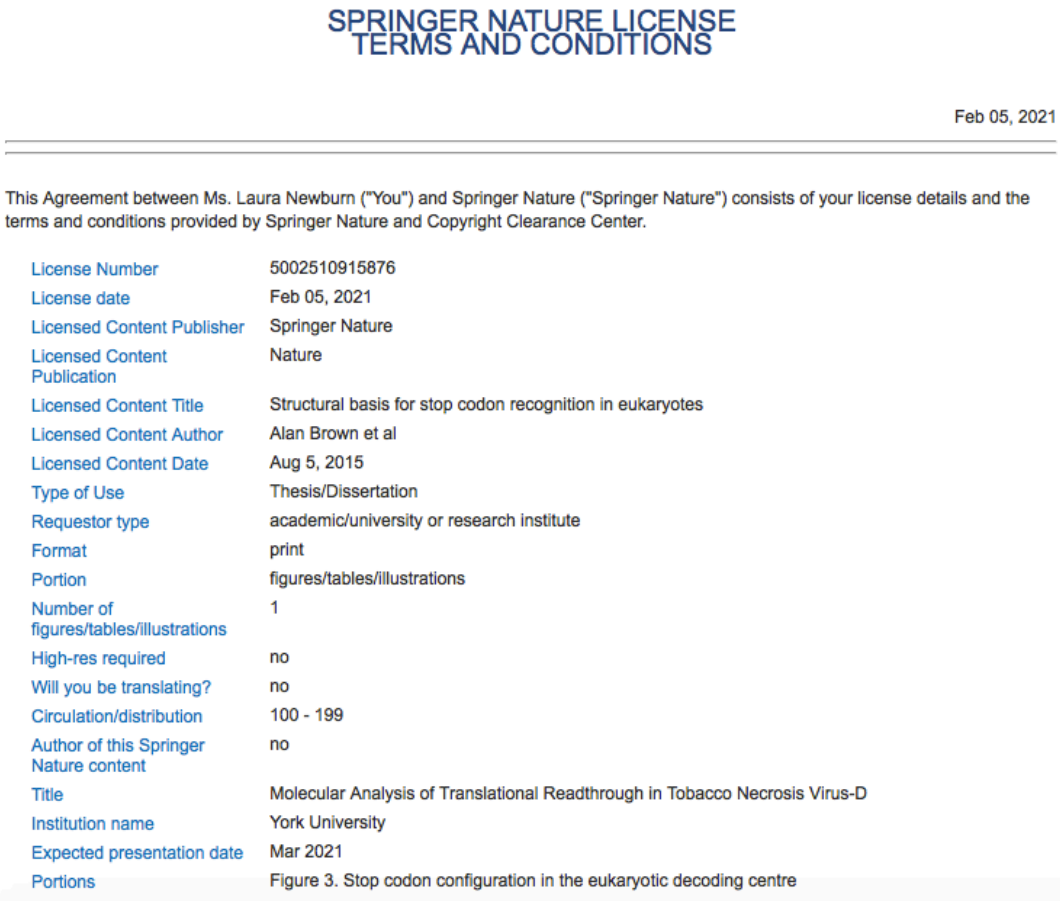

SPRINGER NATURE LICENSE
TERMS AND CONDITIONS

Feb 05, 2021

This Agreement between Ms. Laura Newburn ("You") and Springer Nature ("Springer Nature") consists of your license details and the terms and conditions provided by Springer Nature and Copyright Clearance Center.

License Number	5002510915876
License date	Feb 05, 2021
Licensed Content Publisher	Springer Nature
Licensed Content Publication	Nature
Licensed Content Title	Structural basis for stop codon recognition in eukaryotes
Licensed Content Author	Alan Brown et al
Licensed Content Date	Aug 5, 2015
Type of Use	Thesis/Dissertation
Requestor type	academic/university or research institute
Format	print
Portion	figures/tables/illustrations
Number of figures/tables/illustrations	1
High-res required	no
Will you be translating?	no
Circulation/distribution	100 - 199
Author of this Springer Nature content	no
Title	Molecular Analysis of Translational Readthrough in Tobacco Necrosis Virus-D
Institution name	York University
Expected presentation date	Mar 2021
Portions	Figure 3. Stop codon configuration in the eukaryotic decoding centre

Figure 1. Copyright permission for CHAPTER 1, Figure 4ii.

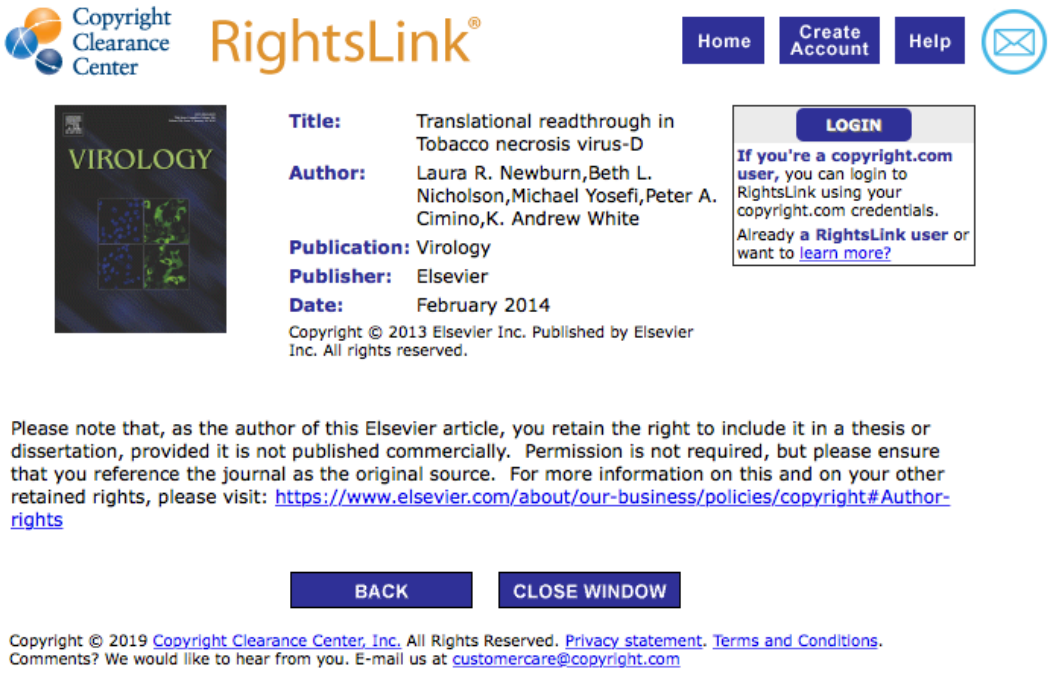

Figure 2. Copyright permission for CHAPTER 2 (Newburn et al., 2014).

Figure 3. Copyright permission for CHAPTER 3 (Newburn and White, 2017).

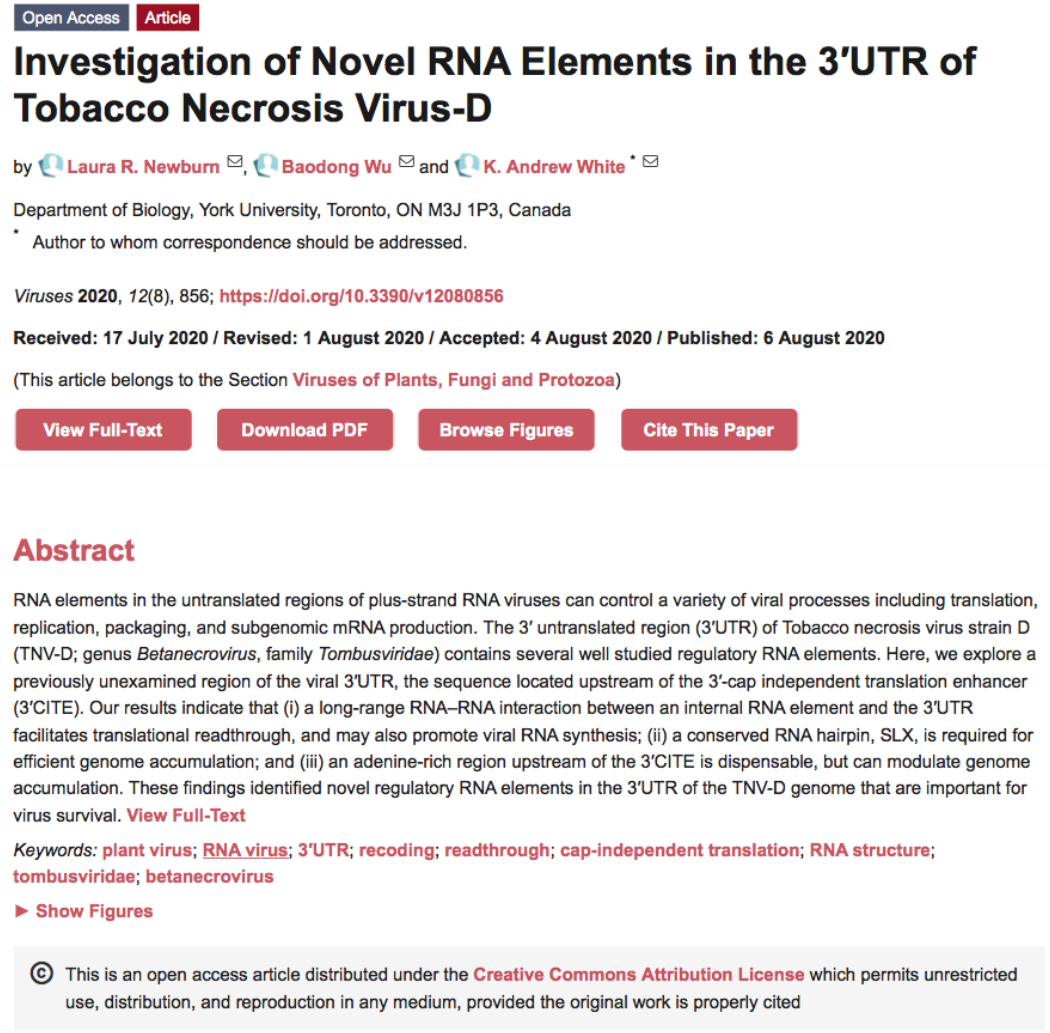

Open Access Article

Investigation of Novel RNA Elements in the 3′UTR of Tobacco Necrosis Virus-D

by Laura R. Newburn, Baodong Wu and K. Andrew White *

Department of Biology, York University, Toronto, ON M3J 1P3, Canada

* Author to whom correspondence should be addressed.

Viruses **2020**, *12*(8), 856; https://doi.org/10.3390/v12080856

Received: 17 July 2020 / Revised: 1 August 2020 / Accepted: 4 August 2020 / Published: 6 August 2020

(This article belongs to the Section Viruses of Plants, Fungi and Protozoa)

View Full-Text | Download PDF | Browse Figures | Cite This Paper

Abstract

RNA elements in the untranslated regions of plus-strand RNA viruses can control a variety of viral processes including translation, replication, packaging, and subgenomic mRNA production. The 3′ untranslated region (3′UTR) of Tobacco necrosis virus strain D (TNV-D; genus *Betanecrovirus*, family *Tombusviridae*) contains several well studied regulatory RNA elements. Here, we explore a previously unexamined region of the viral 3′UTR, the sequence located upstream of the 3′-cap independent translation enhancer (3′CITE). Our results indicate that (i) a long-range RNA–RNA interaction between an internal RNA element and the 3′UTR facilitates translational readthrough, and may also promote viral RNA synthesis; (ii) a conserved RNA hairpin, SLX, is required for efficient genome accumulation; and (iii) an adenine-rich region upstream of the 3′CITE is dispensable, but can modulate genome accumulation. These findings identified novel regulatory RNA elements in the 3′UTR of the TNV-D genome that are important for virus survival. View Full-Text

Keywords: plant virus; RNA virus; 3′UTR; recoding; readthrough; cap-independent translation; RNA structure; tombusviridae; betanecrovirus

► Show Figures

Figure 4. Copyright permission for CHAPTER 4 (Newburn et al., 2020).